UNIVERSITY OF OKLAHOMA

GRADUATE COLLEGE

SINGLE-PROBE MASS SPECTROMETRY AS A BIOANLYTICAL TOOL FOR QUANTITATIVE SINGLE CELL ANALYSIS: FROM CELL LINES TO PATIENTS

A DISSERTATION

SUBMITTED TO THE GRADUATE FACULTY

in partial fulfillment of the requirements for the

Degree of

DOCTOR OF PHILOSOPHY

By

SHAWNA J. STANDKE
Norman, Oklahoma
2019

SINGLE-PROBE MASS SPECTROMETRY AS A BIOANLYTICAL TOOL FOR QUANTITATIVE SINGLE CELL ANALYSIS: FROM CELL LINES TO PATIENTS

A DISSERTATION APPROVED FOR THE
DEPARTMENT OF CHEMISTRY AND BIOCHEMISTRY

BY

Dr. Zhibo Yang, Chair

Dr. Anthony W. G. Burgett

Dr. Michael Patten

Dr. George Richter-Addo

Dr. Si Wu

I would like to dedicate this to all the people I have tutored the past 5 years. Not only have you kept the basics of chemistry fresh in my mind, but I am a firm believer that you never really understand something until you can explain it to someone else. Thank you for always asking me the difficult questions that would make me really have to think about my basic principles, not thinking I'm crazy when I say chlorine is my favorite element because it has my favorite mass, keeping me up-to-date about what is cool, getting me out of lab, and entertaining me with your awesome stories (even your chemistry horror stories).

Acknowledgements

First, I would like to thank my family for their support the past 5 years. Dad, thank you for always pushing me to keep going when things got hard. I don't think I would be writing this if it weren't for you. Mom, thank you for helping me move (and bringing Seth to do the heavy lifting) and for not being ashamed or embarrassed to tell people I am a chemist (unlike Seth). I also really appreciate your help with looking for jobs. Seth, thank you for having "FaceTime Wednesdays" with me. It's been the one thing keeping me from getting extremely homesick, and I love you for that. Jacqueline, thank you for being there whenever I needed to talk and giving me reassurance that I can do anything I put my mind to. You may not be family by blood, but you are by choice, which is just as strong (if not stronger).

Next, I would like to thank my committee members for helping keep me on track. Dr. Yang, thank you for always making time for me and my questions. I appreciate all the skills you have taught me and trusting me to take apart the nano since I am pretty sure it costs more than me. Dr. Burgett, you have been like a Co-PI for me, and I am thankful that you took a chance 5 years ago and let me learn the biochemistry side of things since it has made me a much better analytical chemist. I would like to thank Dr. Libault for being a great out of department member-you may not be in the chemistry department, but you always asked meaningful questions and kept me on track. Dr. Patten, thank you for stepping up to the plate as my outside member the past year. I would like to thank Dr. Richter-Addo for being on top of all the protocols and things I needed to do to receive my PhD and Dr. Wu for always knowing how to rephrase questions, so I understand what was actually being asked. I truly appreciate you guys

for everything you have done. I know you are all busy, and I am grateful you made time to be on my committee.

Additionally, there are faculty members that aren't on my committee that have been critical in my receiving my PhD. Dr. White, thank you for all your stories about industry and your PhD experience, guidance with the program, and help with teaching. Dr. Foster, you have been a great mentor. I appreciate your making time to answer my LC questions, training me on almost all of the instruments in the MS lab, and making me sound cool by telling everyone I am a MS expert.

Finally, I would like to thank all my collaborators without whom I truly couldn't have written this. Dr. Rama Kothapalli, thank you for being there from day 1 and having the patience to teach me skills and develop methods with me. I'd like to thank my undergraduate, Devon Colby, for his help with the ICMP. Dr. Ning Pan and Mei Sun, thank you for all your work helping me with the irinotecan paper. I'd also like to thank the doctors at the OUHSC who made my dream of testing patient samples a reality, and the rest of my group members for being the first to congratulate me on a new paper (and for citing them!). Last, but definitely not least, I would like to thank Ryan Bensen for all his help the past few years. Thank you for doing all the things I don't like to (like write introductions and secure the cell-selection probe), reminding me that I need to eat when we work on data analysis all day so I don't get grumpy, and being an amazing coauthor.

Table of Contents

List of Tables

List of Figures

List of Abbreviations

Abbreviation	Meaning
SCA	Single cell analysis
MS	Mass spectrometry
SCMS	Single cell mass spectrometry
ICMP	Integrated cell manipulation platform
LC	Liquid chromatography
PC	Phosphatidylcholine
PBS	Phosphate buffer serum
FBS	Fetal bovine serum

Abstract

Cellular processes are traditionally characterized using bulk analysis. However, cell population averaging techniques are unable to accurately characterize these processes as each cell is extremely heterogeneous and can have different properties based on cell morphology, size, or growth phase, etc. Additionally, cell population averaging contains extensive sample preparation, which could alter cellular metabolites. Cells are sensitive to environmental perturbation (e.g. centrifugation, trypsinization, temperature fluctuation, etc.), so the sample preparation needed for bulk population analysis may skew results.

With advancements in instrumentation and bioanalytical tools, single cell analysis techniques have been increasingly characterized in the past decade. Single cell mass spectrometry is a popular method for single cell analysis since high resolution mass spectrometers are extremely sensitive and can extract information for a broad range of compounds using only the volume of a single cell (i.e. a few picoliters of solution). Ambient mass spectrometry techniques have been utilized for single cell analysis since they require little to no sample preparation and can give more representative results about each individual cell in a near-native environment. Furthermore, live-video single cell mass spectrometry techniques have been developed to capture real-time analysis of cellular compounds from individual cells.

In this work, the Single-probe mass spectrometry method has been increasingly characterized and developed for use on a variety of cell types. The Single-probe is a

microscale sampling device that couples with a mass spectrometer for the real-time analysis of live, single cells under ambient conditions. First, the Single-probe mass spectrometry technique was used to detect drug compounds from individual cells (results not published). Then, a setup was created to allow for the analysis of suspension cells in solution to enable the testing of a variety of cell types from complex solutions. Next, the Single-probe mass spectrometry method was adapted for the first-time quantification of mammalian cancer cell lines for adherent cells. The quantitative single cell analysis technique was then used to explore drug metabolism on the single-cell level. Finally, cells derived from the urine of bladder cancer patients was tested, and we report the first quantification of anti-cancer compounds from single cells that were collected non-invasively.

Chapter 1 : Single Cell Methods of Analysis

Traditionally, cells are characterized using bulk sampling techniques, such as the use of liquid chromatography mass spectrometry (LCMS) to analyze cell lysate samples. These bulk sampling methods require large sample volume, mask cellular heterogeneity, and require a lengthy sample preparation process, which could alter cellular metabolites and are incapable of providing real-time analysis of cells in a near-native environment.[1,2] Cell population averaging methods assume each cell is identical and will have the same response to environmental or chemical perturbations. However, even in a seemingly homogenous population of cells, cells will exhibit a heterogenous nature based on the rate of growth, phase in the growth cycle, and size, amongst other factors.[3]

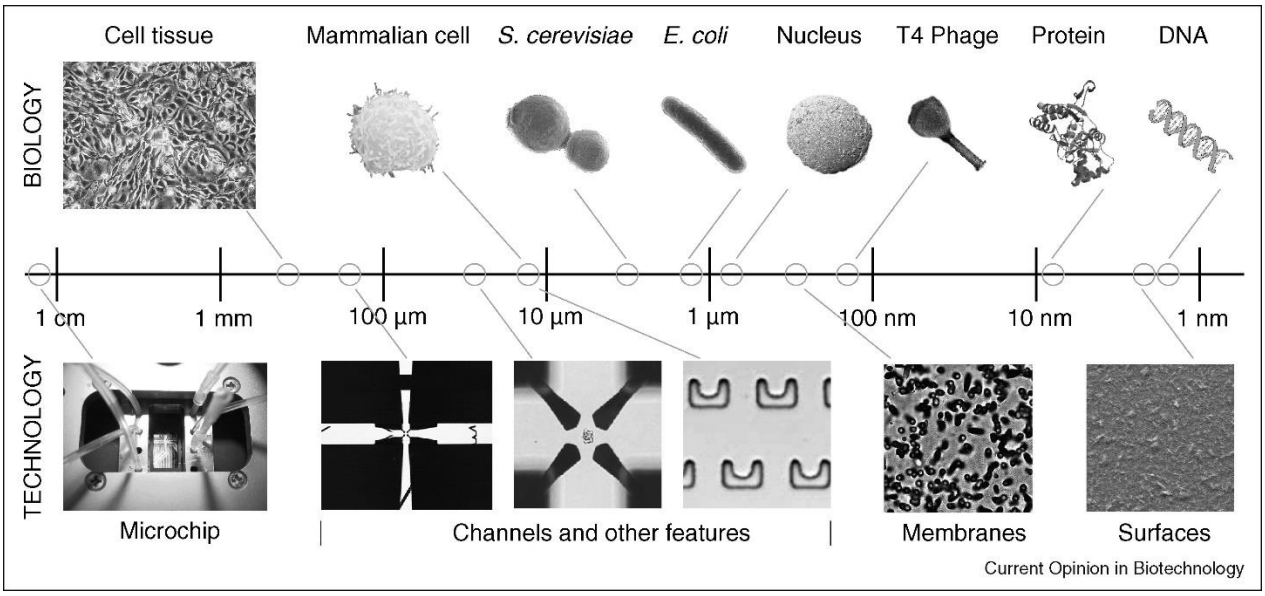

Figure 1-1. Figure of varying cell sizes and the technology the correlating technologies available for cell analysis.[4]

While bulk population averaging requires a large sample volume (e.g. mL's), studying cells on the individual-cell level has been extremely challenging in the past due to the extremely complex composition and small sample volume of a single cell (~ a few picoliters for a single mammalian cancer cell). The majority of single cell analysis techniques were developed on relatively larger cells (e.g. plant cells or embryos) (**Figure 1-1**).[5] However, in the past decade, advancements in instrumentation have made single-cell analysis (SCA) feasible using a variety of bioanalytical techniques. In this work, we will explore the various single cell analysis techniques, with an emphasis on single cell mass spectrometry as that is the technique explored in the upcoming chapters and is one of the most widely-used techniques for single cell analysis high resolution mass spectrometers are capable of extracting information from a variety of compounds simultaneously from a small sampling volume.

1.1 Bioanalytical Techniques for Single Cell Analysis

Single cell analysis techniques can be grouped by which part of the cell is being studied. For example, DNA sequencing and microarrays are traditionally used for the study of genes (i.e., epigenomics and genomics) and transcriptomics at the single-cell level. Mass spectrometry (MS) and protein arrays are used for proteomics, and single-cell metabolomics is characterized using MS and nuclear magnetic resonance (NMR).[6] Other techniques for SCA include microfluidics, spectroscopy, and flow cytometry. As technology advances, the sensitivity and selectivity of each method is improving to give us more information about cellular heterogeneity in a seemingly homogenous cell population.

1.1.1 DNA Sequencing.

DNA sequencing on the single-cell level has important implications in the biomedical community since genes associated with diseases, such as cancer or hereditary illnesses, can be discovered for earlier treatment.[7] These techniques often stem from Sanger sequencing, first implemented in 1977 for the determination of a bacteriophage genome. Sanger sequencing creates multiple copies of the sequenced region, up to ~900 base pairs, by combining the sample with primer, DNA polymerase, and labeled nucleotides in a test tube, heating the mixture to denature the DNA strand, and cooling the newly-created single-stranded DNA so that the primer can bind to it. Once the primer is bound, the mixture is again heated so DNA polymerase can use the primer to incorporate nucleotides until one of the labeled nucleotides is added, which will create a fluorescent base. This process of denaturing, annealing, and extending DNA is known as polymerase chain reaction (PCR).[8] Repeating this cycle ensures that the labeled nucleotides are incorporated into the DNA fragments, and each fragment will have different lengths, ending at the DNA sample initially added into the test tube. Capillary gel electrophoresis can be used to analyze the fragments of different masses since larger masses will move more slowly than smaller fragments, and a fluorescence detector can be used to determine which nucleotide was incorporated into each individual fragment.[9,10]

Genomic DNA from individual eukaryotic cells was first sequenced in 1999 using fluorescently-labeled cells to ensure only one cell was pipetted from the original bone marrow sample, followed by amplification using polymerase chain reaction (PCR) and fluorescence detection to describe regions of the DNA responsible for cancer.[11] DNA sequencing for single molecules via real-time sequencing by a single DNA polymerase

was first achieved by Turner et al in 2009.[12] Instead of using the traditionally-used fluorescent nucleotides that have difficulty incorporating into consecutive positions, which makes real-time analysis impractical, Turner et al utilize a fluorophore that phospholinked into the DNA terminus. The group also adds a zero-mode waveguide nanostructures to aid incorporation by minimizing the volume of observation, which allows for higher concentrations of labeled nucleotides to be used, speeding up the reaction.[12] DNA sequencing at the single-cell level can provide useful information of genetic variants and gene evolution.

1.1.2 Flow Cytometry and Microarrays for SCA.

Flow cytometry is another biochemical method of analysis that involves fluorescence. The sample is exposed to a laser, enabling a readout based on the way in which each cell reflects the light. This technique can be used to separate cells based on their heterogenic properties.[13] Since cellular heterogeneity is a main consideration for SCA techniques, this method is extremely important. It can also be used in conjunction with other techniques to explore heterogeneity at the single-cell level, using MS instead of a fluorescence detector.[14]

A pitfall of flow cytometry is the inability to monitor states before and after laser stimulation, which could alter cellular properties. In addition, the flow cytometer creates significant background noise that could interfere with analyte. To combat these issues, microarrays were introduced in 2005 to measure the amount of intracellular calcium (Ca^{2+}), an important part of the signaling pathway. The polystyrene microarray chip was fabricated to include over 200,000 microchambers 10 μm wide, 12 μm deep, and 30 μm high. Because each chamber is so small, each microchamber can accommodate only

one cell. The fluorescence of each cell was recorded using a microarray scanner, creating a high throughput method for the analysis of many different individual cells simultaneously.[15] Microarrays have been utilized for the single cell analysis of both mammalian and plant cells.[4,6,16,17]

1.1.3. Raman Spectroscopy.

Raman spectroscopy has high spatial resolution (< 1 μm) and does not require any labeling, so it is a good technique for the visualization of cells.[18] Additionally, minimal sample preparation is required since this technique is based on the measurement of photons emitted from samples due to Raman scattering of a light source, such as a laser.[19] Raman spectroscopy has been utilized to characterize the phase in the cell cycle from individual cells or discriminate amongst cell types.[20] Since this method can distinguish between different types of cells, it may be helpful in the future for sorting patient-derived cells. This technique can also be used to study drug-cell interactions since the Raman band intensities will change after the cell is treated.[21] However, current Raman spectroscopy-based single cell measurement methods are not compatible with suspension cells, so cells must be attached to substrates. This sample preparation could change the Raman spectra and give misleading information about the cell.

1.1.4. Microfluidics.

Microfluidics are being increasingly characterized for single cell analysis techniques as the channels are often similar in size to a single cell (~10 μm in diameter) and the chips handle small sample volumes (nL to pL).[22] Microfluidics need to be

coupled with various detection techniques for cell analysis. In 2011, Dochow et al. combined microfluidics with Raman spectroscopy to classify various tumor cells.[23] This could be beneficial to studies in both areas of research since the microfluidic chip allows for the analysis of cells in solution and Raman spectroscopy allows for the analysis of unlabeled compounds. A large number of microfluidic applications on the single cell level have been reported, including the correlation of heavier cells with faster growth rates and characterization of gene or protein expression.[24–30] Although many different detection techniques can be potentially integrated with microchips, a downfall to microfluidic techniques is that they are traditionally coupled to fluorescence detectors, limiting the amount of information that can be obtained simultaneously and requiring labeled samples.[31] However, microfluidic chips can be further developed in conjunction with mass spectrometry to give more molecular information about cellular content in a label-free manner.

1.2 Single Cell Mass Spectrometry Techniques

Single cell mass spectrometry (SCMS) approaches are being increasingly characterized for their ability to identify a wide range of compounds simultaneously in a label-free manner. In general, mass spectrometry (MS) experiments utilize an ionization method (e.g., matrix assisted laser desorption/ionization (MALDI), laser, electrospray ionization (ESI), and electron ionization (EI)), a mass analyzer (e.g., quadruple, time-of-flight (TOF), Fourier-transform ion cyclotron resonance (FT-ICR), and Orbitrap) to filter out neutral species and separate compounds based on their mass-to-charge ratio, and a detector (e.g., electron multiplier, Faraday cup, and mass analyzers based on the

measurement of image current). MS continuously scans a wide mass range, and it utilizes a compound's mass-to-charge ratio to determine its identity.

SCMS methods can be broadly grouped, based on their sampling and ionization environment, into non-ambient (vacuum-based) or ambient techniques. Non-ambient techniques, such as matrix-assisted laser desorption ionization (MALDI) and time-of-flight secondary ion mass spectrometry (TOF-SIMS), require a vacuum environment for sampling and ionization. For example, MALDI has been used to profile molecular components from a variety of single cells, including bacterial cells, frog embryos, plant cells, and mammalian cells.[32–38] Vacuum-based techniques have been used to revolutionize the '-omics' studies, especially peptidomics, proteomics, lipidomics, and metabolomics.[2,6,39–45] These methods have high detection sensitivities, but they also require sample pretreatment, making these methods incapable of real-time analysis or analysis of live cells from a native environment.

Ambient MS methods have been adapted for the analysis of samples in a near-native environment. Ambient techniques can be broadly grouped into microprobe extraction and laser desorption/ionization methods. Microprobe extraction techniques may either use a large probe that encapsulates the cell before being lysed for analysis or use a smaller probe that penetrates the cell membrane and extracts information from the inside. They have been used for the analysis on a variety of cell types, including frog embryos, onions, stem cells, and mammalian cancer cells.[31,46–59] Extraction methods stem from live-video single cell mass spectrometry developed by Masujima's group.[58] Laser desorption/ionization methods have primarily been used to study embryos, but have also been used to analyze oocytes, plant cells, and mammalian cells.[42,60–76]

Additionally, there have been other ambient techniques created for the analysis of cellular compounds at the single-cell level, including separation techniques (e.g. capillary electrophoresis (CE)) or ion mobility mass spectrometry.[60,77–79]

1.3 Single-probe Mass Spectrometry

The Single-probe MS technique is an ambient technique that falls under the microprobe extraction category and is most similar to live-video mass spectrometry. The Single-probe is a microscale sampling and ionization device that can be coupled to a mass spectrometer for studies in multiple research areas. It consists of dual-bore quartz tubing that is transformed into a sharp tip (<10 µm in diameter-similar to the size of an individual cell) using a laser puller. A capillary is placed into each bore: one that will connect to a conductive union and one that is flame-pulled to function as a nano-ESI emitter. The other side of the conductive union is connected to a longer capillary that connects the probe to the sampling syringe. To be conveniently used in the experiment, the Single-probe is attached to a glass slide and secured into a flexible arm clamp on a home-built stage for analysis. The dual-bore probe allows for real-time analysis of intracellular metabolites and drug compounds. As solvent flows through the tip, a liquid junction is formed. Cellular contents are extracted towards the nano-ESI emitter through a self-aspiration process and then ionized for MS analysis. Two digital microscopes are used to monitor the position of the nano-ESI emitter and cell penetration by the Single-probe tip.[46]

The Single-probe MS technique has been modified and utilized for multiple applications, including MS imaging (MSI) to map the spatial distributions of molecules on tissues, analysis of extracellular content from multicellular spheroids, and detection

of intracellular compounds from algal and adherent mammalian cells.[46,48,80–88] In later chapters of this work, we expand the Single-probe MS technique to include the analysis of non-adherent cancer cell lines and quantification of drug compounds from individual cells, including non-adherent cells and cells derived from the urine of bladder cancer patients.[89,90]

1.4 Quantitative Single Cell Mass Spectrometry (qSCMS)

The quantification of molecules on the single-cell level has the potential to enhance our knowledge of biochemical processes or pathways, drug efficacy, or metabolism and revolutionize the standard of care by creating more individualized treatment plans. While there have been a number of qualitative SCMS techniques developed, quantitative MS measurements at the single-cell level is a relatively new field.

Quantification of single cells began with semi-quantitative techniques before progressing onto quantitative methods of analysis. These semi-quantitative techniques compare ratios of an internal standard to see how a compound has changed (i.e. increased or decreased) upon treatment.[91–95] To date, there are very few reports of absolute quantifications of molecules;[66,96,97] however, in chapters 4-6, we report the absolute quantification of drug compounds from individual mammalian cancer cell lines.

1.5 Future Perspectives

Single cell analysis techniques are continually being developed to enhance our understanding of cellular processes since we know studying disease states begins fundamentally at the single-cell level. Due to the heterogeneous composition of cells in

tumors, some tumors may even contain different types of cells, such as cancerous and healthy cells in their masses. Therefore, single cell analysis methods are needed to fully conceptualize these mechanisms of action. As these methods are becoming commercialized, we are learning more about biochemical processes, including drug metabolism, drug-drug interactions, and drug-cell interactions. While there is still a large gap in knowledge, single cell analysis techniques are providing more accurate information that could be useful in increasing our standard of health in the future.

Chapter 2 : Integrated Cell Manipulation Platform Coupled with the Single-probe from Mass Spectrometry Analysis of Drugs and Metabolites in Single Suspension Cells

2.1 Introduction

Human biology, especially disease biology, is increasingly understood to be the result of activities on the level of individual cells, but the traditional analytical methods, such as liquid chromatography mass spectrometry (LCMS), are generally used to analyze samples prepared from populations of cells, whereas the acquired molecular information cannot accurately represent the chemical processes on the individual-cell level. These standard, traditional methods are unable to discern the effects of cellular heterogeneity on an analytical measurement, and the process of destroying and mixing the cells to prepare the lysate potentially leads to the alteration or loss of cellular components.[2,98] These limitations of traditional methods are especially important in the analysis of patient cells, in which the obtained samples can contain a complex mixture of many different cell types. To overcome these deficiencies, single cell molecular analysis methods, including single cell mass spectrometry (SCMS) methods, are increasingly being developed and applied to bioanalysis, especially of cellular metabolites and low molecular weight biomolecules.[42,99]

The first SCMS techniques developed use vacuum-based techniques to perform the analyses under non-ambient conditions.[2,39,43,100–104] Non-ambient SCMS techniques are capable of analyzing cellular lipids and metabolites, but require sample pretreatment under artificial conditions, and therefore are not suitable for real-time analysis. The sample preparation process for non-ambient analysis includes the addition of matrix

components, and this preparation can alter cellular components from their natural environment.[69] Therefore, ambient mass spectrometry (MS) techniques, which do not require a vacuum for the sampling environment, are utilized to analyze cells in a near-native environment. Not having a vacuum environment allows for versatility in the experimental design; cameras can be added to monitor the cellular process and softer ionization techniques can be combined with separation techniques to receive better information from each single-cell experiment.[31,42,46,47,49,52–61,63,64,67–74,77–79,105–108]

The Single-probe SCMS method is an ambient technique that analyzes live, mammalian cancer cell lines in a near-native environment.[46,84,87,90,109] In addition, the Single-probe device has been used for other mass spectrometry applications, including analysis of extracellular molecules in multicellular spheroids and MS imaging of tissues.[48,80,82,83,85,86] However, since cell immobilization on substrates is required for this method, suspension cells cannot be directly analyzed using this technique.[99,110] Therefore, the Single-probe SCMS system could not be directly used to sample non-adherent single cells, such as non-adherent cell lines or suspension cells isolated from a patient's blood or other bodily fluids.[111]

In this work, an integrated cell manipulation platform (ICMP) is coupled with the Single-probe SCMS technique to analyze live, suspension cells on-line with minimal sample preparation (**Figure 2-1**).[90] The ICMP consists of an inverted microscope to monitor cell selection, a glass cell-selection probe, a microinjector to capture individual floating cells, a heated plate to maintain cellular temperature, two cell manipulation systems to control spatial movements of both the glass cell-selection probe and Single-probe, and a digital microscope to observe cell transfer from the cell-selection probe tip

to the Single-probe tip. The fabrication of the Single-probe is detailed in previous publications and will not be addressed here.[46,48] The ICMP/Single-probe system is coupled to a high resolution mass spectrometer. This integrated setup allows for the sampling of identified single cells from complex biological samples with minimal effects from matrix molecules.

2.2 Methods

2.2.1. Glass Cell-Selection Probe Fabrication

Convert single-bore glass tubing into a tapered probe with a sharp tip. Place a single-bore glass tube (ID: 0.3 mm, OD: 1.1. mm) into the clamps of a vertical pipette holder, centering the glass with respect to the heating coil and tighten to secure the tube in place. (The heating coil is comprised of an 18-gauge nickel-chromium resistance wire (~60 mm in length) coiled around a metal rod (diameter = 3.90 mm) 2.5 times.) Set the glass tubing with temperature program 19.5 (manufacturer's unit). Set the solenoid plunger at 4 (manufacturer's unit) and trigger the solenoid to pull the glass tubing. This step creates two probes fused at the tip. Use tweezers to cut ~1 mm away from the tip of each probe, creating an orifice of ~10 µm in diameter at the probe tip.

Bend the glass probe for easy coupling to the ICMP/Single-probe SCMS setup. Set a pulled glass probe into the microforge, positioning the tip ~3 mm above the platinum heating wire. Turn the heat on the platinum wire to 30% of the maximum temperature and bend the probe ~45° from the original position (**Figure 2-2**).

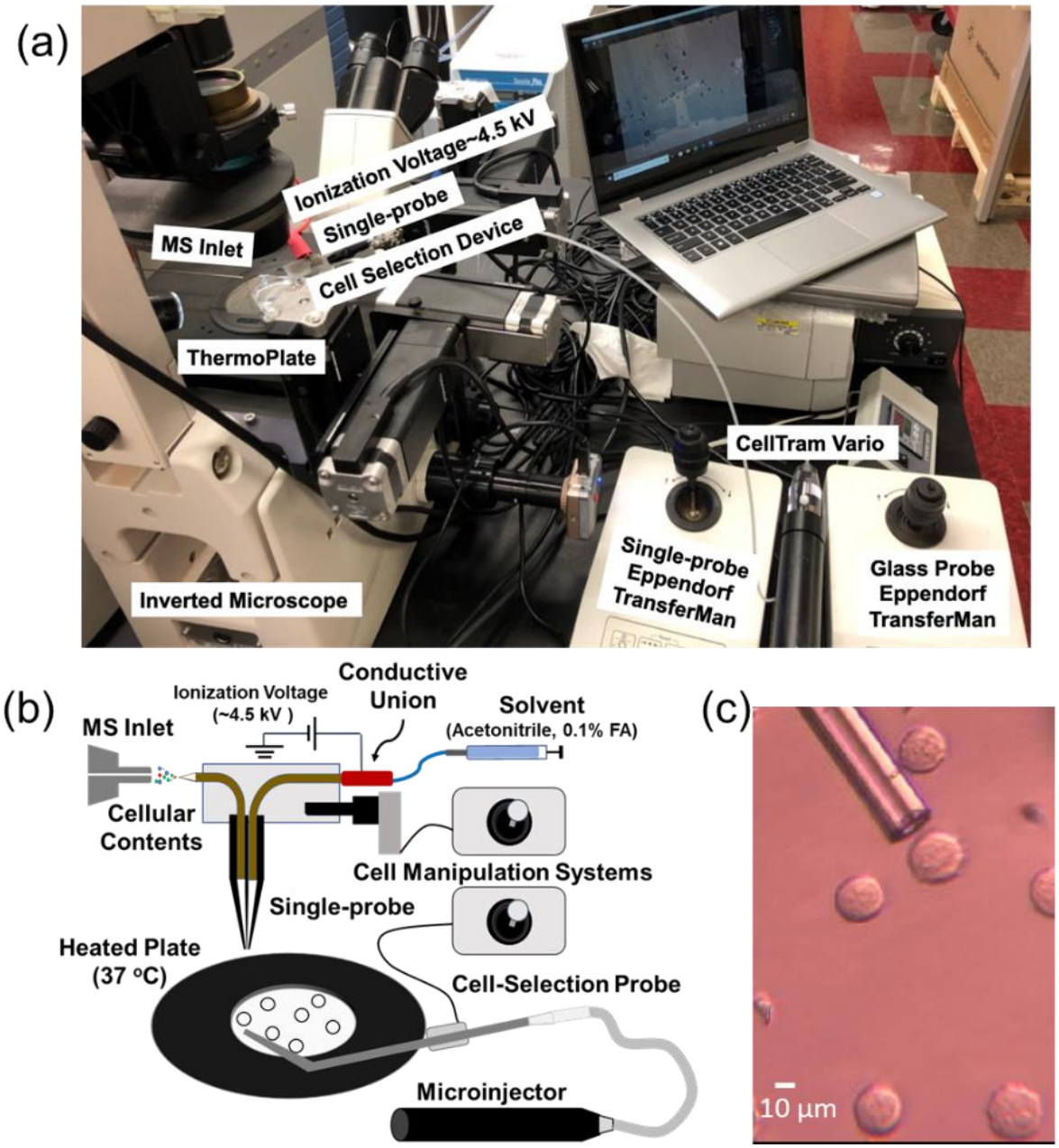

Figure 2-1. Experimental setup for the single suspension cell MS experiments. (A) The integrated cell manipulation platform (ICMP) coupled with a mass spectrometer. (B) Schematic for analysis of suspended cells. (C) Experimental view of K562 cells to be selected using the cell-selection probe. Reprinted with permission from Standke et al.[90] Copyright 2019 American Chemical Society.

2.2.1 Integrated Cell Manipulation Platform Assembly

Place the inverted microscope, microinjector, and two cell manipulation systems on a motorized table for easy coupling with the mass spectrometer. Modify one of the cell manipulation systems to accommodate a Single-probe by replacing the end with an arm clamp. Use a plastic syringe with a needle to fill the microinjector with mineral oil. Avoid bubbles in the tubing as this will affect suctioning. Replace the stage insert of the inverted microscope with the heated plate. Set the heated plate at 37°C prior to analysis.

2.2.2 Set up the glass cell-selection device.

Insert the glass cell-selection probe inside the metal holder of the microinjector by placing the long (non-bent) side into the capillary holder and tightening the screw to secure the probe in place. Position the probe tip's angle parallel to the heated plate.
CAUTION: The glass probe is very sharp and fragile, and it breaks easily. Protect your eyes and be extra cautious while inserting the probe into the microinjector. Secure the metal holder of the microinjector into the cell manipulation system. Position the probe tip near the middle of the inverted microscope light.

2.2.3. Create an Extended Ion Transfer Tube for the Mass Spectrometer Inlet

Use a metal cutter to cut a piece of stainless-steel tubing (OD: 0.0625 (1/16) in, ID: 0.021 in) ~250 mm in length. Measure 135 mm from the end and place a metal feral so ~135 mm will be exposed to the atmosphere and ~115 mm will be inside the mass spectrometer. Secure the feral using two wrenches to tighten it.

2.2.4. Couple the ICMP with Single-probe Setup

Secure the glass slide containing the Single-probe into the arm clamp of the cell manipulation system. NOTE: Single-probes are fabricated according to a previously-published protocol[48] with two minor changes in the current study: the nano-ESI emitter is made longer for easy coupling to the mass spectrometer, and the Single-probes are glued to the glass side on the right-hand side to avoid interfering with the spatial movement of the glass cell-selection device (**Figure 2-2**). Connect the solvent-providing capillary to a conductive union by placing the capillary into the sleeve (1/16 x .005 in) of the plastic ferrule and finger-tightening the fitting. Connect the other side of the conductive union to a capillary (ID: 40 µm, OD: 150 µm), which is connected to a syringe containing the sampling solvent, by placing the capillary into the sleeve (1/32 x .007 in) and tightening the fitting. Acetonitrile with 0.1% formic acid is utilized as the sampling solvent in these experiments. NOTE: The sampling solvent is flexible, but it should primarily contain acetonitrile (or acetonitrile with formic acid for better ionization) for a rapid microscale cell lysis.

Secure the syringe into the syringe pump on the mass spectrometer and place the ionization voltage cord onto a copper wire attached to the conductive union. Then, position the nano-ESI emitter ~ 1mm to the orifice of the extended ion transfer tube. Use the cell manipulation system to control the spatial movements of the Single-probe and position the nano-ESI emitter centrally in front of the extended ion transfer tubing.

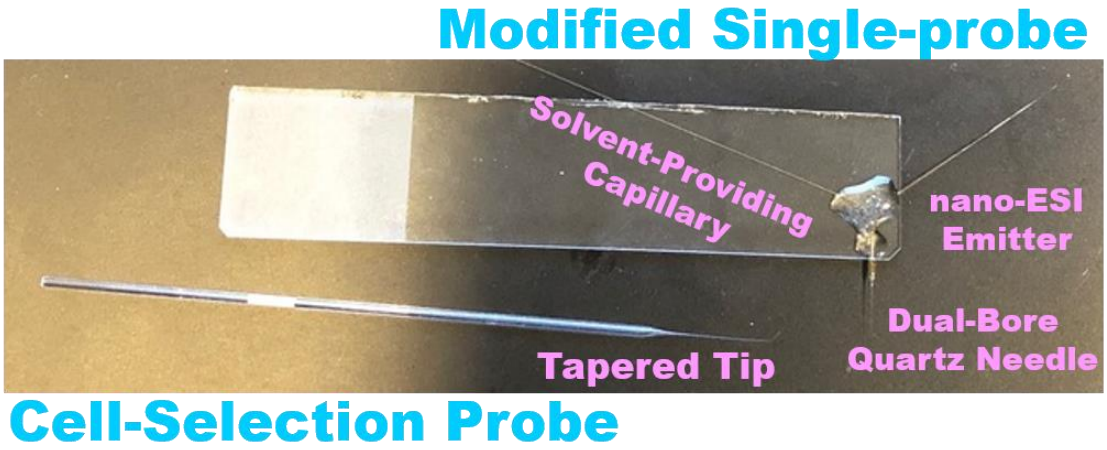

Figure 2-2. Photo of a modified Singe-probe and a cell-selection probe utilized for single suspension cell MS experiments.

2.2.5. Suspended Cell Sample Preparation

The day before analysis (~18-24 h), seed out cells for testing in a cell culture flask (T25). K562 human myeloid leukemia cells are used as models in this study. Heat 1X phosphate buffered saline (PBS) and Roswell Park Memorial Institute (RPMI) medium supplemented with 10% synthetic fetal bovine serum (FBS) and 1% penicillin-streptomycin at 37°C for 30 min. Seed out ~1x10^6 cells in a total volume of 10 mL by combining cells with warm medium. In general, use a 10-mL pipette to place 8 mL of RPMI medium into a cell culture flask. Then, use a 2-mL pipette to put 2 mL of confluent K562 cells the medium for ~1x10^6 cells. Incubate the cells at 37°C and 5% CO_2 until analysis.

Prepare cells for analysis. Pipette cells from the cell culture flask into a 15-mL centrifuge tube. Spin cells down at 400 x *g* and 37°C for 5 min and discard the supernatant. Resuspend cells in 4 mL of RPMI medium containing the drug compound at

the desired treatment concentration. NOTE: For analysis of control cells, resuspend the cells in 4 mL of RPMI medium or PBS and place into the lid of a small Petri dish for analysis. Incubate the cells for the duration of the treatment time at 37°C and 5% CO_2. Spin cells down at 400 x *g* and 37°C for 5 min. Aspirate the supernatant. Cells are resuspended in 10 mL of PBS, and centrifuged at 400 x *g* and 37°C for 5 min. After spinning, discard the supernatant. Repeat this step 3 times to minimize detection of drug from extracellular constituents. Resuspend cells in 4 mL of PBS for analysis.

2.2.6. Perform SCMS Measurements using the ICMP/Single-probe Setup

Customize parameters for the mass spectrometer for the experiment. Under the *Scan Mode* heading of the instrument software, select “Define Scan.” Use a resolution of 60,000 m/∆m at *m/z* 400, 1 microscan, 100 ms maximum injection time, and automatic gain control (AGC) on. A mass range (*m/z*) of 100-1000 was utilized for the experiments. NOTE: Parameters can be modified based on the instrument model. Under *Syringe Pump*, select a flow rate of 150 nL/min. NOTE: Flow rate needs to be optimized for each experiment. Select *NSI Source* and apply a voltage of ~4.5 kV.

NOTE: This parameter also needs to be optimized for each experiment.

Prepare the ICMP for analysis. Turn on the inverted microscope (with 40X magnification selected for both the top plate and bottom lens) and connect it to the USB-port of a laptop to capture live-video feeds. Turn on the heated plate and set it to 37°C. On the computer, go to the *Acquire Data* tab, and select “Continuously” under “Acquire Time.”

Prepare sample for analysis. Pipette 2-3 mL of sample into the lid of a small Petri dish (35x12 mm), positioning the sample in the center of the light from the inverted microscope on top of the heated plate.

Prepare the glass cell-selection probe for analysis. Use the cell manipulation system to move the probe so its tip is focused under the inverted microscope in the same plane as the cells.

Select an individual cell for analysis. Use the cell manipulation system to move the cell-selection probe tip to a targeted cell. This process is monitored using the inverted microscope. NOTE: If the tip of the cell-selection probe cannot be focused in the same plane as the cells, it is possible that the bent part of the probe is not appropriately angled, so adjust the position of the cell-selection probe until both probe tips can be focused along with cells under the microscope.

Gently turn the handle of the microinjector to adjust the position of the mineral oil inside the tubing. A gentle suction is provided by the microinjector to secure the targeted cell to the cell-selection probe tip. NOTE: If the cell cannot be captured by the cell-selection probe through the suction force, check the cell-selection probe to ensure it is fully-inserted into the capillary holder. In addition, inspect the mineral oil levels in the microinjector and tubing, and expel air if there is any.

Use the cell manipulation system to move the cell at the cell-selection probe tip to the Single-probe tip, using a digital microscope focused on the Singe-probe tip to monitor this process. When touching, a small acetonitrile droplet at the Single-probe tip induces a rapid lyses of the cell, and then cell lysate is immediately ionized for on-line MS analysis. NOTE: Because the selected cell is secured to the cell-selection probe tip through a

gentle suction, this cell can be potentially detached during its transfer to the Single-probe tip. Therefore, if ion signals of typical cellular lipids (see **Representative Results**) are not observed within 5 s, it is possible that the cell became unattached, and the selection of a different cell is needed.

2.3. Representative Results

First, untreated K562 cells are used to establish the experimental method. In a typical SCMS experiment, obvious changes of mass spectra can be observed from transferring a cell, during the detection of cellular contents, and after finishing the measurement (**Figure 2-4**). Three common cellular lipid peaks (phosphatidylcholine, PC), including PC(34:4) (*m/z* 754.536), PC(36:4) (*m/z* 782.567), and PC(38:5) (*m/z* 808.583), are monitored to ensure the cell is successfully transferred and cellular contents are detected[46,84,90,112,113] (**Figure 3-3**). If lipid peaks are not seen within 5 s, the mineral oil level in the microinjector is altered to reduce the suction holding the cell at the cell-selection probe tip; caution needs to be taken so that no mineral oil is pushed out from the cell-selection probe. The identity of many PC's in the mass range of *m/z* 750-850 are confirmed using MS/MS on untreated cell lysate samples (**Figure 3-1, Figures A1, A2, Table 2-1**).[90]

Table 2-1. Identified cellular components using the ICMP/Single-probe setup.

Drug Molecule*	***m/z***	**Mass Error (ppm)**
$[Gemcitabine + H]^+$	264.0760	11.32
$[Taxol + Na]^+$	876.3183	2.74
$[OSW\text{-}1 + Na]^+$	895.4448	0.89
Cellular Lipids	***m/z***	**Mass Error (ppm)**
$[PC(34:4) + H]^+$	754.5353	3.71
$[PC(34:3) + H]^+$	756.5512	3.44
$[PC(34:2) + H]^+$	758.5689	0.66
$[PC(36:5) + H]^+$	780.5514	3.07
$[PC(36:4) + H]^+$	782.5677	2.17
$[PC(36:3) + H]^+$	784.5846	0.64
$[PC(38:7) + H]^+$	804.5505	4.10
$[PC(38:6) + H]^+$	806.5674	2.48
$[PC(38:5) + H]^+$	808.5829	2.72
$[PC(38:4) + H]^+$	810.6007	0.00
$[PC(40:7) + H]^+$	832.5825	3.12

*The detection of all drug compounds was confirmed by comparing the MS/MS results with the standard compound.

K562 cells are also subjected to treatment with various drug compounds to expand the versatility of the method. K562 cells are incubated with gemcitabine (1 μM) and taxol (1 μM) for 1 h and OSW-1 (100 nM, 1 μM) for 4 h and 2 h, respectively. Cells are then washed with PBS to minimize the detection of drug compounds from extracellular content. The contribution of matrix (e.g. ions from cell culture medium, PBS, and solvent) to mass spectra of cellular contents can be eliminated through data subtraction, due to their significantly different ion signals (**Figure 2-3**). All three drug compounds are detected using the ICMP/Single-probe MS setup (**Figure 3-4**).[90] These results suggest this method can be used to study intracellular lipids, drugs, and metabolites on the single-cell level from cells in solution in a near-native environment.

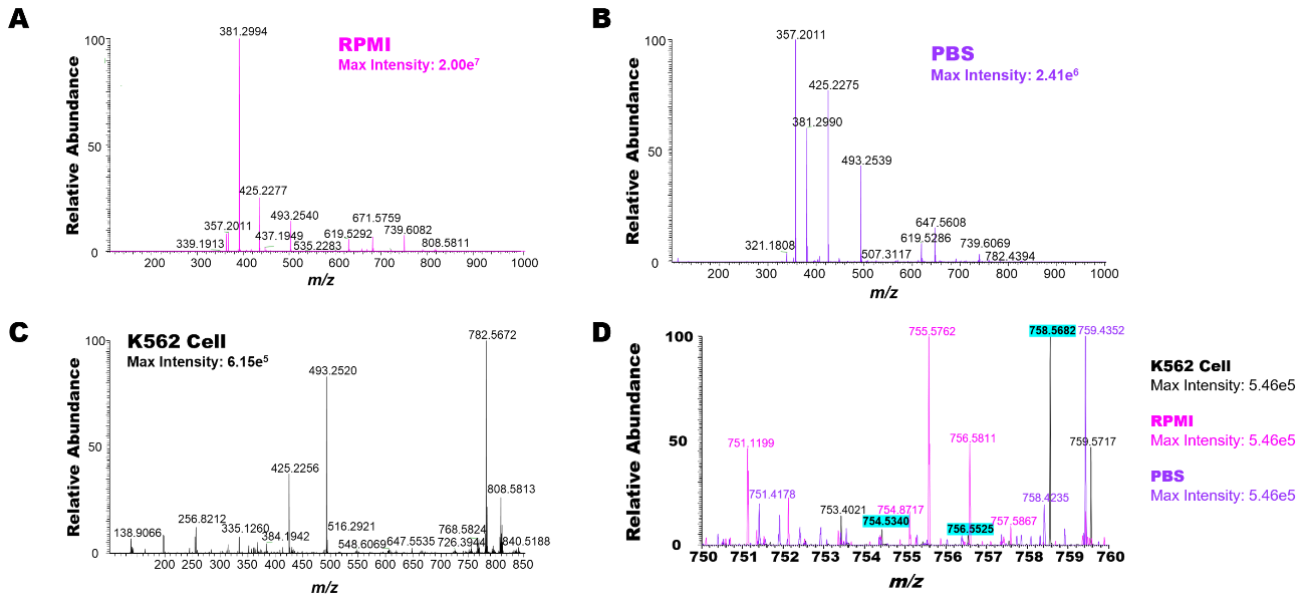

Figure 2-3. Mass spectra of (A) RPMI cell culture medium, (B) PBS, and (C) an individual K562 cell. (D) A zoomed-in region (m/z 750-760) of the combined three spectra (manually combined) from an individual K562 cell, RPMI media, and PBS showing the differences among them, indicating the identified PC species (highlighted) from the cell can be clearly distinguished.

2.4 Discussion of Results

The integrated cell manipulation and analysis platform is constructed to expand the versatility of the Single-probe MS method, allowing for on-line, rapid analysis of non-adherent cells in a near-native environment. A major advantage of the technique is that minimal sample preparation is required, so the cells are analyzed in conditions that mimic their standard state. Particularly, individual cells of interest can be visually identified and selected, minimizing the influence of matrix effect on MS ionization efficiency while maintaining cells in their natural environment, so the results are more representative cells' native status (**Figure 2-3**).

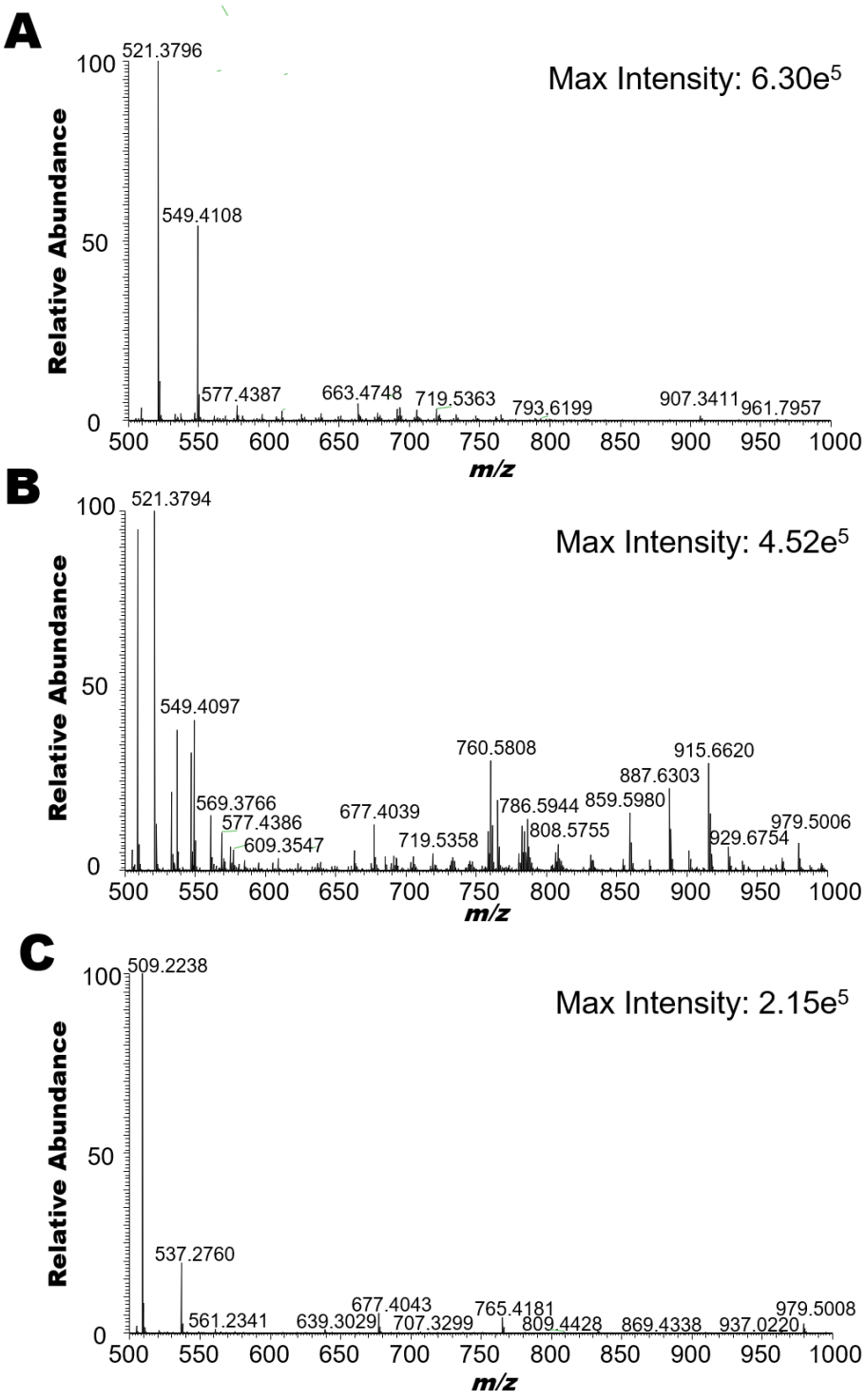

Figure 2-4. The zoomed-in mass spectra (m/z 500-1000) showing changes of ion signals (A) before analysis of a cell, (B) during acquisition of the cell, and (C) after cell analysis using the suspended cell platform.

This technique can be potentially used to study patient cells suspended in biofluids in future studies. Another advantage of this technique is the flexible selection of the sampling solvent. It is important to include acetonitrile as the main sampling solvent so that microscale lysis can occur rapidly. Potentially, internal standards (e.g. isotopically-labeled drug compounds) can be added into the sampling solvent for quantification of molecules of interest (e.g. drug molecules) from individual cells, including those can play a key role in revolutionizing personalizing drug treatments in the future.[111]

Although this integrated system can be conveniently used to analyze broad ranges of cells, a limitation of the method is that neither the Single-probe nor cell-selection probe is commercially-available; dictating the need for optimization of many parameters (e.g. flow rate, voltage, length between the nano-ESI emitter and ion transfer tubing, etc.) prior to each experiment. In addition, due to the smallness of the Single-probe and cell-selection probe, environmental perturbation (e.g. air flow) may result in difficulties establishing a junction between the two probes. A short-term solution is the bending of the cell-selection probe close to the end to minimize the length of tapering. Future work includes the development of a housing to enclose the critical parts of the setup to minimize environmental effects. Due to the limited amount of cellular contents and short acquisition time (~2-3 s) from a cell, MS/MS analysis can be only conducted for relatively abundant species. Other factors influencing the detection sensitivity include the suppressed ionization efficiency due to the introduction of matrix along with the cell and potential ion loss through the extended ion transfer tubing.

*The materials in **Chapter 2** are adapted from an article just accepted in *JoVE* April 2019.

Chapter 3 : Mass Spectrometry Measurement of Single Suspended Cells using Combined Cell Manipulation System and the Single-probe Device

3.1 Introduction

Liquid biopsy samples from patients, such as blood plasma, saliva, urine, or fine needle aspiration, are a complex milieu of different types of individual cells, and therefore any bioanalysis of the multi-cellular patient sample would likely be extremely heterogenous.[114] Moreover, patient-derived cells are typically converted into lysate and then analyzed using a bulk sampling technique, such as liquid chromatography mass spectrometry (LCMS). However, bulk analysis masks cellular heterogeneity, and the cellular characteristics, metabolites, and responses to drug administration in an abnormal subpopulation would be mixed with signals from healthy cells.[14,115] A better approach would be to focus the bioanalysis on the individual patient cells levels, but the limited volume of an individual cell (i.e., ~1-3 picoliters),[5] along with spectral interferences from sampling medium, make analysis on the single-cell level extremely challenging. Additionally, many cellular bioanalytical methods, including some single cell methods, require complex sample preparation prior to measurement.[116] Extensive sample preparation, including cell attachment and detachment, centrifugation, and changes to the cellular environment can alter cellular metabolites and morphologies.[98] Therefore, a rapid, real-time analysis is necessary to study cells in a near-native state.[14,115] Advancements in instrumentation over the past decade have allowed single cell analysis (SCA) to become increasingly popular as a means to characterize heterogeneity that is

unable to be accounted for using bulk sampling techniques. Current methods of SCA include flow cytometry,[4,6,16,17] microfluidics,[25,31] RNA sequencing,[117,118] and mass spectrometry (MS) methods of analysis.[2,4,99,119]

Single cell mass spectrometry (SCMS) is becoming popular due to its label-free approach and ability to detect broad ranges of analytes, including lipids, peptides, and metabolites.[69,99] SCMS can be characterized into two groups, ambient and non-ambient analysis, according to their sampling and ionization environment. Non-ambient techniques are vacuum-based and require sample pretreatment, while ambient techniques are often performed in a near-native environment with minimal sample preparation. A pitfall of non-ambient SCMS techniques is the inability to study live cells in real time in normal cellular environments. Changes to the cellular environment could alter cellular metabolites. Thus, a number of ambient SCMS techniques have been developed for the measurement of live mammalian cells. These techniques analyze cellular contents obtained from individual cells using micro-probe extraction[31,46–48,50–59,108,109,120] or laser desorption/ionization.[60–66,68,69,71–75,121] Among these ambient SCMS techniques, the Single-probe SCMS technique allows for real-time, *in situ* analysis of live cells, including mammalian and plant cells.[82,83,87,122–125] Microscale separation methods, such as capillary electrophoresis (CE), and post-ionization methods, such as ion mobility (IM)[99] have been coupled to MS to minimize spectral interferences during single cell analysis.[78,79] A prerequisite of many non-ambient SCMS techniques is the need for an immobilized substrate to secure cells, such as preparing a frozen, hydrated sample or utilizing micropatterned poly stencil film.[99] Because cellular metabolites are sensitive to the microenvironment, any perturbation, including cell attachment and changing culture

medium, may potentially affect the molecular composition inside cells. A bioanalytical method capable of rapidly measuring drug pharmacology on single cells isolated from patients under ambient conditions could be used to develop personalized drug therapeutic regimens tailored to the individual's response to a drug.[110]

SCMS techniques are often limited by the amount of content available from an individual cell. Single cells have a much smaller sample volume than bulk samples used in traditional analytical techniques, but still maintain extremely complex compositions without extensive sample pretreatment. For example, typical cultured mammalian cells contain only a few picoliters of solution (individual cell size ~10-20 μm in diameter), but it is estimated that more than 10^9 proteins and 10^{10} lipids are present in one single cell.[42] Limited amount and complex composition of cellular contents from individual cells lead to challenges generally present in SCMS studies, particularly for cancer cells with small sizes (e.g., ~10-13 μm).[54,70,106,126–130]

Despite the small sampling size of cultured cells, the Single-probe SCMS technique has demonstrated its success qualitatively with metabolic profiling in individual mammalian cancer cell lines. In addition, this technique has been used for other applications, including MS tissue imaging[28,30] and analysis of extracellular molecules inside live multicellular spheroids.[56,57] There are a number of advantageous features unique to the Single-probe SCMS technique, including versatile selection and composition of the sampling solvent, capabilities for real-time and *in situ* analysis, and potential compatibility with broad types of mass spectrometers. However, this technique was previously used only for analysis of cells on an immobilized substrate (e.g., on glass cover slips).

In this work, we report the development of an integrated cell manipulation platform (ICMP), which combines the Single-probe SCMS method with a single cell manipulation platform, to analyze individual, suspended cancer cells in real time in a near-native environment with minimal sample pretreatment. This new instrumental setup allows for the direct selection and analysis of individual cells present in their original complex matrices. Because matrix molecules in the sample solution are generally eliminated upon analysis, the matrix effect, which results in reduced ionization efficiency and detection sensitivity, is minimized. While **Chapter 2** focused on the methodology behind the ICMP, this chapter focuses on the versatility of the method and the potential impact that analyzing a variety of cell types from solution can have for various disease states in the future.

3.2 Experimental Setup

To conduct SCMS of suspended cells, this ICMP setup is coupled to a high-resolution Thermo LTQ Orbitrap XL mass spectrometer, and a Single-probe is used as the sampling and ionization device. This multifunctional cell manipulation system **(Figure 2-1)** consists of two Eppendorf TransferMan cell micromanipulation devices (to control spatial movements of both the glass cell-selection device and Single-probe), a Nikon Eclipse TE300 inverted microscope (for cell monitoring), and a Tokai Hit ThermoPlate system (to mimic the temperature of the cells' natural environment). A cell-selection probe, which is a glass tubing with a small tip size, is connected to a microinjector, which is coupled with one of the Eppendorf manipulation systems to capture target cells. The other Eppendorf manipulation system is modified to allow a Single-probe interface with the mass spectrometer via an extended ion transfer tube, which is used to replace the standard

one. Cells are randomly selected with the cell-selection device using a digital stereomicroscope, and then transferred to the Single-probe tip for real-time microscale lysis followed by MS analysis (**Figure 3-1**).

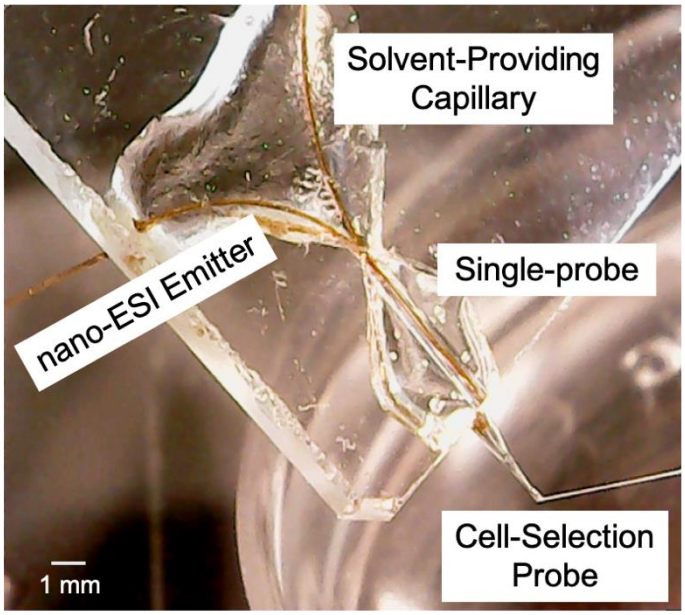

Figure 3-1. Transferring a live single cell from the cell-selection probe tip to the Single-probe tip. Solvent (acetonitrile) droplet created between the Single-probe and cell-selection probe induces a rapid microscale lysis of the cell followed by MS analysis. Reprinted with permission from Standke et al.[90] Copyright 2019 American Chemical Society.

3.2.1 Fabrication of the cell-selection probe

A single-bore glass tubing (ID: 0.3 mm, OD: 1.1 mm, RSC, Rochester, NY) was tapered to act as a cell-selection device (with a tip size ~15 µm) using a vertical pipette puller (KOPF, Tujunga, CA). To adapt this glass needle for the suspended cell setup, its tapering part was bent ~45° using a microscope microforge (MF-9, Narishige, Amityville, NY).

3.2.2. Single-probe fabrication

Single-probes were fabricated using a previously published protocol, so only a brief summary will be given here.[46] Dual-bore quartz tubing (Friedrich & Dimmock, Millville, NJ; OD: 500 µm, ID: 127 µm) was pulled into a sharp needle (OD ~ 5 µm) using a micropipette laser puller (Sutter, Novato, CA). Fused silica capillary (OD: 110, ID: 40 um) was inserted into one bore to act as a solvent-providing capillary. The same diameter capillary was flame-pulled and inserted into the other channel of the dual-bore quartz needle to act as a nano-ESI emitter. The probe was sealed using UV resin (Prime-Dent, Chicago, IL) and secured on a glass slide with Epoxy glue (Devcon, Hartford, CT) for easy coupling to the flexible arm clamp.

3.2.3. Sample preparation

For suspended cell experiments, K562 cells were utilized. K562 cells (ATCC, Manassas, VA) are derived from chronic myeloid leukemia. This cell line was chosen for its non-adherent culture conditions and relatively large size (~15-20 µm diameter) among all cancer cell lines.[131] K562 cells were maintained in T25 flasks at 37°C and 5% CO_2 in RPMI media supplemented with 10% FBS and 1% penicillin-streptomycin. Cells were seeded out at $5.0e^5$ cells per flask 24 hr prior to treatment and transferred to a 12-mL centrifuge tube for treatment with various drug compounds, including taxol, gemcitabine, and OSW-1. Prior to analysis, cells were pelleted at 500 RCF for 5 minutes at 37°C and washed with 10 ml of PBS (x3) to avoid detection of the drug compound from extracellular content. K562 cells were then resuspended with PBS (4 mL) for SCMS analysis.

For metabolomic analysis, K562 cells were seeded at $5.0e^5$ cells per flask 24 hours prior to treatment. 100-nM Taxol was added to one flask and left to incubate for 24 hours. Following the incubation, cells were directly analyzed using the integrated cell manipulation platform. A minimum of 22 cells were analyzed for each treatment condition.

3.2.4. Experimental parameters

Mass spectrometer. A Thermo LTQ Orbitrap XL mass spectrometer (Thermo, Waltham, MA) was utilized in positive ionization mode with an ionization voltage of +4.5 kV applied to the conductive union during analysis. Settings of the mass spectrometer used in experiments include 60,000 resolution (m/Δm) at *m/z* 400, 1 microscan, 100 ms maximum injection time, and AGC (automatic gain control) on. The mass range used was *m/z* 100-1500.

Coupling the integrated cell manipulation platform with the Single-probe mass spectrometry technique. To perform experiments on live suspension cells, the ICMP was positioned such that the Single-probe's nano-ESI emitter was centrally positioned at the inlet of the extended ion transfer tube. The solvent-providing capillary of the Single-probe was programmed to deliver solvent (acetonitrile with 0.1% formic acid (FA)) at a flow rate of ~150 nL/min. K562 cells (2 mL) were added to the lid of a 35x12-mm petri dish (Thermo, Waltham, MA) on top of the ThermoPlate, which was set to 37°C to maintain a living environment of cell. Cells in the petri dish lid were monitored using the inverted microscope. Once a cell of interest was determined, the cell-selection probe was moved adjacent the cell. A gentle suction was applied to the cell-selection probe by precisely manipulating the CellTram Vario. The captured single cell at the cell-

selection probe tip was then transferred to the tip of the Single-probe. A digital stereomicroscope was used to monitor the approach of the cell-selection probe tip towards the Single-probe tip for cell transfer. Once the cell-selection probe and Single-probe created a junction, the suction from the cell-selection device was released to transfer the cell into the solvent (acetonitrile) bridge at the tip of the Single-probe for in situ, real-time microscale cell lysis (**Figure 3-1**). The released cellular contents were carried by a continuous flow of the solvent and transported to the nano-ESI emitter for ionization and MS analysis.

A delay time between releasing the cell from the cell-selection probe and MS detection of cellular species was observed. For most experiments, ion signals of cellular contents were observed within 3 seconds after releasing the cell into the Single-probe tip. Ion signals for analyte from each individual cell usually lasts for around 3 seconds under optimized experimental conditions. However, this time length may vary depending on the individual cell volume, flow rate, and size of the solvent droplet formed between the tips of cell-selection probe and Single-probe.

3.3 Results

3.3.1. Optimization of ion transfer tubing length

Prior to coupling the ICMP with the mass spectrometer, the setup was tested using suspended HCT-116 and HeLa cells. The optimized tip size for the cell-selection probe was found to be ~50 µm (with the diameter of the orifice ~12 µm) to allow a gentle suction from the CellTram Vario without obviously changing the morphology of cells. To couple the integrated cell manipulation system to the Single-probe device and

the mass spectrometer, an extended ion transfer tube was used to replace the standard one equipped with the mass spectrometer. The length of the ion transfer tube was altered to give the best conditions for coupling the system to the mass spectrometer without sacrificing ion intensity since the signal from an individual cell can be similar to background (~$1e^4$). Using a flow rate of 1 µL/min, the total ion current was compared for the different ion transfer tubing lengths (100 and 135 mm) for an internal standard (50-nM deuterated-Irinotecan (m/z 587.28)) diluted with acetonitrile containing 0.1% formic acid. The total ion currents were $6.33e^8$, and $2.02e^8$ for the 100-mm, and 135-mm ion transfer tubing, respectively. However, signal was unable to be seen when coupling the transfer tubing with the Single-probe positioned above the ThermoPlate where the sampling solution is located due to the large gap between the emitter and mass spectrometer inlet. The gap was unable to be decreased due to the position of the instruments being coupled. Therefore, the 135-mm ion transfer tubing was utilized for further SCMS experiments. The total ion currents were compared between the 135-mm ion transfer tubing and the 20-mm ion transfer tubing utilized in previous Single-probe MS experiments. Using 50-nM standards of ^{15}N-gemcitabine (*m/z* 267.075) and d-OSW-1 (*m/z* 895.463) dissolved in acetonitrile, the analyte signal was tested for each compound. For the extended ion transfer tubing, the average relative abundance was $4.65x10^4 \pm 1.56x10^4$ compared to $3.98x10^5 \pm 2.28x10^5$ using the shorter ion transfer tube to test ^{15}N-gemcitabine. However, the higher-mass compound (d-OSW-1), more indicative of analyte extracted from cellular content, gave more similar abundances of $9.28x10^4 \pm 8.51x10^4$ and $7.45x10^4 \pm 4.18x10^4$ for the shorter and longer ion transfer tubing, respectively. The length of the optimized ion transfer tube (inner diameter: 410

μm) was found to be 250 mm with ~135 mm external part exposed to ambient conditions.

3.3.2. Optimization of ion transfer tubing heating parameters

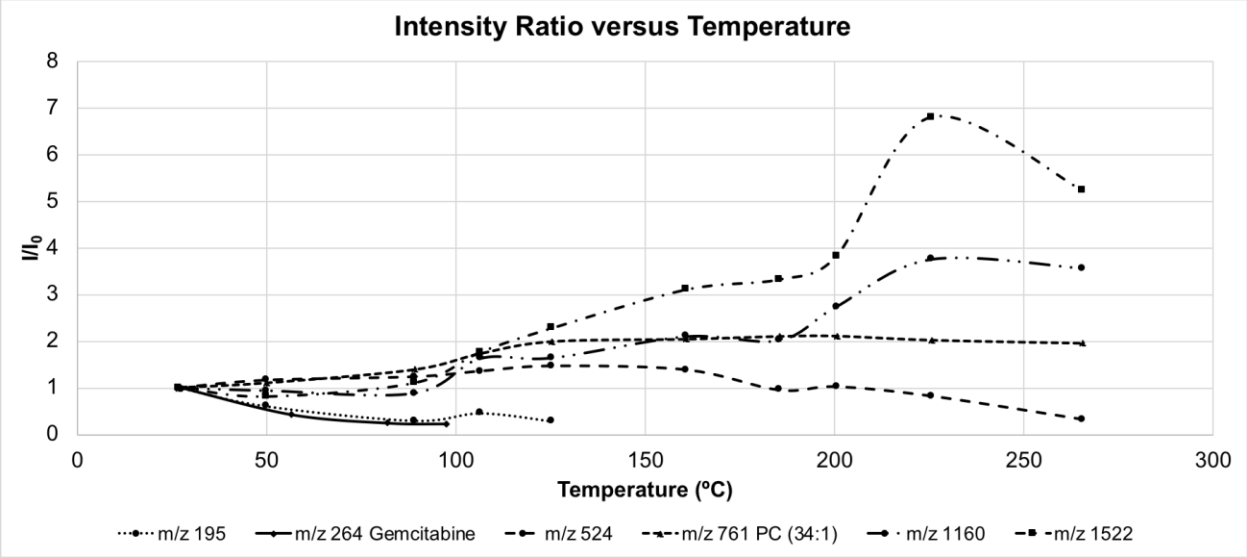

Figure 3-2. Graph depicting the temperature dependence on intensities for compounds of various masses. Reprinted with permission from Standke et al.[90] Copyright 2019 American Chemical Society.

To minimize the ion loss due to a longer ion transfer tube, experiments were performed to evaluate the effect of temperature of the extended ion transfer tubing on ion intensities (**Figure 3-2**). A heating coil with the temperature control unit was wrapped around the external part of the ion transfer tube, and the ion intensities of the standard calibration solution containing the drug compound was measured under a series of temperatures. In general, the ion signal intensities for analytes in higher mass ranges increased with increasing temperature and reached a maximum around 225°C. However, due to the breakdown of gemcitabine and cellular metabolites at elevated temperature (i.e., T > 100°C) the heating coil was not utilized for further experiments.

The ion transfer tube was wrapped with coiled fiberglass insulating tubing (MULTICOMP, Newark element14, Chicago, IL) and heated using a POWERSTAT Variable Autotransformer (Superior Electric Co, Bristol, CT). Temperature was measured using a 6802 II Digital Temperature Thermometer (Signstek, Wilmington, DE). Positive ionization mode calibration solution (Caffeine *m/z* 195, MRFA *m/z* 524, and Ultramark *m/z* 1322, 1422, and 1522) was supplemented with gemcitabine (*m/z* 264.077) and PC 34:1 (*m/z* 760.588) to give a broad mass range of analyte to monitor. A flow rate of 0.5 µL/min was used to continuously deliver solution to the tip for ionization using a voltage of 2.5 kV for direct injection. Signals for analyte under m/z 500 decreased as the ion transfer tubing was heated and were at or below noise level after heating the ion transfer tube past 100°C with no signal after 150°C.

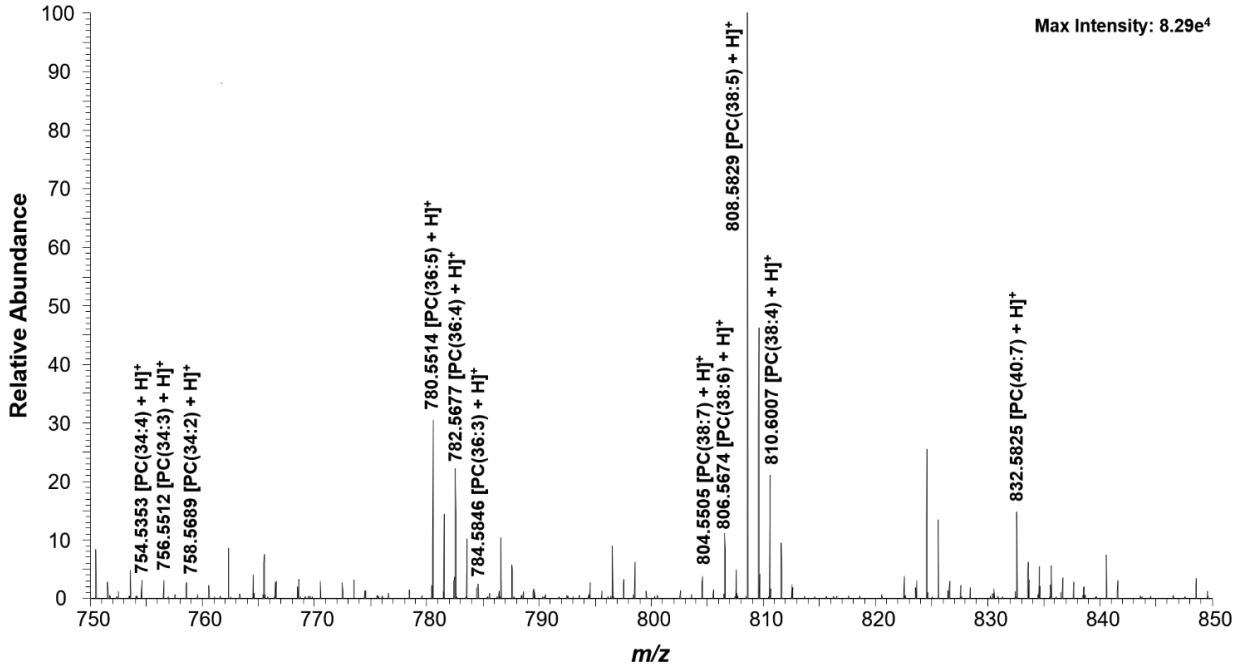

Figure 3-3. Zoomed in spectrum from a single cell showing the representative species (*m/z* 750-850). Structure confirmation of the labeled ions was performed through MS/MS analysis (**Figure A1**). Reprinted with permission from Standke et al.[90] Copyright 2019 American Chemical Society.

K562 cells in both control and drug-treated groups were subjected to the SCMS measurement. Three abundant cellular lipid (phosphatidylcholine (PC)) peaks (PC(34:4), PC(36:4), and PC(38:5) at m/z 754.536, 782.567, and 808.583, respectively (**Figure 3-3**)) were monitored throughout the experiment to ensure cells were transferred and analyzed.[112,113,122] These common species have been observed in our previous studies using adherent cell lines.[84,87,122]

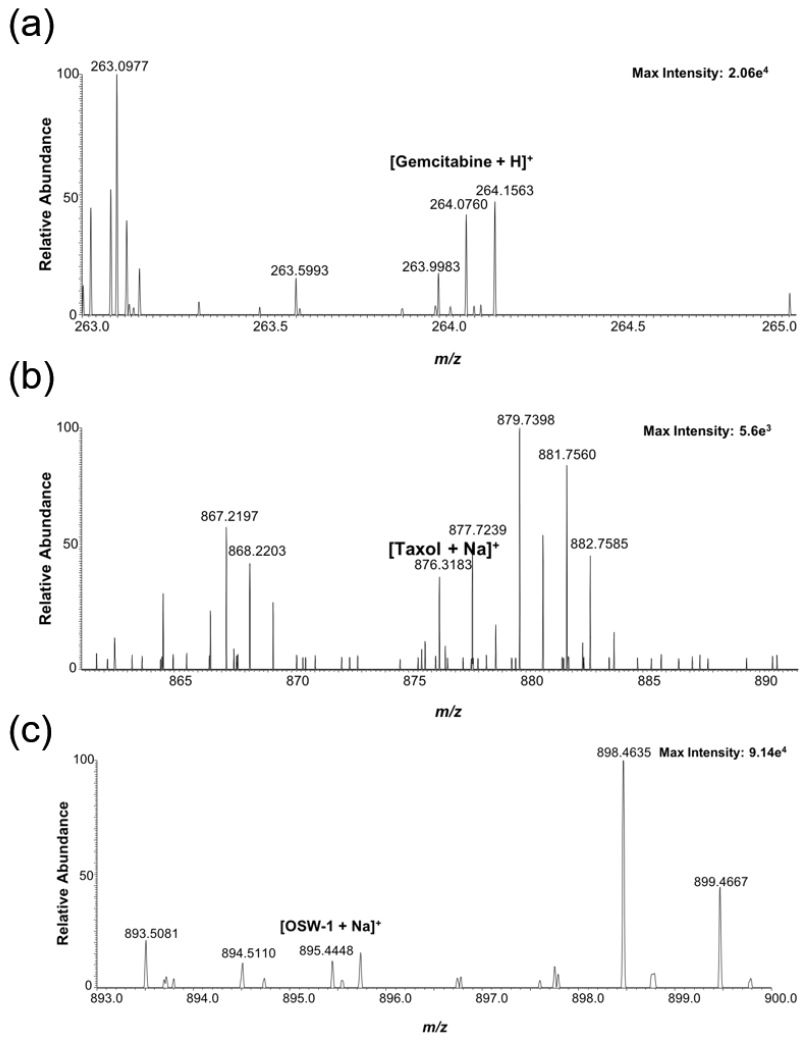

Figure 3-4. Mass spectra obtained from treating individual K562 cells with: (A) gemcitabine (1 µM, 1 hr) (B) taxol (1 µM, 1 hr) and (C) OSW-1 (100 nM, 4 hr). Reprinted with permission from Standke et al.[90] Copyright 2019 American Chemical Society.

K562 cells were subjected to treatment with various anticancer drug compounds (gemcitabine, Taxol, and OSW-1) to demonstrate the versatility of analyte that could be extracted from individual suspended cells. Gemcitabine (1 µM) and Taxol (1 µM) were incubated with cells for 1 hr. OSW-1 (100 nM and 1 µM) were incubated with cells for 4 hours and 2 hours, respectively. In addition to a large number of cellular metabolites, all three drug compounds were detected from individual cells (**Figure 3-2**, **Table 2-1**). The

drug compounds were unable to be detected in the PBS, in which the K562 cells were suspended or untreated cells (**Figure 3-4**), indicating that they were released from cells during cell lysis and not from the sampling solution.

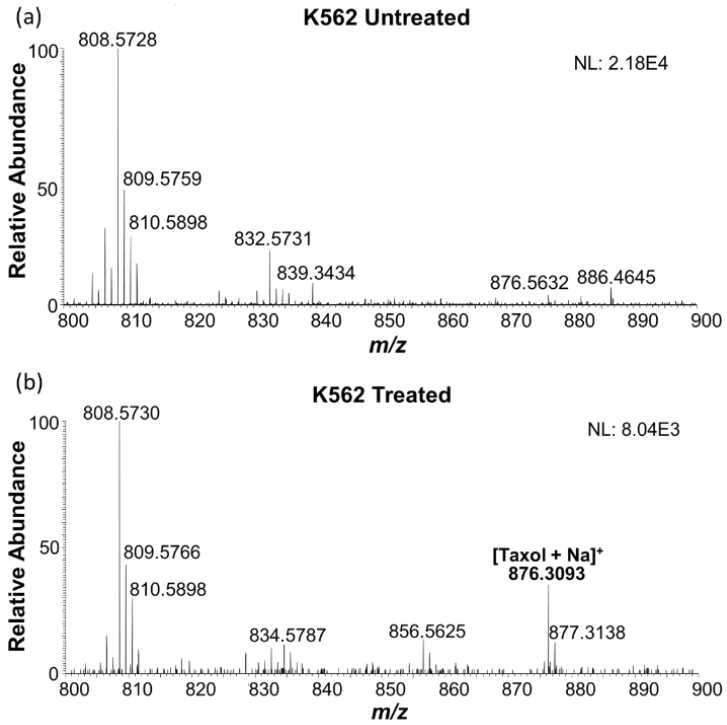

Figure 3-5. Zoomed-in mass spectra showing molecular profiles (*m/z* 800–900) for (A) untreated and (B) treated (100 nM Taxol for 24 hours) single K562 cells. Reprinted with permission from Standke et al.[90] Copyright 2019 American Chemical Society.

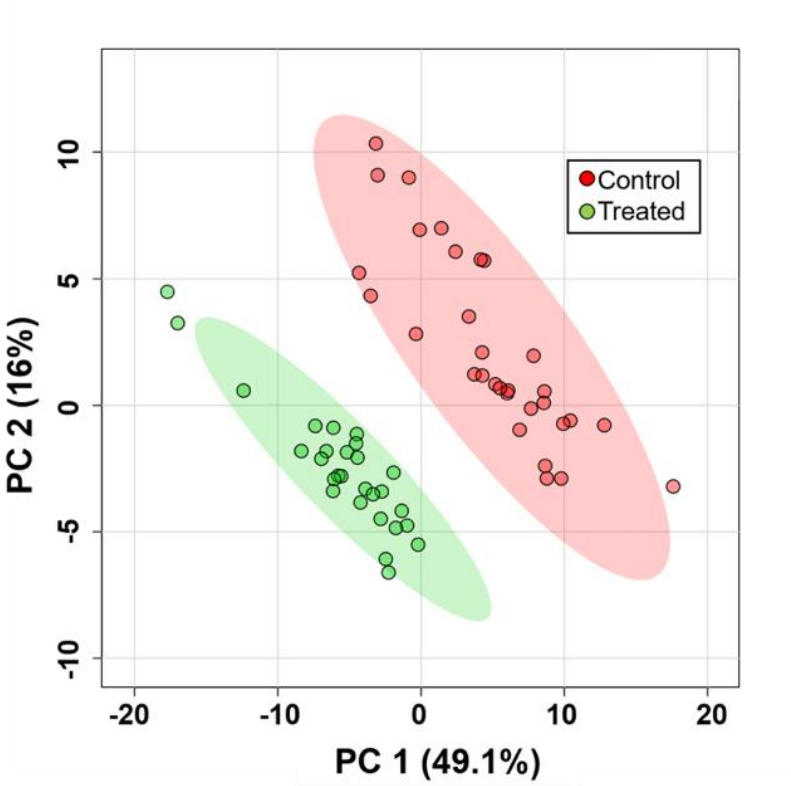

Figure 3-6. PCA showing the overall difference of metabolic compositions of single K562 cells in the control and drug treated (100 nM Taxol for 24 h) groups. Reprinted with permission from Standke et al.[90] Copyright 2019 American Chemical Society.

The ICMP coupled to the Single-probe SCMS was also utilized for the analysis of global metabolic changes in K562 cells following a 24-hour treatment with Taxol (100 nM). The SCMS data were subjected to pretreatment, including background removal, noise reduction, peak alignment, and intensity normalization using Geena2 prior to analysis using MetaboAnalyst.[132,133] Under our experimental conditions, the physiological profiles of cells were not significantly changed by drug treatment; however, their molecular compositions were drastically changed (**Figure 2-4**). Principle Component Analysis (PCA) was performed to illustrate the differences of molecular profiles of cells between control and treatment groups (**Figure 3-6**). In addition, the within-group spread of SCMS

data points in the PCA plot reflects the heterogeneity of cells in the same group.[134] In total, the abundances of 78 metabolites were significantly changed ($p<0.05$ from *t*-test) upon drug treatment. For further identification of compounds of interest determined from SCMS experiments, cell lysates were prepared using drug treated cells (100 nM Taxol for 24 hours) and subjected to the complementary MS/MS analysis. Monoglycerides (MG) and diglycerides (DG) comprised many of the significantly-changed metabolites. For example, upon treatment with Taxol, DG(44:6) is significantly down-regulated, while MG(16:0) and MG(18:0) are significantly up-regulated (**Figure A2**). These results illustrate a stark difference between these two groups, including multiple significantly up/down- regulated metabolites, which demonstrates the capability of this technology to identify global metabolic changes within individual, live suspension cells.

3.4 Conclusion

In summary, the Single-probe SCMS technique has successfully been coupled with an integrated cell manipulation platform for the analysis of suspended cells (K562) in solution. This integrated system allows us to observe and select individual cells suspended in solution. The selected cell is transported to the Single-probe tip, where a rapid single cell lysis occurs in an acetonitrile droplet. Released cellular contents are then immediately analyzed by a high-resolution mass spectrometer. More than 30 total cells were analyzed using this integrated SCMS system, and different cellular metabolites were found between treated and control cell groups. Complementary MS analysis of cell lysate can be performed for identification of species of interest obtained from the SCMS experiments.

This integrated system is suitable for the analysis of cells present in solutions, such as bodily fluids, with minimum sample preparation. The complex matrix is largely excluded from MS analysis by selecting a cell of interest for analysis with a probe not utilized for analysis, so minimal or no solution is extracted. With the ability to analyze small sampling volumes, it is feasible that the integrated cell manipulation platform can be used for rapid analysis of individual cells derived from patients *in situ*, which could allow for unprecedented personalization of drug administration.

*Safety Considerations***.** Both glass and silica capillaries pose a needle-stick hazard, so these items must be handled with caution. Standard safety protocols were enforced for the handling of chemicals and culturing and treating of cell lines.

3.5 Acknowledgements

The author would like to thank Mr. Devon H. Colby for his work in developing the integrated cell manipulation platform for analysis. Additionally, the author would like to thank Mr. Ryan C. Bensen for his work in preparing cell samples. This work is adapted with permission from *Analytical Chemistry*.[90] Copyright 2019.

Chapter 4 : Quantification of Drug Molecules in Live Single Cells using the Single-probe Mass Spectrometry Technique

4.1. Introduction

Single cell analysis (SCA) is transforming the biological sciences, making its greatest impact in the fields of neuroscience, immunology, and oncology, and it promises to enhance our understanding of individual cells in numerous other contexts.[42] Cell-to-cell heterogeneity dictates a multitude of functions for homeostasis and development of disease states. Since a cell is the basic unit of multicellular organisms, understanding functions of organisms in health and disease is aided by understanding cell heterogeneity and how it changes during these processes. Compared with the traditional methods that are based on the population-averaged studies, SCA can provide a more nuanced analysis of the underlying biological mechanics of the system being studied.[135] SCA encompasses a variety of analytical techniques, including single cell genomics (e.g., DNA and RNA sequencing), single cell transcriptomics, single cell fluorescent tagging, Raman spectroscopy imaging, and others.[6]

Single cell mass spectrometry (SCMS) is a nascent field that has gained great interest in broad areas of research.[2,42,106,136,137] Mass spectrometry (MS) is a versatile technique to simultaneously analyze a large number of molecules in a short period of time. Traditional MS approaches to cell analysis are restricted to a population of cells (e.g., cell lysate), where an averaged result is obtained. Recent advancements in high mass resolution MS have allowed for the confident identification of a large number of molecules,[138] and improved sensitivity enables MS to be applied at the single-cell level, mostly in the field of metabolomics,[57,76,120,137] and potentially even single cell

peptidomics[45,139] and proteomics.[91] Current SCMS techniques can be broadly categorized into two main approaches, non-ambient and ambient techniques, based on their sampling and ionization environments. Non-ambient techniques include matrix assisted laser desorption/ionization (MALDI) MS[100,119,140,141] and time-of-flight secondary ion MS (TOF-SIMS),[102,103] which are capable of high spatial resolution[43] for cellular and sub-cellular resolution analysis of the cell organelles.[39,101,142] However, non-ambient techniques require obligatory sample pretreatment and a vacuum sampling environment, which is not suitable for live cell analysis. Ambient SCMS techniques enable the study of single cells in their native conditions with little or no sample preparation, allowing live cells to be analyzed. Because cells' metabolites can rapidly change upon the variation of their environment, molecular information obtained from live cells has higher fidelity reflecting cell status.[91] Reported ambient SCMS techniques include laser assisted electrospray ionization (LAESI) MS, single cell capillary electrophoresis (CE) ESI MS, probe ESI MS, and live single-cell video-MS (live MS).[69]

Recently, we have introduced the Single-probe MS technique for *in situ* MS analysis of live eukaryotic cells in real time.[46,48,109] The Single-probe is an integrated micro-scale sampling and ionization device that can be coupled with a mass spectrometer for multiple applications. The Single-probe tip (~6-10 μm) is small enough to be inserted into single cells for direct liquid-microextraction of cellular contents followed by immediate MS detection. This technique has been used to analyze cellular metabolites of single cells, including cancer cells[48,80,85,86,90,109] and algae cells.[88] In addition, the Single-probe device can be used for other applications, including high spatial resolution ambient MS

imaging of biological samples[48,82,83] and analysis of extracellular molecules inside live multicellular spheroids.[87]

Discoveries in fundamental research as well as industrial and clinical applications often require reporting relative or absolute quantities of target molecules. Unfortunately, many of the existing spectroscopic[143] and MS methods cannot perform quantitative analysis on broad ranges of molecules. Over the last decade, researchers have devised various MS techniques to quantify analyte from prepared biological samples. Most metabolomics studies introduce an internal standard, such as a stable isotope-labeled compound, to aid in quantification by plotting relative intensities of the ion pairs to estimate the relative amount of target molecules. Although progress has been made in quantifying molecules from live single cells, quantitative analysis of species of interest at the single-cell level is still extremely challenging due to the limited amount of sample present in individual cells and a lack of sensitive bioanalytical techniques.

Semi-quantitative MS analysis has been performed using vacuum-based techniques. MALDI was used for one of the earliest reported quantifications of low molecular compounds, including the neurotransmitter acetylcholine and peptides from biological samples of interest.[92] Since then, MALDI-TOF and MALDI-MSI (MS imaging) have been explored for semi-quantitative analysis using stable isotope labeling, relative ratio comparisons, or mapping cellular images for quantitation at the single-cell level.[91]

Ambient MS techniques have also been developed at the individual-cell level. For example, the Masujima group reported relative quantification of molecules at the cellular level using live single-cell video-mass spectrometry to obtain a ratio of isotopically-labeled compound to the analyte for comparison with a standard curve of known labeled- to

unlabeled-compound ratios. Recently, label-free quantification of proteins in individual frog embryos was performed using ion currents to estimate concentrations using capillary electrophoresis micro-electrospray ionization (μ-ESI) for high resolution MS.[91] In addition, nano-ESI with electroosmotic extraction has been used to quantify the amount of glucose in onions,[66] and nano-DESI has quantified phosphatidylcholine from human cheek cells.[72]

New developments in label-free MS increase the feasibility of the methods for use in individualized chemotherapeutic regimens since one of the aims in metabolomics is quantitation of metabolites to evaluate changes in response to disease, treatment, and environmental and genetic perturbations. Successfully quantifying molecules (e.g. drug compounds) in single cells can potentially revolutionize fundamental research and clinical tests. In the present study, we employed the Single-probe SCMS technique to directly quantify the absolute amount of the drug molecule, irinotecan,[74] inside live single cancer cells.

4.2 Methods

4.2.1. Single-probe fabrication protocol.

The fabrication protocols of the Single-probe are detailed in our previous publications,[46,48,82] and only brief procedures are provided here. Single-probe fabrication utilizes a laser puller (P-2000 Micropipette Laser Puller, Sutter Instrument Co., Novato, CA) to evolve dual-bore quartz tubing (outer diameter (OD) 500 μm; inner diameter (ID) 127 μm, Friedrich & Dimmock, Inc., Millville, NJ, USA) into a sharp-tipped needle. A solvent-providing capillary (OD 105 μm; ID 40 μm, Polymicro Technologies, Phoenix, AZ, USA) and a nano-ESI emitter produced from the same fused silica capillary are embedded into the dual-bore quartz needle and sealed using UV curing resin (Light Cure

Bonding Adhesive, Prime-Dent, Chicago, Il, USA). To conveniently use the Single-probe in the experiment, the device is secured onto a glass slide using regular epoxy glue. The glass slide is then held by a flexible clamp holder (MXB-3h, Siskiyou, Grants Pass, OR) as shown in **Figure 4-1**. For SCMS experiments, the Single-probe tip is inserted into a cell, and the sampling solvent, which contains the internal standard, is continuously delivered into the cell through the solvent-providing capillary. The cellular contents are extracted by the sampling solvent and withdrawn by capillary action towards the nano-ESI emitter, where the extracted molecules and internal standard are immediately ionized for MS analysis (**Figure 4-1**).

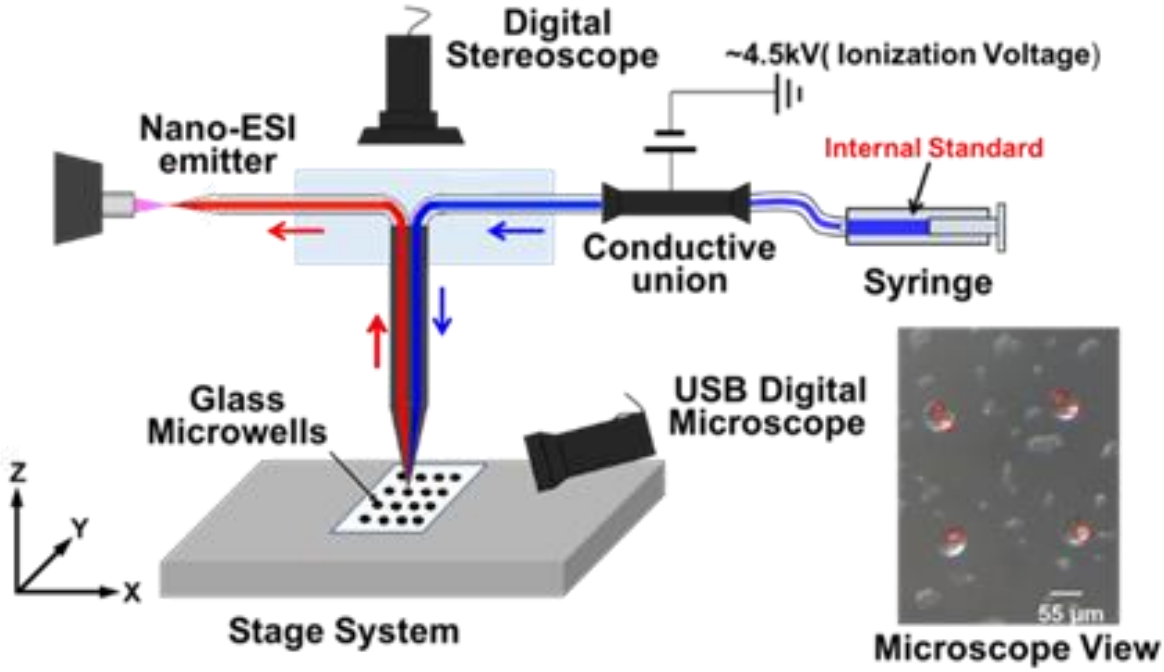

Figure 4-1. qSCMS experimental setup with individual cells highlighted in the microscopic image of glass microwells.

4.2.2. Glass chips containing microwells for qSCMS experiments.

In our qSCMS experiments, it is critical to extract the entire cellular contents and delivered solution of the internal standard, which are needed to derive the quantity of species of interest inside single cells. Custom glass microchips with microwells (radius: 55 µm, depth: 25 µm; Blacktrace Inc., MA) were utilized, in which cells were retained in microwells through overnight incubation prior to MS measurements (described in the following section). Single cells from wells are monitored using a top-view digital stereomicroscope (**Figure 4-1**).

*4.2.3. Cell sample preparation***.**

The adherent, mammalian cell lines used in these experiments included HeLa (cervical cancer) and HCT-116 (colon cancer), which were cultured using DMEM and McCoy's 5A media, respectively. Each media was supplemented with 10% FBS and 1% penicillin-streptomycin. Cell lines were passaged around 85% confluency.

Cell Preparation for qSCMS Experiments*.* For single-cell experiments, a glass microchip containing microwells was placed into each well of a 6-well plate. 400 µL of cell suspension (~150,000 cells) solution was added into 3.6 mL of cell culture medium for overnight incubation, allowing cells to be attached to the glass microchip.

For drug treatments, the growth media in the well was first aspirated. Then, an appropriate amount of irinotecan solution dissolved in complete media (media that contains FBS and penicillin-streptomycin) was added into the well containing the glass microchip with cells, adding 4 mL of solution to ensure the chip is fully covered (with final drug concentrations to be 0.1 and 1.0 µM), and incubating cells for different time lengths

(0.5 and 1 h). Cell-containing glass microchips were then rinsed with 5 mL of incomplete cell culture media (FBS- and penicillin-streptomycin-free media) to remove residual drug molecules on the cell and slide surfaces prior to measurement. Single cells retained in individual microwells (i.e., one cell per microwell) were selected for quantitative SCMS measurements.

Cell Lysate Preparation. The results obtained from our SCMS studies were compared with those from the traditional cell population analyses: LC/MS analysis of cell lysates. In the traditional LC/MS studies, the moles of analyte inside of a single cell were estimated by taking the total amount of analyte divided by the total number of cells. For cell lysate preparation, cells were cultured in 6-well plates under the same conditions as those used in the cell preparation for SCMS experiments as described in the previous section. To duplicate the cell growth environment in the SCMS experiments, a glass slide was placed at the bottom of each well for cell attachment. Upon finishing drug treatment, cells were rinsed using PBS (phosphate buffered saline) and detached from cell culture plate using trypsin. Cells were then transferred into 1.5-mL Eppendorf tubes and centrifuged to prepare cell pellets. One tube of cells was used to count the cell number. The remaining five tubes were used to prepare cell lysate samples through a solvent extraction approach, which was conducted by adding ACN(50%) / MeOH(50%) solution that contains the internal standard (i.e., deuterated-irinotecan) into each tube. Cell extraction was centrifuged, and the supernatant was withdrawn followed by drying. The dried samples were dissolved in 200 µL of ACN (12%):H_2O (88%), and then analyzed using a Waters nanoACQUITY UPLC (C-18 column) coupled to a Thermo LTQ Orbitrap XL mass spectrometer (Waltham, MA).

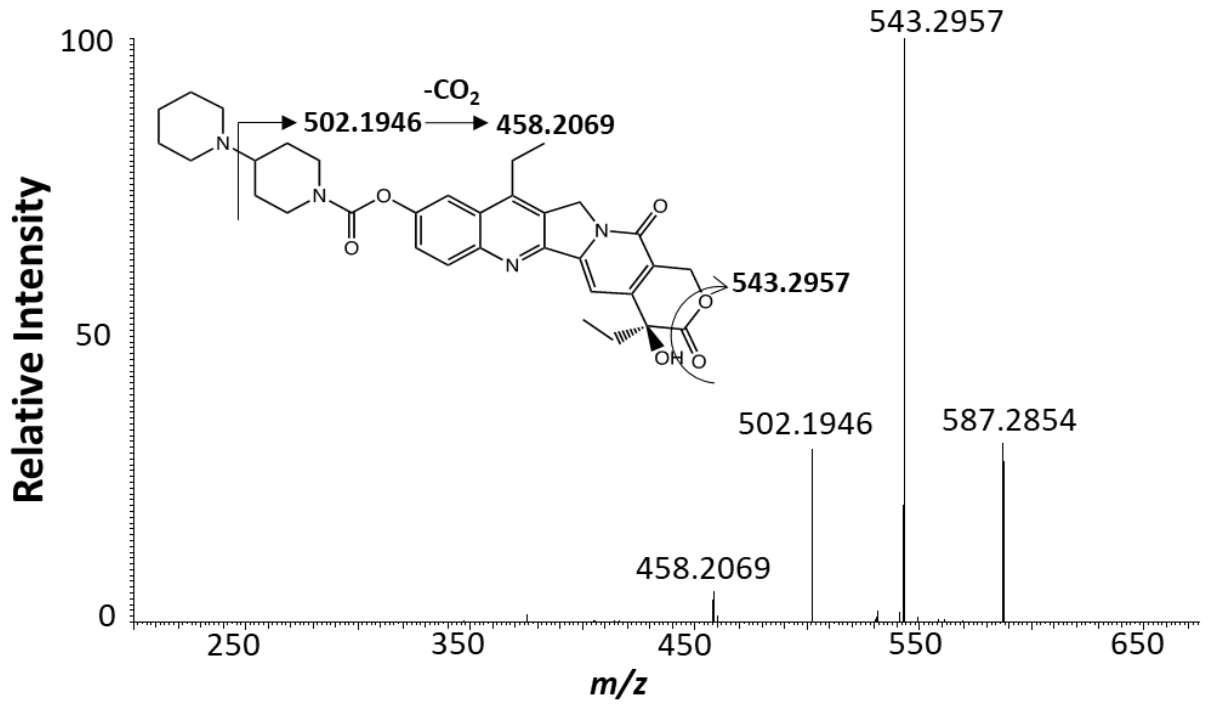

Figure 4-2. MS/MS of irinotecan from an individual HCT-116 cell.

*4.2.4. qSCMS experiments and data processing***.**

The qSCMS experiments were carried out using the same experimental setup with similar operation procedures as detailed in our previous publications,[46,48] and only outlined information is provided here. The Single-probe SCMS setup includes a Single-probe (attached to a glass slide), a digital stereomicroscope, a USB digital stereomicroscope, a computer-controlled XYZ-translational stage system, and a Thermo LTQ Orbitrap XL mass spectrometer (**Figure 4-1**). To conduct a quantitative SCMS experiment, the microwell slide containing cells is attached to the motorized XYZ-stage, and sample movement is controlled using the LabView software.[144] Upon finding a target cell in a microwell, the Z-stage is precisely lifted (0.1-μm increments) for cell insertion

monitored using microscopes. The sampling solution was prepared by adding the deuterated-irinotecan into methanol (50%)/water (50%), and it was continuously delivered using a syringe pump at a flow rate of ~25 nL/min; the actual flow rate needs to be optimized for each Single-probe device. To determine the optimal concentration of deuterated-irinotecan used in the experiments, a series of concentrations ranging from 10 nM to 1 uM were tested. 50 nM was selected as the optimized concentration of deuterated irinotecan because it provided ion intensities that were within ~10 times of the regular irinotecan, allowing for accurate quantitative MS measurements to be conducted within a relative narrow linear dynamic range. To eliminate any potential artifacts related to the selections of sampling solvent flow rate and internal standard concentration, we have carried out statistical analysis of results obtained under different conditions, and no significant difference was observed. MS analyses were performed using the following parameters: mass resolution 60,000 (m/Δm), 4.5 kV (positive mode), 1 microscan, 100 ms max injection time. For more confident identification of species of interest, MS/MS analyses were conducted using collision induced dissociation (CID) (**Figure 4-2**). MS/MS was performed to confirm the detection of both irinotecan and deuterated-irinotecan using following parameters: isolation width 1.0 *m/z* (± 0.5 *m/z* window) and normalized collision energy 20–35 (manufacturer's unit).

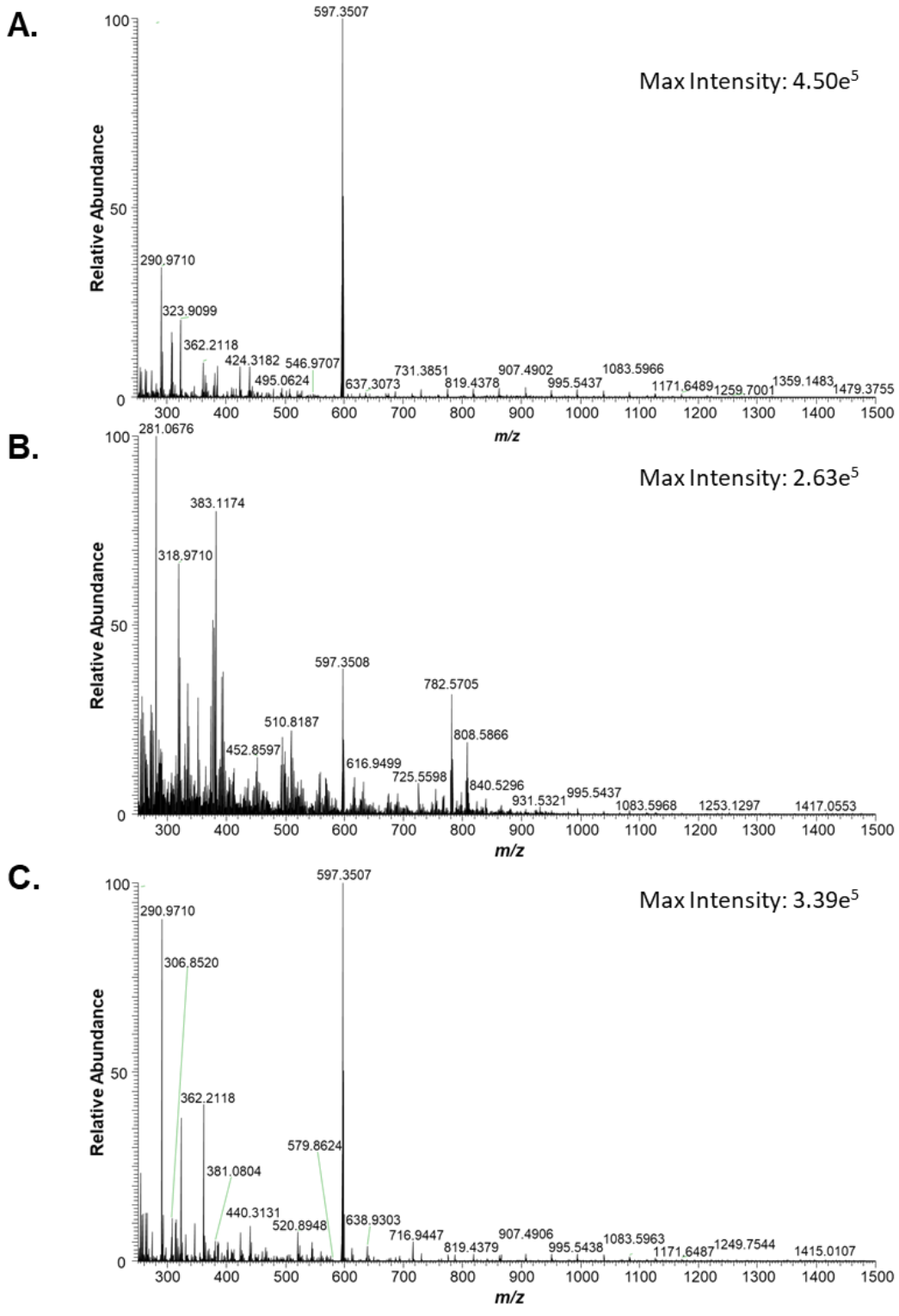

Figure 4-3. Spectra depicting ion signals (a) before cellular analysis, (b) during analysis, and (C) after analysis of an individual HeLa cell treated with irinotecan (100 nm, 1 h).

To quantify the total amount of irinotecan inside of live single cells, a comprehensive MS data analysis was carried out. The insertion of the Single-probe tip into an individual cell and extraction of intracellular molecules were confirmed from significant changes of mass spectra during the experiment: ion signals changed from the solvent background through the culture medium to the cellular metabolites (**Figure 4-3**). Particularly, for the drug treated cells, the ion signal of the regular irinotecan ($[C_{33}H_{38}N_4O_6 + H]^+$) was only observed after the cell was penetrated by the Single-probe, whereas the deuterated drug compound ($[C_{33}H_{28}D_{10}N_4O_6 + H]^+$) was continuously observed through the entire data acquisition time. We estimated the moles of irinotecan inside of live single cells (x) by taking into account multiple factors, including the integration of the ion intensities of the target molecule (∑A) and internal standard (∑B), the concentration of the internal standard (c), the flow rate of the sampling solution containing the internal standard (*v*), the MS data acquisition time (t) (**Equation 4.1**, **Figure 4-4**).

$$\frac{\Sigma A}{\Sigma B} = \frac{X}{c \cdot t \cdot v} \qquad \textbf{(Equation 4.1)}$$

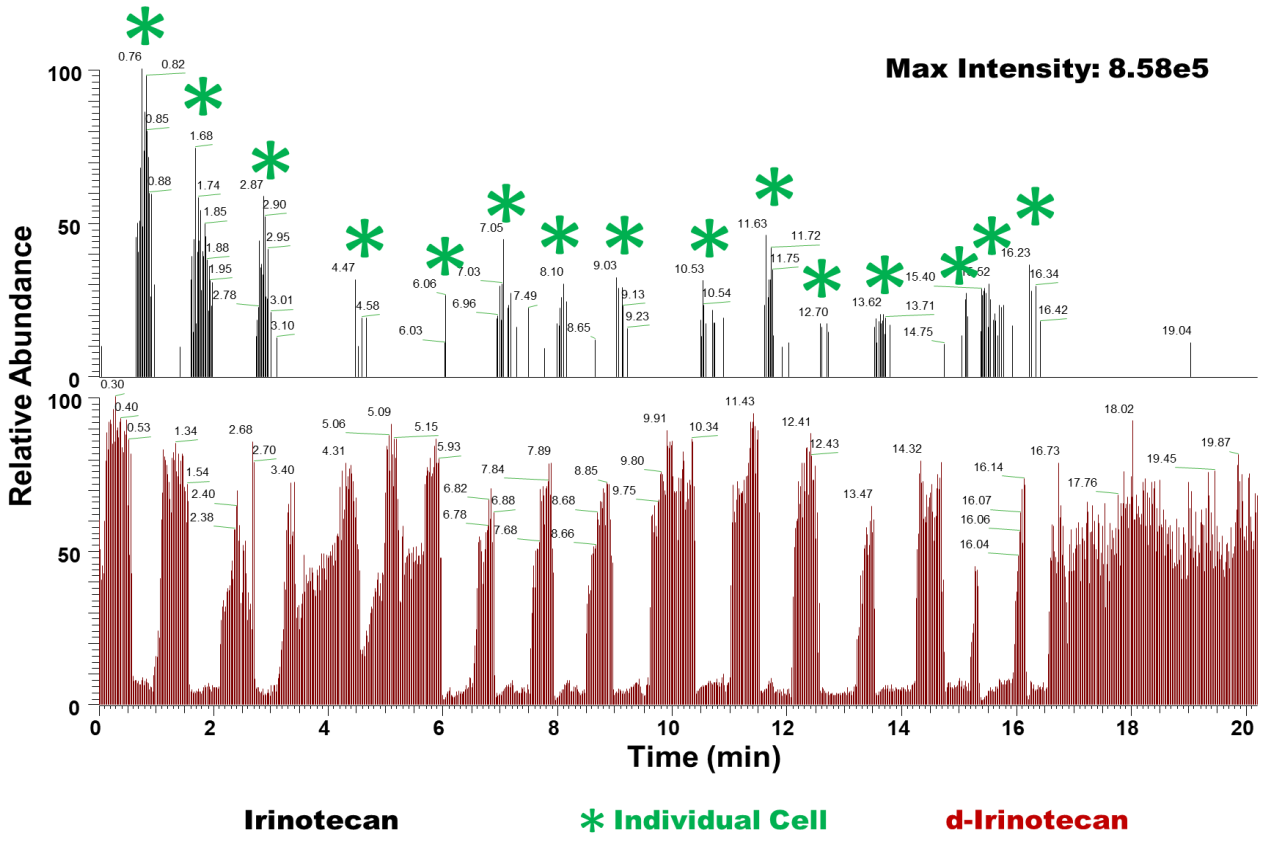

Figure 4-4. Extracted ion chromatogram for irinotecan (top) and d-irinotecan (50 nM) (bottom) depicting the time for drug signal from individual HCT-116 cells (100 nM, 1 h).

4.3 Results

4.3.1. Experimental Setup for Quantitative SCMS Experiments.

Previous Single-probe MS studies have qualitatively obtained the chemical profiles of a wide range of metabolites present in cultured mammalian cells.[46,82,83,109] Two major modifications were incorporated to the establish quantitative SCMS (qSCMS) capabilities. First, methodology for internal standard introduction was established. The unique design of the Single-probe allows for versatile compositions of sampling solvent to be used in the SCMS experiments. For example, reagents, such as dicationic compounds (2+ charged),

were utilized in our previous reactive SCMS experiments to detect molecular anions in positive ionization mode of the mass spectrometer.[109] In the current study, the isotopically-labeled drug compound (i.e., internal standard) at predetermined concentrations in the sampling solvent allows for the quantification of analytes present in the individual cells. The second major new experimental modification to the Single-probe SCMS method for quantitation is the use of glass microchips containing microwells for cell culture and analysis. Previous SCMS experiments were conducted using non-differentiated surfaces, such as glass microscope cover slides, to immobilize cells for convenient cell sampling. However, partial loss of cellular components through diffusion may occur during SCMS measurement. In the qSCMS experiments, only individual cells inside hemisphere microwells (radius 55 µm; depth 25 µm, Blacktrace Inc.) were selected (**Figure 4-1**), confining any potential analyte release to the well where the cellular compounds can be recaptured for analysis. Microscope-guided visualization of the Single-probe sampling individual cells in the microwell is performed until sampling the microwell contents cease to detect cellular ion signals in the MS data.

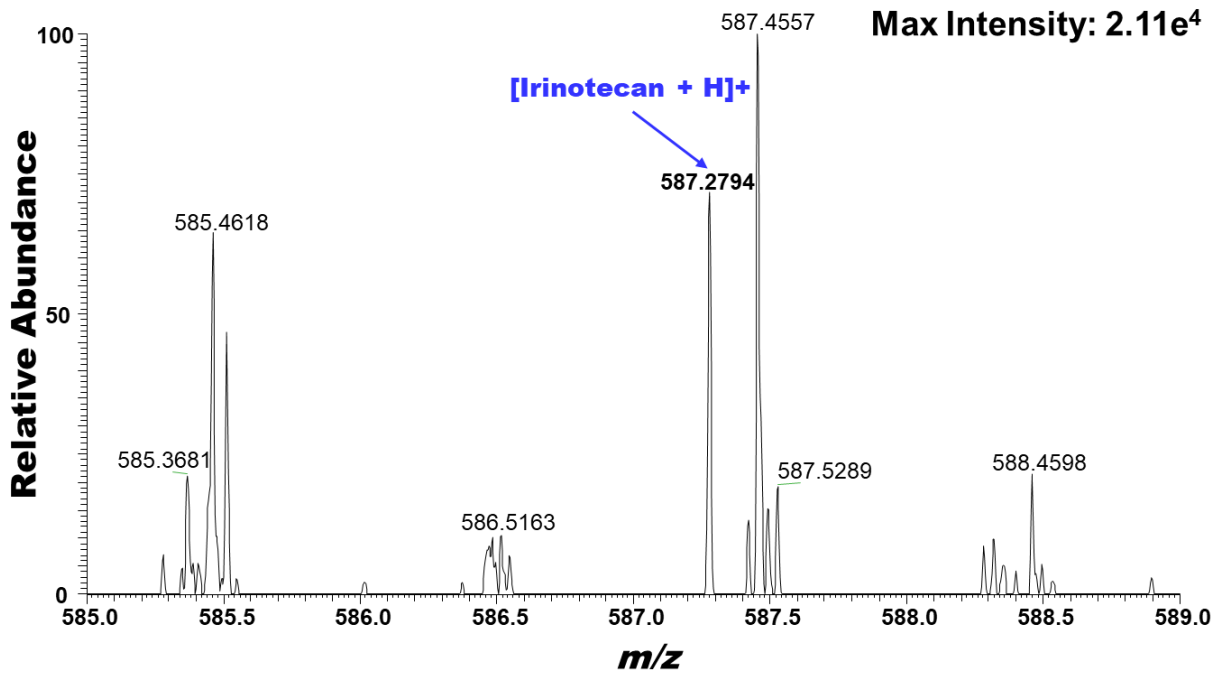

Figure 4-5. Limit of detection for irinotecan using the Single-probe qSCMS method (10 fM).

4.3.2. Limit of Detection.

The limit of detection (LOD) was determined by sampling solutions of irinotecan at various concentrations using the qSCMS setup. The LOD was determined to be 10 fM, while the limit of quantification (LOQ) was measured to be 100 fM (**Figure 4-5**).

4.3.3. Influence of Flow Rate and Concentration of Internal Standard.

Flow rate of the sampling solvent, which contains the internal standard, is an experimental parameter that must be optimized for each experiment since it varies with tip size, emitter length, and distance between the emitter and the mass spectrometer inlet. Therefore, it is important to determine if varying the flowrate affects the amount of drug calculated inside an individual cell. For this experiment, over 27 cells treated under the

same condition were measured at two different flowrates (25 and 50 nL/min). The amounts of drug molecules measured at different flowrates were not significantly different ($p > 0.05$). The concentration of internal standard is also critical for qSCMS experiments, and it needs to be carefully selected. Excessively high concentrations of the internal standard may suppress the ion signals of analytes; however, inadequate abundance of internal standard may not be observed during the experiment. To study the effect of internal standard concentration, two different concentrations of deuterated-irinotecan were tested (25 nM and 50 nM). Over 45 cells treated using the same condition were measured using each concentration of internal standard, and the obtained amounts of drug molecule were not significantly different ($p > 0.05$).

4.3.4. Method Validation.

Validation experiments were carried out to verify the Single-probe qSCMS technique is capable of highly efficiently sampling and detecting target analytes from single cells retained in microwells on the glass chip. To split the flow of irinotecan solution, three fused silica capillaries were connected to a µT-connector. For precise delivery of irinotecan solution into target microwells, the first fused silica capillary (ID: 25 µm, OD: 360 µm) was chemically etched (using HF) into a sharp needle, which was placed into a microwell on the glass chip with the flat end connected to one channel of a T-junction. A second capillary with the same length but a larger ID (ID: 50 µm, OD: 360 µm) was connected to another channel of the T-connector. The third capillary was connected the other channel of the T-connector to deliver the irinotecan solution from the syringe. A series of volumes (2-9 nL) of irinotecan solution (10 nM) were delivered into individual microwells on the glass chip to acquire known amounts (22.7-93.7 amol) drug compound

in those microwells. Similar to the Single-probe qSCMS measurements, this experimental setup was utilized with a continuous flow of internal standard (deuterated-irinotecan with the same concentration 10 nM) to extract irinotecan in microwells for MS analysis.

$$Q = \frac{\Delta P \pi r^4}{8 \eta l} \qquad \textbf{(Equation 4.2)}$$

where Q is the volume flux, P is the change in pressure, r is the capillary radius, η is the viscosity, and l is the capillary length.

Poiseuille's Law (**Equation 4.2**) was used to calculate the flow rate from the chemically-etched probe, which was used to deliver the irinotecan solution into each microwell. We then used the Single-probe qSCMS technique to measure the amounts of irinotecan in each well by placing the Single-probe tip into individual microwells containing irinotecan. Similar to the measurement operation and data analysis of qSCMS of cells, the deuterated-irinotecan internal standard was also used (flow rate was 150 nL/min), and the amounts of irinotecan deposited in microwells were calculated. Using Excel, we plotted the correlations between the ratio of the areas of irinotecan to deuterated-irinotecan and the ratios of the volumes of irinotecan to deuterated-irinotecan.

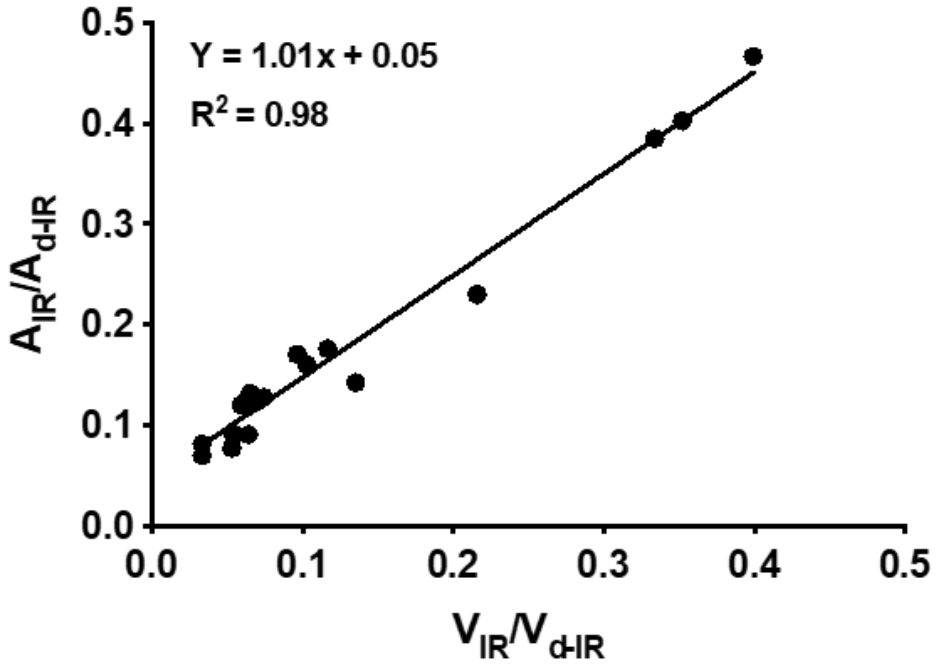

Figure 4-6. Graph of the ratio of the areas of irinotecan to deuterated-irinotecan versus the ratio of the volumes of irinotecan to deuterated-irinotecan for method validation.

A y-intercept of 0 would indicate all the irinotecan loaded into each microwell was captured. Our y-intercept of 0.05 suggests most of the irinotecan was captured (**Figure 4-6**). Error could come from the small volume available for each microwell, making it difficult to inject volumes smaller than individual microwells as well as from capillary action, which could draw some irinotecan solution back inside the capillary. A slope of 1 and a high R^2 value would indicate the ratio of volumes and areas of drug compound to internal standard are equal, which is a major factor for qSCMS calculations since we are using the total intensities as areas under the curve. A slope of 1.01 with an R^2 value of 0.98 suggests the ratios are similar and can be used for calculations (**Figure 4-6**). These results suggest our method is robust and can be used for quantitative experiments.

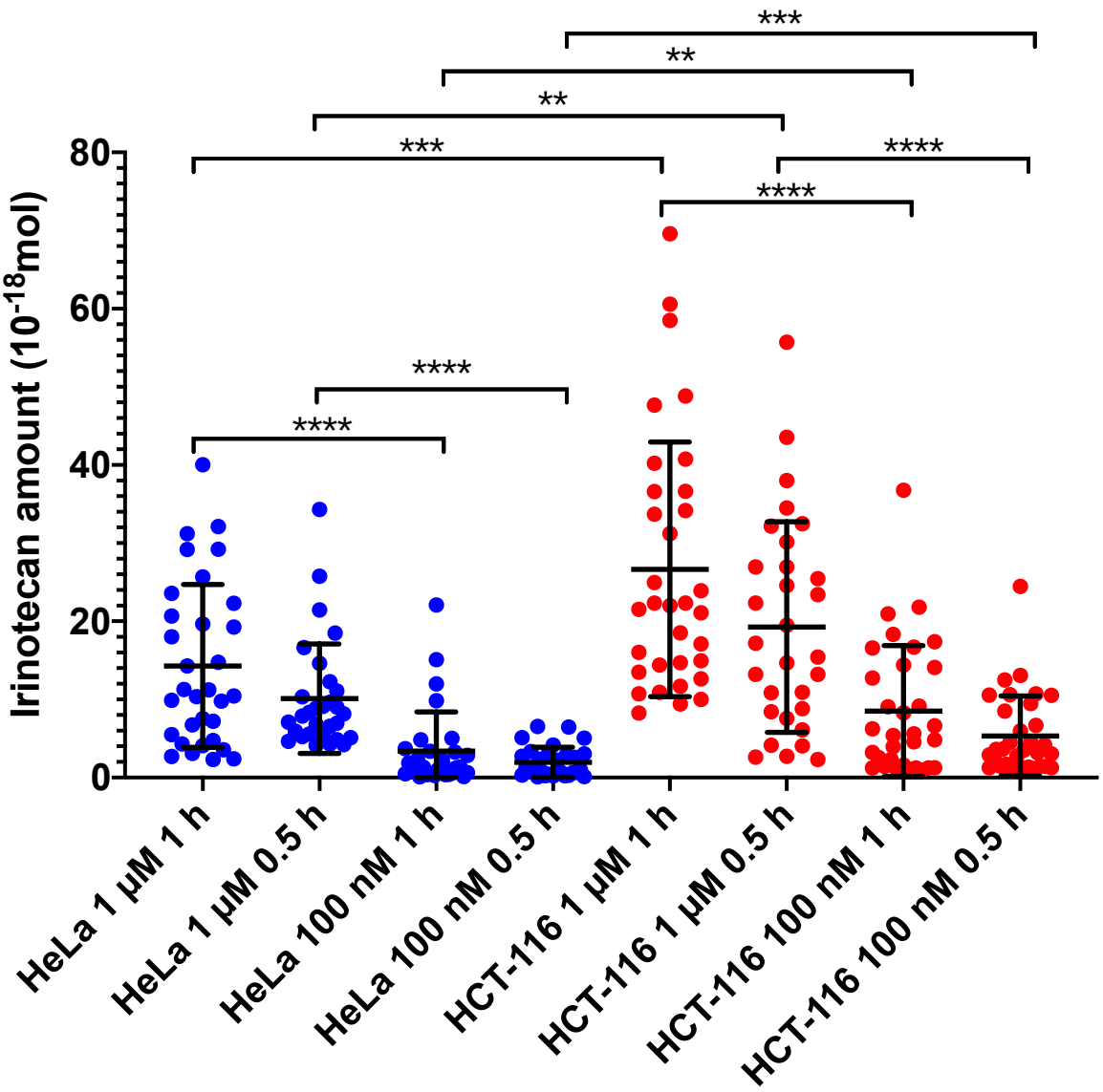

Figure 4-7. Box plot depicting the amount of irinotecan (amol) inside individual HeLa and HCT-116 cells at varying treatment concentrations and times.

4.3.2. qSCMS of the Anti-Cancer Drug Irinotecan in Human Cancer Cell Lines.

Single-probe qSCMS analysis of the standard-of-care anti-cancer drug irinotecan in individual HCT-116 and HeLa human cancer cells is reported (**Figure 4-7** and **Table 4-1**). The adherent HCT-116 colon adenocarcinoma and HeLa cervical cancer cell lines were treated with irinotecan using a range of concentrations and treatment times (**Figure**

4-7 and **Table4- 1**). Single cells inside microwells (i.e., one cell/microwell) were used in the quantitative SCMS measurements. Internal standard (d-irinotecan) concentrations of 25 and 50 nM were used. We collected eight sets of data from both cell lines treated under different conditions, and more than 30 cells were measured for each set of SCMS experiments. Rank sum tests (Mann-Whitney)

were conducted to determine whether there is a statistically significant difference of drug quantity between each pair of datasets. In general, the drug uptake amounts from individual cells exhibit a broad range of values, which are likely attributed to the heterogeneity of individual cells.

The Single-probe qSCMS measurements show several clear trends connecting cellular treatment with intracellular drug levels. Increasing irinotecan treatment concentrations in the HCT-116 cellular media from 0.1 to 1.0 μM increased the average intracellular irinotecan levels in individual cells. Using the lower drug concentration (0.1 μM Irinotecan), the drug update amounts were measured as $5.3 \pm 5.1 \times 10^{-18}$ and $8.5 \pm 8.4 \times 10^{-18}$ mole (attomole or amole) for cells treated for 0.5 and 1.0 hour, respectively. Larger amounts of intracellular drug molecules were obtained from cells treated with a higher concentration (1.0 μM): 15.2 ± 14.1 and 23.1 ± 16.7 amol for the treatment time of 0.5 and 1 hour, respectively. The increased drug uptake amounts from individual cells in different groups are statistically significant ($p < 0.01$) (**Figure 4-7**). In contrast, increasing the treatment time from 0.5 to 1.0 hour, while keeping the same drug concentration, has no significant effect ($p > 0.05$) on drug uptake.

For HeLa cells, a similar trend was found: increasing the drug concentration from 0.1 to 1.0 μM significantly ($p < 0.001$) increases the drug uptake amounts (**Figure 4-7**).

Cells treated with 0.1 μM irinotecan reported intracellular drug amounts of 1.9 ± 1.8 and 3.2 ± 3.0 amol for 0.5- and 1.0-hour treatment times, respectively. Increasing the drug treatment concentration to 1.0 μM increases the drug uptake amount to 9.8 ± 7.1 and 14.7 ± 10.4 amol for 0.5- and 1.0-hour treatment times, respectively. Additionally, keeping the same drug treatment concentrations (0.1 or 1.0 μM) while increasing the treatment time from 0.5 to 1.0 hours has no significant influence ($p > 0.05$) on intracellular drug levels. The qSCMS studies suggest that both HCT-116 and HeLa cells rapidly absorb drug compound from media.

Our experiments clearly show that cellular drug uptake amounts vary between HCT-116 and HeLa cell lines (**Figure 4-7**). Although both cell lines exhibit very similar trends of drug uptake amount, the intracellular drug amounts in single HCT-116 cells are significantly higher ($p < 0.001$) than those in single HeLa cells treated under the same conditions in all cases. These differences are likely attributed to multiple reasons. First, the cell sizes of these two cell lines are different. The average volume of an HCT cell (3.26 ± 0.11 picoliters) is about 1.3 times as the volume of a single HeLa cell (2.6 ± 0.4 picoliters),[127,145] so larger cells may have higher drug uptake amount. Second, it is possible that HCT-116 cells have a higher efficiency of irinotecan uptake since irinotecan has shown to have a greater aptitude towards the treatment of colon cancer than cervical cancer.[146]

4.3.3. Comparison of SCMS and LC/MS Results.

For comparison studies, we prepared cell lysate samples (see “Cell Sample Preparation”) and conducted traditional LC/MS experiments to measure the average amount of irinotecan inside of a single cell for both lines. Deuterated-irinotecan at known

concentrations was added during the preparation of cell lysate. Using nano-UPLC/MS, ion signals of both regular and deuterated-irinotecan were measured. The average drug amount in a single cell was estimated by considering multiple factors, including the peak areas of both regular and deuterated-irinotecan, the concentration of deuterated-irinotecan in cell lysate samples, and the total number of cells in each sample.

In general, a similar trend for both SCMS and LC/MS has been observed: a higher drug treatment concentration and/or longer treatment time results in higher drug uptake for both cell lines. However, the amounts of irinotecan measured from quantitative SCMS experiments are significantly higher than those from LC/MS experiments for both cell lines treated under all conditions (**Table 4-1**). For example, HCT-116 cells that underwent 0.1 μM treatment for 1 hour gave values of 8.5 ± 8.4 amol and 2.5 ± 0.8 amol for SCMS and LC/MS experiments, respectively. The t-test results indicate that these results are significantly different ($p < 0.001$). Similarly, treating cells with 1 μM irinotecan for 1 hour gave averaged values of 23.1 ± 16.7 amol and 11.6 ± 3.4 amol for SCMS and LC/MS measurements ($p < 0.001$), respectively. A similar trend was found for 0.5-hour drug-treated groups under different drug treatment concentrations (0.1 μM and 1 μM) in HeLa cell line experiments.

The difference between these two methods is likely due to two major reasons. Cell heterogeneity in SCMS experiments can attribute to the large standard deviation, and the possible drug loss during the lengthy LC/MS sample preparation process could contribute to SCMS having larger values. First, cellular heterogeneity is likely to influence cellular phenotypes since every cell is unique and is the product of its own particular genome, epigenome, and cell status.

Table 4-1. Amount of irinotecan (amol) found inside single cells for varying treatment times and concentrations using both qSCMS and LCMS analysis. (a) Results from HeLa cells. (b) Results from HCT-116 cells.

(a)

Treatment Conditions	**SCMS Results** ($x10^{-18}$ moles)	**LCMS Results** ($x10^{-18}$ moles)
100 nM, 0.5 h	1.9 ± 1.8	1.3 ± 0.5
100 nM, 1 h	3.2 ± 3.0	1.9 ± 1.1
1 μM, 0.5 h	9.8 ± 7.1	3.9 ± 3.0
1 μM, 1 h	14.7 ± 10.4	4.2 ± 1.2

(b)

Treatment Conditions	**SCMS Results** ($x10^{-18}$ moles)	**LCMS Results** ($x10^{-18}$ moles)
100 nM, 0.5 h	5.3 ± 5.1	2.5 ± 0.2
100 nM, 1 h	8.5 ± 8.4	2.5 ± 0.8
1 μM, 0.5 h	15.2 ± 14.1	10.5 ± 1.7
1 μM, 1 h	23.1 ± 16.7	11.6 ± 3.4

It is becoming clear that the differences among individual cells, even within a supposedly homogeneous cell-type, can influence the behavior of a biological system.[72] All of these differences among individual cells are critical for the cell functions, which may alter the capability of drug uptake. Second, the difference of cell sample preparation is likely to induce variance between the different measurements. SCMS involves minimal sample preparation, so there is less of a chance of drug compound loss between sample preparation and measurement. In contrast, cell lysate samples used for traditional LC/MS experiments involve multiple-step preparation. After anti-cancer drug treatment, cells undergo multiple steps that can possibly result in drug compound loss, such as trypsin

detachment, multiple rounds of rinsing cells and centrifugation, and organic solvent extraction. Unfortunately, the internal standard cannot be added into cell samples during these steps to compensate for drug compound loss during these steps, and it is impractical to measure the portion of drug compound lost during these steps. In contrast, drug treated cells are rinsed with either untreated (FBS-free) culture media or PBS and followed by immediate analysis for qSCMS experiments, minimizing drug compound loss from target single cells.

Since cells were measured in a near-native environment in SCMS experiments, the results are likely more representative of cellular status than LC/MS experiments. However, our quantitative SCMS approach has its own limitations. First, solvent extraction is performed at the single-cell level to extract drug compounds for MS analysis, which makes this method suitable to detect and quantify free and loosely-bonded drugs inside single cells. However, if drug compounds form covalent bonds with DNA or proteins,[91,147] they are not likely to be extracted by solvent during the SCMS measurement. Second, we measured approximately 30 cells for each treatment condition due to the limited SCMS experimental throughput. An increased throughput of the quantitative SCMS technique will significantly enhance experimental efficiency. Third, our current studies provide the absolute amount of drug compound inside single cells. However, we were unable to measure the volume of cells using the current experimental setup to provide intracellular drug concentration, which is likely to be of great interest for fundamental research and the pharmaceutical industry. Therefore, future technology development and more detailed studies are needed to enable deeper understanding of anti-cancer drug uptake and pharmacokinetics studies.

4.4 Conclusion

In the present study, we utilized the Single-probe qSCMS technique to measure the absolute amount of the anti-cancer drug compound irinotecan from live single cells in real time. Two cell lines, HCT-116 and HeLa, were used as the model systems and subjected to drug treatment using a series of concentrations and times. The sampling solvent containing deuterated-irinotecan, the internal standard, was delivered to the Single-probe device to perform microscale extraction of cellular contents. Both irinotecan and its internal standard were simultaneously detected in real-time MS analysis, and the absolute drug uptake amounts from individual cells were estimated. Our results indicate that for single cells treated using the same conditions, drug uptake amounts were broadly distributed. For cells treated under different concentrations and times, drug concentration is likely to have a more significant influence on the drug uptake amount than treatment time. Comparison between the two cell lines indicate that HCT-116 cells contain significantly more irinotecan than HeLa cells. Drug uptake amounts obtained from single cells were also compared with the results measured from cell lysates using LC/MS. The results obtained at the single-cell level were significantly higher than those from population cell measurements, which can be attributed to cell heterogeneity and potential drug compound loss during cell lysate preparation. This qSCMS technology is applicable of the analysis of many other types of drug compounds, drug metabolites, and cellular metabolites of interest and can lead to better understanding of pharmacokinetics and potential applications of compounds in precision medicine, including patient samples, to revolutionize personal chemotherapeutics.

4.5 Acknowledgements

The author would like to thank Dr. Ning Pan Bernhardt for her contribution in helping develop the quantitative single cell mass spectrometry method for Single-probe mass spectrometry and data analysis. Dr. Naga Rama Kothapalli created the cell lysate experiments used for method validation. Additionally, Ms. Mei Sun helped perform method verification experiments. This manuscript is currently under review (*Analytical Chemistry* April 2019).

Chapter 5 : Single Cell Mass Spectrometry Quantification of OSW-1 Kinetics

5.1 Introduction

Intracellular drug incorporation provides information that is essential for the advancement of personalized cancer therapeutics. The time for incorporation of anti-cancer compounds in cancer cells can provide insight towards the toxicity and metabolism of the drug, which can determine drug candidacy for a patient.[148] In drug development, quantitative measurement of drug uptake rate is essential to evaluate the efficacy of the drug towards a specific type of cancer. OSW-1 (3beta,16beta,17alpha-trihydroxycholest-5-en-22-one 16-O-(2-O-4-methoxybenzoyl-beta-D-xylopyranosyl)-(1-->3)-(2-O-acetyl-alpha-L-arabinopyranoside)) is a naturally-occurring compound isolated from the chincherinchee bulbs (Ornithogalum saundersiae) exhibiting antiproliferative properties of cultured human cell lines with half-maximal inhibitory concentrations (IC_{50}) in the sub-nanomolar range.[149,150] OSW-1 belongs to the ORPphil-in family of natural products due to its targeting of oxystersterol binding protein (OSBP) and OSBP-related protein 4L (ORP4L).[151] Although it is suggested that OSBP and ORP4 are the efficacy targets of OSW-1, its cytotoxic mechanism of action is highly enigmatic.[150,152] Understanding the pharmacokinetic and pharmacodynamic properties of OSW-1 and other potential chemotherapeutic agents could lead to important discoveries regarding the effectiveness of their dosages. The average amount of drug compounds in individual cells is traditionally measured using bulk analysis methods, such as liquid chromatography mass spectrometry (LCMS), of samples prepared from populations of cells (i.e. cell lysate experiments). Major pitfalls of quantifying cell lysates through liquid chromatography

mass spectrometry (LCMS) include a lengthy sample preparation process, requirement of a large number of cells, and inability to describe cellular heterogeneity. Particularly, the lengthy sample preparation process is needed for these traditional experiments, resulting in inaccurately studying of pharmacokinetic or pharmacodynamic properties of anti-cancer compounds. To thoroughly understand the efficacy of these compounds on various cell types (i.e. cancerous or non-cancerous), it is important to investigate drug interactions on the single-cell level.

Single cells analysis (SCA) techniques for eukaryotic cells currently include microfluidics, DNA and RNA sequencing,[117,118,153] mass spectrometry (MS),[2,4,42,108,119,137] cytometry,[4,6,16,17] and Raman spectroscopy imaging,[154] amongst others. However, the need for sample preparation for many of these methods could change the morphology of cells and deter their ability to retain cellular characteristics. Thus, it is critical to develop bioanalytical techniques capable of analyzing cells in real time in a near-native environment. Single cell mass spectrometry (SCMS) is becoming more widely used, especially the subcategory of SCMS involving ambient ionization, for the ability to give an abundance of information utilizing a label-free process with minimal sample preparation. Recently, our lab has used the Single-probe MS technique to analyze various cellular metabolites and drug molecules real time, both qualitatively[46,48,83,87,109] and quantitatively (**Chapter 4**), inside individual mammalian cell lines for SCA or tumor imaging. In this work, we expand the versatility of quantitative single cell mass spectrometry (qSCMS) to include the analysis of pharmacokinetic and pharmacodynamic data for OSW-1 in both HCT-116 and T24 (colon and bladder cancer, respectively) cell line models.

5.2 Experimental Section

5.2.1. Materials and Reagents.

LCMS grade acetonitrile and methanol were purchased from Sigma Aldrich (Saint Louis, MO) and used as solvents for both SCMS and LCMS experiments. A P-2000 Micropipette Laser Puller from Sutter Instrument Company (Novato, CA) was used to pull Friedrich & Dimmock, Inc. (Millville, NJ) dual bore quartz tubing for both sets of experiments. Fused silica capillaries were purchased from Polymicro Technologies (Phoenix, AZ). Glass microchips were purchased from Blacktrace (Norwell, MA), a sister company of Dolomite Centre (Royston, Herts, UK). Before use, each microchip was coated with poly-D-lysine (MW 70,000 – 150,000) to improve cell attachment.

5.2.2. Glass Microchip Maintenance.

Prior to use, glass microchips were coated with poly-D-lysine. Poly-D-lysine (5 mL) was placed into 3 wells of a 6-well plate, and PBS was placed in the other 3 wells. Using forceps, a microchip was inserted into a poly-D-lysine-containing well for 5 minutes. After 5 minutes, the chip was transferred to a well containing PBS. After washing, the glass microchips were exposed to UV light for 2 hours prior to being used for plating.

Before use, glass microchips were rinsed with complete McCoy's media (5 mL, 3 times). After use, the chips were exposed to UV for at least 2 hours prior to reuse. Before plating, each chip was trypsinized (4 mL/well) for at least 2 hours and rinsed with complete media.

5.2.3. Sample Preparation.

Both HCT-116 and T24 cell lines were grown in McCoy's medium supplemented with 10% synthetic fetal bovine serum and 1% penicillin-streptomycin. All cells were maintained in an incubator at 37°C under 5% CO_2, and they were passaged around 75% confluency. T24 and HCT-116 cells were grown up for 2 days prior to treatment. To avoid mutations, only cells under passage number 25 that were in culture less than 2 months were utilized in the experiments.

Cells were plated in 6-well plates on glass microchips (28 mm) containing chemically-etched microwells (width: 55 µm; depth: 25 µm) to prevent sample loss that could occur as the Single-probe penetrates each cell. For each treatment, culture medium for the desired well was aspirated and replaced with fresh medium containing 100-nM OSW-1 (4 mL) and allowed to incubate at 37°C for the duration of the treatment time. Prior to analysis, each microchip was washed with FBS-free media (5 mL) to avoid detection of the drug from extracellular content.

5.2.4. Single Cell Mass Spectrometry Protocol.

Single-probe Fabrication. Single-probes were fabricated utilizing a previously published protocol;[155] therefore, only a brief summary is given here. Dual-bore quartz tubing (OD: 500 µm, ID: 127 µm) was pulled into a sharp needle using a laser puller to give a final tip diameter of ~5 µm. A silica capillary (OD: 105 µm, ID: 40 µm) was placed into one bore to act as the solvent-providing capillary, and a nano-ESI emitter pulled from the same capillary was placed into the other bore. The capillaries were held in place with

UV curing resin, and the finished probe was secured to a glass slide using Epoxy glue for easy coupling to the mass spectrometer with a flexible clamp holder.

Single-probe Mass Spectrometry Setup. The nano-ESI emitter was aligned with an extended ion transfer tube for coupling with the Thermo LTQ Orbitrap XL mass spectrometer (60,000 m/Δm, 1 microscan, 1 ms maximum injection time). The cell-containing glass microchip was then placed on an X, Y, Z-translational stage controlled by the LabView software package that allows the stage to be moved precisely in 0.1-μm increments. High voltage (~4 kV) was applied to a conductive union that connected the probe to a syringe containing the internal standard (50 nM d-OSW-1) dissolved in acetonitrile with 0.1% formic acid. Once a single cell was selected using a top-view stereomicroscope, penetration was achieved by raising the stage in the Z-direction.

Data Analysis. Data analysis was attained by exporting the scans from the Xcaliber software package into Excel. Then, the analyte signal time and total intensities (integral) for both OSW-1 and d-OSW-1 were calculated. By factoring in the flow rate and concentration of the internal standard (d-OSW-1), the absolute number of moles of OSW-1 could be calculated for each cell using a ratio of analyte to internal standard. The relative concentration of drug in each cell was estimated using the average cell volume of each cell line.

5.3 Results

The absolute number of moles of OSW-1 in each individual cell was calculated at various time points to determine the pharmacokinetic and pharmacodynamic data, and the relative concentration can be estimated using an average cell volume of 3.26 pL and 7.2 pL for HCT-116 and T24 cells, respectively.[127,128] In HCT-116 cells, the drug

compound is present within 15 minutes after OSW-1 treatment (100 nM), and its abundance is significantly increased ($p < 0.01$) until 1 hour for cells treated with 100 nM OSW-1 (**Table 5-**1, **Figure 5.1**). However, it is likely that OSW-1 establishes intracellular concentration equilibrium in HCT-116 cells around 1 hour because the drug amount is not significantly changed after that time ($p < 0.01$).

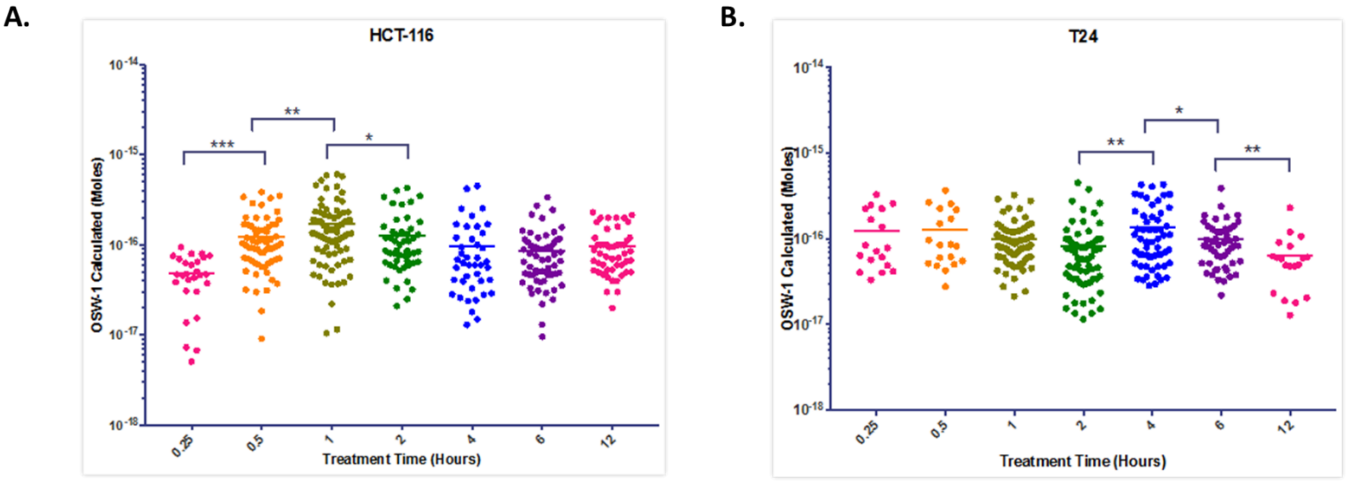

Figure 5-1. Box plots showing the amount of OSW-1 accumulated in each cell line. (a) HCT-116 cells, and (b) T24 cells. (n>20 for each treatment)

In comparison, T24 cells appear to establish concentration equilibrium at a slower rate than HCT-116 cells upon treatment using the same drug concentration. Longer treatments (>2 h) lead to drug accumulation, and the greatest values are reached after 4 hour-treatments (**Table 5-1**). Our experimental results suggest that the drug uptake rate is time-dependent, and it may vary for different cell lines.

Washout experiments were performed in HCT-116 cells to determine how long the drug is retained inside each cell. HCT-116 cells were treated with OSW-1 (100 nM) for 1 h, which correlates to the treatment time with the maximum amount of drug accumulated. The washout experiments showed OSW-1 at an unquantifiable amount inside individual

HCT-116 cells for up to 24 hours (limit of detection is 10 nM).[89] The amount of OSW-1 is significantly decreasing from 6 hours to 12 hours, suggesting the drug is metabolizing. However, the metabolites of OSW-1 are currently unknown, so they were not able to be monitored during this timeframe.

Table 5-1. Uptake amount (mol) of OSW-1 (100 nM) by HCT-116 and T24 cells in time-dependent treatments.

Treatment Time (Hours)	Moles Calculated (& Estimated Concentrations) HCT-116	Moles Calculated (& Estimated Concentrations) T24
0.25	$4.79 \pm 2.47 \times 10^{-17}$	$1.30- \pm 0.892 \times 10^{-16}$
0.5	$7.85 \pm 4.93 \times 10^{-17}$	$1.31- \pm 0.939 \times 10^{-16}$
1	$1.72 \pm 1.33 \times 10^{-16}$	$9.82- \pm 5.95 \times 10^{-17}$
2	$1.27 \pm 0.982 \times 10^{-16}$	$8.45- \pm 8.02 \times 10^{-17}$
4	$9.80- \pm 9.80 \times 10^{-17}$	$1.33- \pm 1.10 \times 10^{-16}$
6	$8.52- \pm 6.30 \times 10^{-17}$	$9.82- \pm 6.54 \times 10^{-17}$
12	$9.64 \pm 6.30 \times 10^{-17}$	$6.42 \pm 5.04 \times 10^{-17}$

5.4 Conclusions

The Single-probe qSCMS was used to quantitatively measure the dynamics of drug uptake, particularly at time points that are too short (e.g., within 15 min) to measured using traditional analytical methods, such as LCMS, in which lengthy steps of sample preparation are obligatory. In addition, our technique is capable of quantifying the absolute drug amount inside individual cells, whereas traditional methods, which are based on bulk sample measurements, can only provide averaged results with an unrealistic assumption that each cell is the exact same size and in the same growth state.

Due to the complexity of cell heterogeneity, even for the cultured cell lines, it is challenging to depict the quantitative SCMS results, as the amount of drug measured in individual cells, regardless of cell lines or treatment conditions, exhibit a wide distribution. Therefore, it is expected to obtain relatively large standard deviations of experimental results, especially compared to the small standard deviations of traditionally-established methods. It is worth noting that the measurement of each cell cannot be repeated because each cell contains a limited volume that is enough for only one measurement. Although obtaining the absolute drug concentration in individual cells will tremendously affect fundamental studies and clinical applications, our technique cannot provide such information at the current state. With microscope-guided experiments, a general cell size can be seen before analysis, but wells are chosen without bias: only wells with one cell are targeted for analysis, regardless of the size of cell within the well. Without accounting for the actual cell volume of each individual cell, it is difficult to give a more accurate information of drug concentration. Future work will include establishing a protocol to determine both the cell volume and absolute amount of drug during the SCMS experiments and provide concentrations of drug compounds in individual cells (**Chapter 6**).

The amount of OSW-1 measured at various time points within each cell line demonstrate the minimum exposure time required for the drug to be absorbed within each cell, the length of time to establish chemical equilibrium, and how long the drug is retained within each cell. This technology can be applied to other drugs to determine pharmacokinetic or pharmacodynamic data towards the metabolism of drugs in various cell lines. By monitoring anti-cancer drug metabolites, specifically active metabolites, the

aptitude of the drug compound towards killing cancer cells can be determined. Our technique can be potentially applied to cells from patients to revolutionize personalized cancer regimens in the future (**Chapter 6**).

5.5. Acknowledgements

The author would like to thank Dr. Anh T. Le for synthesizing the internal standard used in these experiments. Also, the author would like to thank Mr. Ryan C. Bensen for his help in sample preparation and writing of this manuscript (to be submitted by May 2019).

Chapter 6 : Single Cell Mass Spectrometry Quantification of the Anti-Cancer Compound Gemcitabine: From Cell Lines to Patients

6.1 Introduction

Personalized medicine maximizes the efficacy of one's treatment by accounting for the biological makeup of the individual.[156] This practice is currently best characterized in oncology, primarily through genotypical identification of key cancer-related genes for proper identification and characterization of the tumor.[157] However, current drug-dosage determination is typically chosen in correlation to the patient's physical characteristics, such as body surface area, and is administered in a scheduled manner.[158,159] The efficacy of this treatment course is generally conducted through an endpoint analysis, typically weeks or months following initial treatment administration. This translates into extended periods of time in which patients are required to endure chemotherapy medication with its potential associated adverse side effects to determine if the initial treatment was effective in overall cancer regression.

Therapeutic Drug Monitoring (TDM) is currently used for the determination of drug efficacy through quantification of the chemotherapeutic agent in serum at designated time points throughout a drug administration regimen.[160] The following dosage is administered considering the previously- calculated serum concentrations, resulting in a constant serum concentration of the chemotherapeutic agent. A major drawback associated with TDM arises from the pharmacokinetic/ pharmacodynamic diversity of each individual, which skews drug quantification at the primary tumor site.[160,161] Alternatively, the drug could be quantified within accessible tumor sample biopsies, but this utilizes invasive

sampling and lacks the validation of therapeutically-relevant drug concentrations within cancer-specific cells.

The heterogenetic disease state of cancer is becoming increasingly characterized as an abnormal cellular process originating at the single-cell level, contributing to the development of the cancer stem cell theory and clinical relevance of circulating tumor cells.[162–165] Therefore, the development of bioanalytical methods for the detection and quantification of disease-relevant compounds on the single-cell level would be a powerful tool by providing real-time feedback of therapeutically-relevant treatment efficacy.[46] Single cell analyses have been developing over the past decade, including DNA and RNA sequencing, microfluidics, imaging, cytometry, and mass spectrometry (MS).[2,117–119,166–170] New and innovative mass spectrometry methodologies utilizing unique apparatuses, ionization technologies, and microscopy could also be applied to single cell mass spectrometry (SCMS) technology, progressing the applicability and accessibility of SCMS.[101,106,171–178]

The prodrug gemcitabine (2′,2′-difluoro-2′-deoxycytidine; dFdC) is a commonly-used drug known for its synergy with the anti-cancer compound cisplatin and, together, form a regimen for the treatment of many cancers, including bladder cancer.[179] After intracellular uptake, the prodrug is phosphorylated into its active form (2′,2′-difluoro-2′-deoxycytidine triphosphate; dFdCTP) or is deaminated into its inactive form (2′,2′-difluoro-2′-deoxyuridine; dFdU).[180,181] Gemcitabine has been previously quantified in extracted tumor tissue, peripheral blood mononuclear cells (PBMCs), and in plasma.[182–185] However, these methods lack the ability to analyze drug pharmacology in a non-invasive manner or characterize cellular heterogeneity on the single-cell level.

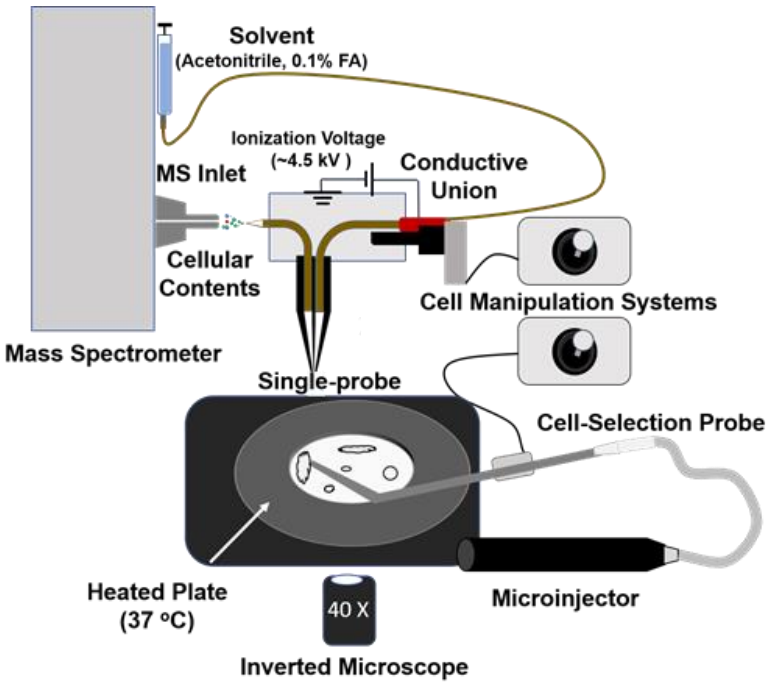

Figure 6-1. Schematic of the setup for non-adherent cells, including cells derived from the urine of bladder cancer patients.

Here, gemcitabine is quantified from individual cells of an adherent bladder cancer cell line (T24), non-adherent chronic myeloid leukemia, (K562), and cells isolated from the urine of gemcitabine-treated bladder cancer patients using the Single-probe MS technique previously used for the real-time analysis and quantification of individual adherent cancer cell lines, algal cells, and spheroids utilizing an integrated cell manipulation platform (ICMP) **(Figure 6-1)**, for the analysis of non-adherent cells.[46,81,83–90]

6.2 Methods

6.2.1. Sample Preparation.

Adherent Cell Lines. For the adherent bladder cancer cell line model, T24, cells were plated according to a previously published protocol. Cite IR. Briefly, T24 cells ($1x10^5$) are plated into each well of a 6-well plate containing a poly-D-lysine-coated glass microchip with chemically-etched microwells (25 μm x 55 μm) and McCoy's Media 5a supplemented with 10% synthetic fetal bovine serum (FBS) and 1% penicillin-streptomycin (4 mL). Approximately 36 hours after initial seeding, the media in each well is replaced with Gemcitabine-containing media at the indicated concentrations and incubated at 37°C and 5% CO_2 for the duration of the treatment time (1 hour). Prior to analysis, each glass microchip is rinsed with FBS-free media (5 mL) to avoid the detection of Gemcitabine from extracellular species. Cells were tested using the traditional Single-probe setup, modified for quantification **(Figure 6-1).**

Non-Adherent Cell Lines. The human chronic myeloid leukemia cell line, K562, was used as a cell line model for the proposed suspended cell manipulation system. Cells were grown in T25 flasks at 37°C and 5% CO_2 in RPMI media supplemented with 10% FBS and 1% penicillin-streptomycin. Prior to treatment (~24 hours), K562 cells ($\sim 1x10^5$) were seeded out in a T25 flask. The cells were spun at 1500 RPM for 5 min and treated with Gemcitabine at the indicated concentrations at a 4-mL volume in a 15-mL Falcon tube. After treatment, cells were pelleted at 1500 RPM for 5 minutes at 37°C and washed 3 times with PBS (10 mL). All tubes were resuspended in PBS (3 mL/tube) and were used for analysis in a 3-mL petri dish. K562 cells were analyzed using the integrated cell

manipulation platform (ICMP) in conjunction with quantitative single cell mass spectrometry using the Single-probe mass spectrometry technique. Cite Tech.

Bladder Cancer Patient Samples. Two separate groups of bladder cancer patients' urinary cells were analyzed in this study. One group (n=2) was not subjected to gemcitabine (untreated), while the other (n=2) received 1000 mg/m^2 infusion of gemcitabine. The urine was collected in a specimen jar for the analysis of the non-treated patients and collected an hour after infusion for the treated patients. The urinary sample was processed and analyzed within 3 hours after collecting. Each sample was processed as followed: sample was spun at 1500 RPM for 5 minutes at 37°C, followed by washing with pre-warmed PBS (20 mL) 3 times. The cells were resuspended in PBS (2 mL), and the cell solution was placed into a 3-mL petri dish for analysis using the ICMP.

6.2.2. Integrated Cell Manipulation Platform.

The Single-probe setup has been modified to accommodate an Eppendorf cell manipulation system, which utilizes both a Single-probe and a cell-selection device that allows the analysis of samples from a complex matrix with minimal sample preparation (**Figure 6-1**). The system is composed of an Eppendorf TransferMan cell manipulation system, Nikon inverted microscope, a Tokai Hit ThermoPlate, and a glass cell-selection device. The cell-selection device was held in place and controlled through an Eppendorf TransferMan cell manipulation system. The Single-Probe was controlled through a second TransferMan system and stabilized with a flexible arm clamp. This system was constructed on a motorized table for convenient coupling to the Thermo LTQ Orbitrap XL mass spectrometer.

6.2.3. Glass Cell-Selection Probe Fabrication.

Single-bore glass tubing (ID: 0.3 mm, OD: 1.1 mm) was transformed into a glass cell-selection device using a vertical pipette puller. Briefly, the glass was heated to create a tapered tip (~15 μm in diameter) to encompass an individual cell. Once the probe was pulled apart, it was placed in a Microforge MF-9 and bent ~45° from its original position.

6.2.4. Single-probe Fabrication.

Single-probes were fabricated using a previously published protocol.[186] Briefly, dual-bore quartz tubing (OD: 500 μm; ID: 127 μm) was pulled into a sharp needle (OD: ~5 μm) using a micropipette laser puller. Fused silica capillary (OD: 110 μm, ID: 40 μm) was placed into one bore as a solvent-providing capillary. The same diameter capillary was flame-pulled and placed into the other channel of the dual-bore quartz needle as a nano-ESI emitter. The probe was sealed using UV resin and secured on a glass slide with Epoxy glue for easy coupling to the flexible arm clamp of either the X, Y, Z-translational stage (adherent cells) or TransferMan manipulation system (non-adherent cells).

6.2.5. Mass Spectrometry Analysis of Individual Cancer Cells.

The Single-probe's nano-ESI emitter was aligned with the extended ion transfer tube's inlet. The solvent-providing capillary of the Single-probe was programmed to deliver solvent (internal standard dissolved in acetonitrile with 0.1% formic acid) at a flow rate of ~100 nL/min. Information regarding the synthesis of ^{15}N-gemcitabine can be found in **Appendix B**. Analysis was performed using a Thermo LTQ Orbitrap XL mass spectrometer. Positive ionization mode was used with a voltage of ~4.5 kV applied to the conductive union during analysis. (The flow rate and ionization voltage were optimized

for each experiment due to varying tip size, emitter length, and emitter distance from the mass spectrometer's inlet). A resolution of 60,000 and 1 scan/100 ms maximum injection time were used.

Adherent Cell Line Analysis. The glass microchip was placed on an X, Y, Z-translational stage controlled through the LabView software package, which allows controlled movements in 0.1 μm increments. Cells are monitored using a top-view digital stereomicroscope. Once an individual cell is selected, the stage is lifted in the z-direction for insertion. Microscale extraction of cellular content occurs and is introduced to the mass spectrometer after ionization using the nano-ESI emitter.

Non-Adherent Cell Line Analysis. Cells are placed in the lid of an 18-mm petri dish placed on a ThermoPlate at 37°C to mimic the cellular environment. During analysis, cells are monitored using an inverted microscope. Once a cell is chosen, suction is gently applied to the glass cell-selection device by changing the mineral oil in the CellTram Vario microinjector to secure a cell, and the cell-selection device is lifted in the Z-direction until aligned with the Single-probe tip. Once a liquid junction is formed between the two probes, suction from the cell-selection device is released for cell transfer. The cell undergoes microscale lysis and extraction and is taken up through drag force and capillary action before being sprayed into the mass spectrometer for analysis.

6.2.6. Gemcitabine Quantification.

For data analysis, files were exported from XCaliber to Excel, and the ratio of the intensities between gemcitabine and ^{15}N-labeled gemcitabine was calculated. Taking into consideration the flow rate, concentration of internal standard, and signal time for

gemcitabine, the absolute amount of compound (mol) was calculated for each individual cell. The relative cellular concentrations were estimated using the average cell volumes for each cell line (T24: 7.2 pL, K562: 2.8 pL).[131,187]

6.3 Experimental Section

Gemcitabine (*m/z* 264.0781) quantification was performed with the addition of an internal standard of isotopically-labeled (^{15}N-labeled) gemcitabine (*m/z* 267.0703) **(Scheme B1, Figures B1, B2)** into the sampling solvent (acetonitrile with 0.1% formic acid). Gemcitabine was first quantified in individual cells of an adherent bladder cancer cell line (T24) utilizing the Single-probe quantitative single cell mass spectrometry (qSCMS) method previously published in our lab (**Chapter 4, 5**). Analysis was performed following a 1-h incubation of gemcitabine at either 0.1, 1, or 10 μM (**Figure 6-2, Table 6-1, Figure B3**). For method validation, 1-μM gemcitabine-treated T24 cells were trypsinized, washed with PBS, and analyzed using the ICMP. The amount of gemcitabine calculated from both methods was not significantly different ($P > 0.05$), verifying the Single-probe/ICMP method for quantification of non-adherent cells.

Table 6-1. The concentrations of individual cells at the provided treatments using the averaged cell volume of K562 cells (Relative) ($n > 20$) and the measured volumes (Absolute) ($n > 20$)

Treatment Concentration	Relative Concentration	Absolute Concentration
0.1 μM	14.2 ± 9.0 μM	10.9 ± 7.1 μM
1 μM	17.4 ± 10.1 μM	17.9 ± 11.9 μM
10 μM	32.2 ± 21.5 μM	37.3 ± 26.1 μM

An advantage of the ICMP is that it allows for the analysis of a variety of cell types with minimal interferences from complex sampling matrices. The ICMP, consisting of an inverted microscope, two cell manipulation systems, a microinjector, a glass cell-selection probe, and a Single-probe, is capable of distinguishing cell types, morphologies, and sizes **(Figure 6-1).** The Single-probe/ICMP was further expanded to calculate the absolute concentration of gemcitabine from non-adherent chronic myeloid leukemia cells (K562) by measuring the diameter of each cell.[90] K562 cells were treated under the same conditions as the adherent T24 cells. The absolute concentration of gemcitabine was compared with the relative concentrations achieved using the average volume of K562 cells (2.6 pL) (**Table 6-2**).[131] There was no statistical difference between the concentrations calculated or the deviation within each data set between the two methods. Future work can be done using statistical analysis to determine how absolute concentrations correlate with cell size compared to the number of moles taken up.

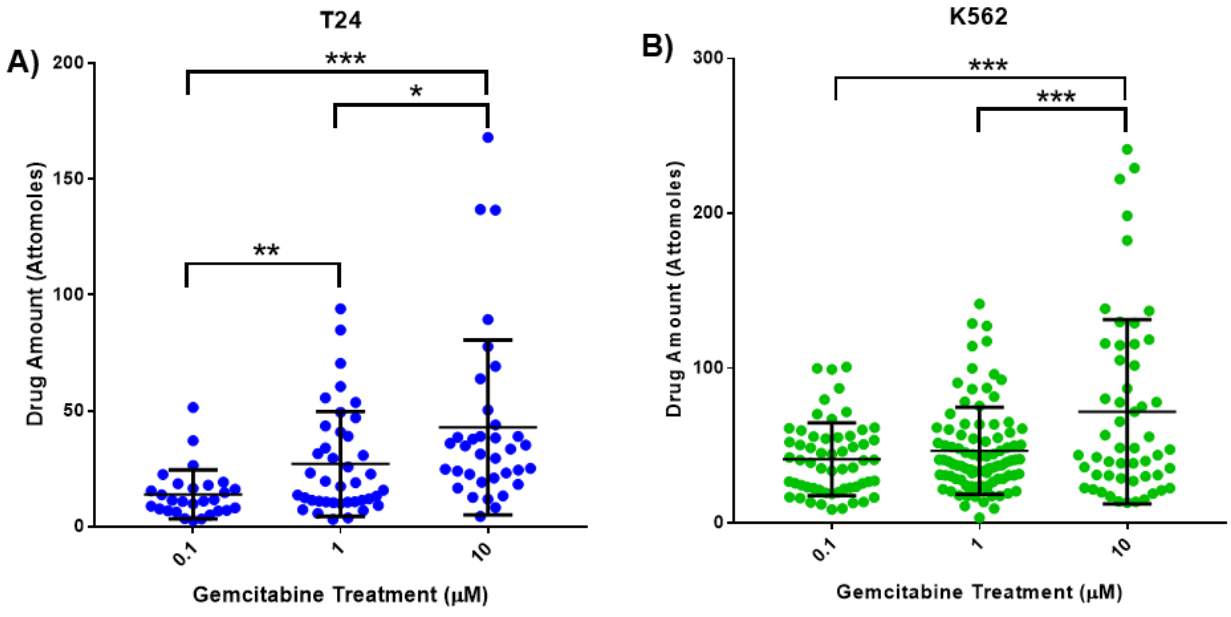

Figure 6-2. Moles (x10^{-18}) of gemcitabine calculated inside individual cells. (a) Adherent T24 cells and (b) non-adherent K562 cells.

Table 6-2. Moles ($x10^{-18}$) of gemcitabine calculated inside individual T24 and K562 cells. (n>30 for each treatment)

Treatment Concentration	T24 (Attomole)	K562 (Attomole)
0.1 μM	13.9 ± 10.6	41.3 ± 23.5
1 μM	27.0 ± 22.6	46.7 ± 28.2
10 μM	42.8 ± 37.7	72.0 ± 59.5

The amount of gemcitabine inside K562 cells followed a similar trend to T24 cells (**Figure 6-2, Figure B3**). There was an increase in intracellular gemcitabine quantification upon an increase in treatment condition and the 10-μM treatment also resulted in a significant increase in intracellular gemcitabine compared to 1 and 0.1 μM treatments. Additionally, the deviation of intracellular moles quantified within a treatment condition also increased with increasing treatment concentrations: the 10 μM treatment resulted in the greatest deviation (82%) followed by 1 μM (60%) then 0.1 μM (57%) **(Figure 6-2)**.

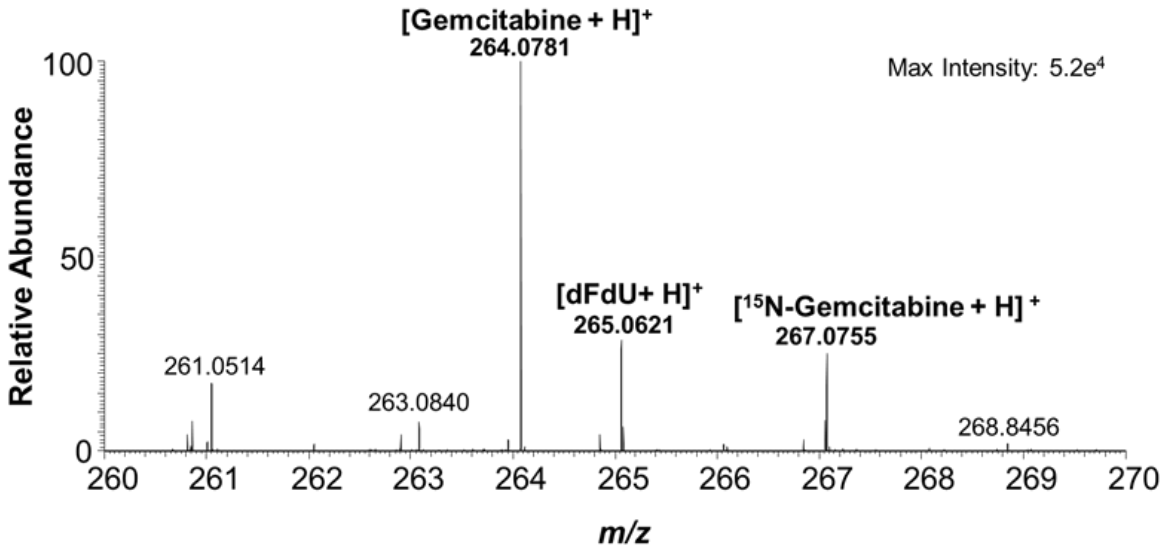

Figure 6-3. Mass spectrum of gemcitabine and 1-µM $^{15}N_3$-gemcitabine from an individual cell isolated from the urine of a bladder cancer patient 1 h after a 1000 mg/m^2 infusion of gemcitabine.

After the method was validated *in vitro*, the Single-probe/ICMP method for qSCMS was expanded to include the analysis of single cells isolated from the urine of bladder cancer patients (n=4). An initial qualitative analysis was performed on two patients who served as a control and were not subjected to gemcitabine chemotherapy. Phosphatidylcholines were qualitatively detected in single cells isolated from the urine of the bladder cancer patients **(Figure B4)**, validating the capability of detecting small molecules from isolated clinical samples.

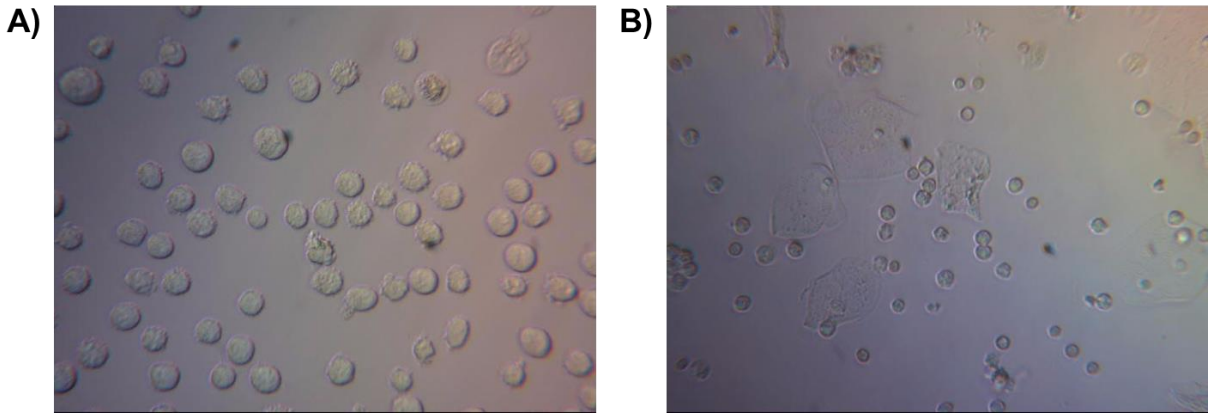

Figure 6-4. Experimental view of cells. (a) K562 cells and (b) Patient-derived cells.

Following the qualitative analysis, gemcitabine quantification inside single cells was performed using the ICMP setup on two patients who underwent gemcitabine chemotherapy (1000 mg/m^2 gemcitabine/treatment). Urine was collected from chemotherapy patients 1-h post-infusion **(Figures 6-3 and 6-4, Figures B5-B7**). Gemcitabine identification was validated through MS/MS analysis from a single patient-isolated cell and standard solution **(Figure B6)**. Gemcitabine was quantified from the patients who underwent chemotherapy but was not present in cells from the control group **(Figure 6-3, Figure B5)**. The amount of drug calculated from gemcitabine patient 1 is significantly higher than patient 2, suggesting the regimen is more effective for patient 1 **(Table 6-3)**. There also seems to be a general trend that the amount of gemcitabine is increasing with increasing round of chemotherapy, suggesting that gemcitabine is accumulating between treatments.

The urine of gemcitabine-exposed patients was also tested by spiking the sample with internal standard (100 μM ^{15}N-gemcitabine). Patient 1 had a gemcitabine concentration

of 1,490 ± 470 μM and patient 2 had a concentration of 585 ± 159 μM, which shows a relatively large amount of the anti-cancer compound being excreted through the urine within an hour after infusion. Additionally, the urine and the isolated cells also showed the non-active metabolite of gemcitabine, 2',2'-difluorodeoxyuridine (dFdU) (*m/z* 265.0621) **(Figure 6-3)**, which could be quantified in the future to further determine efficacy of the drug treatment.

6.4 Conclusion

In summary, we have developed a method for the quantification of the chemotherapeutic agent, gemcitabine, from single cells isolated from the *in vitro a*dherent (T24) and non-adherent (K562) cell line models and, ultimately, from *in vivo* clinically isolated cells from bladder cancer patients. Furthermore, this technique can be applied for the metabolomic analysis of individual clinical cells, detecting significantly modified molecules between two populations of cells (i.e. healthy vs. cancerous).

Table 6-3. Gemcitabine quantification from single isolated cells from two bladder cancer patients undergoing gemcitabine chemotherapy.

Infusion	**Patient 1** (Attomoles)	**Patient 2** (Attomoles)
1	-	45.8 ± 39.4
2	473 ± 187.7	79.4 ± 50.9
3	-	-
4	1,557 ± 1,004	-

Further clinical studies are currently being set up to assess the therapeutically-relevant levels of gemcitabine within the cell to apply this technique for personalized chemotherapeutic drug monitoring. Single-cell quantification of drug compounds isolated from non-invasive patient samples is a major advancement for the bioanalytical community and expanding this technology to include metabolites could improve personalized health care in the future, especially with regards to chemotherapeutic agents.

6.4 Acknowledgements

The author would like to thank the collaborators from the OU Health and Science Center, especially Drs. Heinlen, Weger, and Tripathi for making the analysis of patient-derived samples possible. Additionally, Dr. Naga Rama Kothapalli aided in the development of the technique for handling patient samples. Dr. Anh T. Le synthesized the internal standard utilized in the experiments and contributed **Scheme B1** and **Figures B1** and **B2**. Mr. Ryan C. Bensen helped in sample preparation and the writing of the manuscript to be submitted in April 2019.

Chapter 7 : Conclusions and Future Directions of Quantitative Single Cell Mass Spectrometry using the Single-probe Mass Spectrometry Technique

7.1 Summary of Work

In this work, we expanded the versatility of the Single-probe mass spectrometry technique. First, an integrated cell manipulation platform was built. This platform consists of an inverted microscope to monitor cell selection, two Eppendorf cell manipulation systems to control the spatial movements of each of the probes, a ThermoPlate to mimic the cells' native environment, a glass cell-selection device, and a Single-probe. This setup was then utilized for the detection of lipids from untreated cells, the detection of compounds from drug-treated cells, and untargeted analysis of cells from both drug-treated and control (untreated) groups. Then, the Single-probe mass spectrometry technique was adapted for quantitative analysis of drug compounds from adherent cell lines. First, quantitative single cell mass spectrometry was validated by comparing the amount of drug compound from single cell analysis to the traditional method of LCMS analysis of cell lysate samples. Then, quantitative analysis was used to explore the kinetics of OSW-1 inside different cell lines. Finally, quantitative analysis was expanded to include the analysis of patient-derived cell samples.

7.2 Implications of Work and Future Directions

The work presented in this manuscript has the potential to revolutionize personalized chemotherapeutic regimens for a variety of cancers. Since the tip of the glass cell-selection device can be as small as ~5 μm, this technique may be expanded to

any type of cell, adherent or non-adherent, as long as the cell is at least 5 μm in diameter. This method can also be applied to other disease states, since it is capable of providing information about cellular metabolites, both qualitatively and quantitatively, in a near-native environment. The ambient conditions with minimal (or even no sample preparation for qualitative experiments using the ICMP/Singe-probe setup) can enhance our understanding of cellular processes. Since the "-omics" techniques are becoming popular, this method can be expanded to include peptidomics, metabolomics, lipidomics, etc.

There are a few studies that could be done to strengthen this technique in the future. First, the integration of a miniaturized plasma device or coupling the Singe-probe mass spectrometry method with inductively-coupled plasma (ICP) MS would allow for the analysis of compounds like cisplatin, a common chemotherapeutic drug, that cannot be easily quantified through this technique since its mechanism of action includes binding to DNA. Second, drugs could be studied as part of "co-treatments." For example, cisplatin and gemcitabine are often used together as part of one chemotherapy regimen. Using multiple drugs to treat cell lines could be used to expand our knowledge of drug-drug interactions. Third, more patient samples can be analyzed. These samples can be broken down into analysis of cell type (i.e. cancer, healthy, red blood cell, etc.) or metabolites can be quantified to determine drug efficacy and better evaluate the course of chemotherapy for the individual patient.

References

1. Mao, S. *et al.* In Situ Scatheless Cell Detachment Reveals Correlation between Adhesion Strength and Viability at Single-Cell Resolution. *Angew. Chemie Int. Ed.* **57,** 236–240 (2018).
2. Rubakhin, S. S., Romanova, E. V, Nemes, P. & Sweedler, J. V. Profiling metabolites and peptides in single cells. *Nat. Methods* **8,** S20–S29 (2011).
3. Ginzberg, M. B., Kafri, R. & Kirschner, M. Cell biology. On being the right (cell) size. *Science* **348,** 1245075 (2015).
4. Kortmann, H., Dittrich, P. S. & Blank, L. M. Chemical and biological single cell analysis. *Curr. Opin. Biotechnol.* **21,** 12–20 (2010).
5. Moran, U., Phillips, R. & Milo, R. SnapShot: Key Numbers in Biology. *Cell* **141,** 1262–1262.e1 (2010).
6. Wang, D. & Bodovitz, S. Single cell analysis: the new frontier in 'omics'. *Trends Biotechnol.* **28,** 281–290 (2010).
7. Schuster, S. C. Next-generation sequencing transforms today's biology. *Nat. Methods* **5,** 16 (2007).
8. Ho, S. N., Hunt, H. D., Horton, R. M., Pullen, J. K. & Pease, L. R. Site-directed mutagenesis by overlap extension using the polymerase chain reaction. *Gene* **77,** 51–59 (1989).
9. Sanger, F. *et al.* Nucleotide sequence of bacteriophage φX174 DNA. *Nature* **265,** 687 (1977).
10. Shendure, J. & Ji, H. Next-generation DNA sequencing. *Nat. Biotechnol.* **26,** 1135 (2008).
11. Klein, C. A. *et al.* Comparative genomic hybridization, loss of heterozygosity, and DNA sequence analysis of single cells. *Proc. Natl. Acad. Sci.* **96,** 4494 LP-4499 (1999).
12. Eid, J. *et al.* Real-Time DNA Sequencing from Single Polymerase Molecules. *Science (80-.).* **323,** 133 LP-138 (2009).
13. Nebe-von-Caron, G., Stephens, P. J., Hewitt, C. J., Powell, J. R. & Badley, R. A. Analysis of bacterial function by multi-colour fluorescence flow cytometry and single cell sorting. *J. Microbiol. Methods* **42,** 97–114 (2000).
14. Bendall, S. C. *et al.* Single-Cell Mass Cytometry of Differential Immune and Drug Responses Across a Human Hematopoietic Continuum. *Science (80-.).* **332,** 687 LP-696 (2011).
15. Yamamura, S. *et al.* Single-Cell Microarray for Analyzing Cellular Response. *Anal. Chem.* **77,** 8050–8056 (2005).
16. Davey, H. M. & Kell, D. B. Flow cytometry and cell sorting of heterogeneous microbial populations: the importance of single-cell analyses. *Microbiol. Rev.* **60,** 641–96 (1996).
17. Andersson, H. & van den Berg, A. Microtechnologies and nanotechnologies for single-cell analysis. *Curr. Opin. Biotechnol.* **15,** 44–49 (2004).
18. Kann, B., Offerhaus, H. L., Windbergs, M. & Otto, C. Raman microscopy for cellular investigations — From single cell imaging to drug carrier uptake visualization. *Adv. Drug Deliv. Rev.* **89,** 71–90 (2015).

19. Bumbrah, G. S. & Sharma, R. M. Raman spectroscopy – Basic principle, instrumentation and selected applications for the characterization of drugs of abuse. *Egypt. J. Forensic Sci.* **6,** 209–215 (2016).
20. Konorov, S. O., Schulze, H. G., Piret, J. M., Blades, M. W. & Turner, R. F. B. Label-Free Determination of the Cell Cycle Phase in Human Embryonic Stem Cells by Raman Microspectroscopy. *Anal. Chem.* **85,** 8996–9002 (2013).
21. Nawaz, H. *et al.* Evaluation of the potential of Raman microspectroscopy for prediction of chemotherapeutic response to cisplatin in lung adenocarcinoma. *Analyst* **135,** 3070–3076 (2010).
22. Yin, H. & Marshall, D. Microfluidics for single cell analysis. *Curr. Opin. Biotechnol.* **23,** 110–119 (2012).
23. Dochow, S. *et al.* Tumour cell identification by means of Raman spectroscopy in combination with optical traps and microfluidic environments. *Lab Chip* **11,** 1484–1490 (2011).
24. Godin, M. *et al.* Using buoyant mass to measure the growth of single cells. *Nat. Methods* **7,** 387 (2010).
25. Lecault, V., White, A. K., Singhal, A. & Hansen, C. L. Microfluidic single cell analysis: from promise to practice. *Curr. Opin. Chem. Biol.* **16,** 381–390 (2012).
26. Köster, S. *et al.* Drop-based microfluidic devices for encapsulation of single cells. *Lab Chip* **8,** 1110–1115 (2008).
27. Falconnet, D. *et al.* High-throughput tracking of single yeast cells in a microfluidic imaging matrix. *Lab Chip* **11,** 466–473 (2011).
28. Huang, B. *et al.* Counting Low-Copy Number Proteins in a Single Cell. *Science (80-.).* **315,** 81 LP-84 (2007).
29. Leung, K. *et al.* A programmable droplet-based microfluidic device applied to multiparameter analysis of single microbes and microbial communities. *Proc. Natl. Acad. Sci.* **109,** 7665 LP-7670 (2012).
30. Shi, Q. *et al.* Single-cell proteomic chip for profiling intracellular signaling pathways in single tumor cells. *Proc. Natl. Acad. Sci.* **109,** 419 LP-424 (2012).
31. Sims, C. E. & Allbritton, N. L. Analysis of single mammalian cells on-chip. *Lab Chip* **7,** 423–440 (2007).
32. Stahl, B., Linos, A., Karas, M., Hillenkamp, F. & Steup, M. Analysis of Fructans from Higher Plants by Matrix-Assisted Laser Desorption/Ionization Mass Spectrometry. *Anal. Biochem.* **246,** 195–204 (1997).
33. Rubakhin, S. S., Garden, R. W., Fuller, R. R. & Sweedler, J. V. Measuring the peptides in individual organelles with mass spectrometry. *Nat. Biotechnol.* **18,** 172 (2000).
34. Li, L. *et al.* Egg-laying hormone peptides in the aplysiidae family. *J. Exp. Biol.* **202,** 2961 LP-2973 (1999).
35. Redeker, V., Toullec, J.-Y., Vinh, J., Rossier, J. & Soyez, D. Combination of Peptide Profiling by Matrix-Assisted Laser Desorption/Ionization Time-of-Flight Mass Spectrometry and Immunodetection on Single Glands or Cells. *Anal. Chem.* **70,** 1805–1811 (1998).
36. van Striena, F. J. C., Jespersen, S., van der Greef, J., Jenks, B. G. & Roubos, E. W. Identification of POMC processing products in single melanotrope cells by matrix-assisted laser desorption/ionization mass spectrometry. *FEBS Lett.* **379,**

165–170 (1996).
37. Vázquez-Martínez, R. M. *et al.* Analysis by mass spectrometry of POMC-derived peptides in amphibian melanotrope subpopulations. *Life Sci.* **64,** 923–930 (1999).
38. Jespersen, S., Chaurand, P., van Strien, F. J. C., Spengler, B. & van der Greef, J. Direct Sequencing of Neuropeptides in Biological Tissue by MALDI−PSD Mass Spectrometry. *Anal. Chem.* **71,** 660–666 (1999).
39. Lanni, E. J., Rubakhin, S. S. & Sweedler, J. V. Mass spectrometry imaging and profiling of single cells. *J. Proteomics* **75,** 5036–5051 (2012).
40. Guillaume-Gentil T.; Kiefer, P.; Ibanez, A. J.; Steinhoff, R.; Bronnimann, R.; Dorwling-Carter, L.; Zambelli, T.; Zenobi, R.; Vorholt, J. A., O. . R. Single-Cell Mass Spectrometry of Metabolites Extracted from Live Cells by Fluidic Force Microscopy. *Anal. Chem.* (2017). doi:10.1021/acs.analchem.7b00367
41. Zenobi, R. Single-Cell Metabolomics: Analytical and Biological Perspectives. *Science (80-.).* **342,** 1243259 (2013).
42. Chen, X. *et al.* Single-cell analysis at the threshold. *Nat. Biotechnol.* **34,** 1111 (2016).
43. Ibáñez, A. J. *et al.* Mass spectrometry-based metabolomics of single yeast cells. *Proc. Natl. Acad. Sci. U. S. A.* **110,** 8790–8794 (2013).
44. Nemes, P., Knolhoff, A. M., Rubakhin, S. S. & Sweedler, J. V. Single-cell metabolomics: changes in the metabolome of freshly isolated and cultured neurons. *ACS Chem. Neurosci.* **3,** 782–792 (2012).
45. Neupert, S., Rubakhin, S. S. & Sweedler, J. V. Targeted single-cell microchemical analysis: MS-based peptidomics of individual paraformaldehyde-fixed and immunolabeled neurons. *Chem. Biol.* **19,** 1010–1019 (2012).
46. Pan, N. *et al.* The Single-Probe: A Miniaturized Multifunctional Device for Single Cell Mass Spectrometry Analysis. *Anal. Chem.* **86,** 9376–9380 (2014).
47. Phelps, M., Hamilton, J. & Verbeck, G. F. Nanomanipulation-coupled nanospray mass spectrometry as an approach for single cell analysis. *Rev. Sci. Instrum.* **85,** 124101 (2014).
48. Rao, W., Pan, N. & Yang, Z. Applications of the Single-probe: Mass Spectrometry Imaging and Single Cell Analysis under Ambient Conditions. *J. Vis. Exp.* 53911 (2016). doi:10.3791/53911
49. Fujii, T. *et al.* Direct metabolomics for plant cells by live single-cell mass spectrometry. *Nat. Protoc.* **10,** 1445 (2015).
50. ALI, A. *et al.* Quantitative Live Single-cell Mass Spectrometry with Spatial Evaluation by Three-Dimensional Holographic and Tomographic Laser Microscopy. *Anal. Sci.* **32,** 125–127 (2016).
51. Fujita, H. *et al.* Comprehensive chemical secretory measurement of single cells trapped in a micro-droplet array with mass spectrometry. *RSC Adv.* **5,** 16968–16971 (2015).
52. Gong, X. *et al.* Single Cell Analysis with Probe ESI-Mass Spectrometry: Detection of Metabolites at Cellular and Subcellular Levels. *Anal. Chem.* **86,** 3809–3816 (2014).
53. Lorenzo Tejedor, M., Mizuno, H., Tsuyama, N., Harada, T. & Masujima, T. In Situ Molecular Analysis of Plant Tissues by Live Single-Cell Mass Spectrometry. *Anal. Chem.* **84,** 5221–5228 (2012).

54. Shimizu, T. *et al.* Live Single-Cell Plant Hormone Analysis by Video-Mass Spectrometry. *Plant Cell Physiol.* **56,** 1287–1296 (2015).
55. Yamamoto, K. *et al.* Cell-specific localization of alkaloids in Catharanthus roseus stem tissue measured with Imaging MS and Single-cell MS. *Proc. Natl. Acad. Sci.* **113,** 3891 LP-3896 (2016).
56. DATE, S., MIZUNO, H., TSUYAMA, N., HARADA, T. & MASUJIMA, T. Direct Drug Metabolism Monitoring in a Live Single Hepatic Cell by Video Mass Spectrometry. *Anal. Sci.* **28,** 201 (2012).
57. HIYAMA, E. *et al.* Direct Lipido-Metabolomics of Single Floating Cells for Analysis of Circulating Tumor Cells by Live Single-cell Mass Spectrometry. *Anal. Sci.* **31,** 1215–1217 (2015).
58. TSUYAMA, N., MIZUNO, H., TOKUNAGA, E. & MASUJIMA, T. Live Single-Cell Molecular Analysis by Video-Mass Spectrometry. *Anal. Sci.* **24,** 559–561 (2008).
59. Phelps, M. S. & Verbeck, G. F. A lipidomics demonstration of the importance of single cell analysis. *Anal. Methods* **7,** 3668–3670 (2015).
60. González-Serrano, A. F. *et al.* Desorption Electrospray Ionization Mass Spectrometry Reveals Lipid Metabolism of Individual Oocytes and Embryos. *PLoS One* **8,** e74981 (2013).
61. Shrestha, B., Nemes, P. & Vertes, A. Ablation and analysis of small cell populations and single cells by consecutive laser pulses. *Appl. Phys. A* **101,** 121–126 (2010).
62. Shrestha, B. & Vertes, A. In Situ Metabolic Profiling of Single Cells by Laser Ablation Electrospray Ionization Mass Spectrometry. *Anal. Chem.* **81,** 8265–8271 (2009).
63. Stolee, J. A., Shrestha, B., Mengistu, G. & Vertes, A. Observation of Subcellular Metabolite Gradients in Single Cells by Laser Ablation Electrospray Ionization Mass Spectrometry. *Angew. Chemie Int. Ed.* **51,** 10386–10389 (2012).
64. Stolee, J. A. & Vertes, A. Toward Single-Cell Analysis by Plume Collimation in Laser Ablation Electrospray Ionization Mass Spectrometry. *Anal. Chem.* **85,** 3592–3598 (2013).
65. Chen, F. *et al.* Single-Cell Analysis Using Drop-on-Demand Inkjet Printing and Probe Electrospray Ionization Mass Spectrometry. *Anal. Chem.* **88,** 4354–4360 (2016).
66. Yin, R., Prabhakaran, V. & Laskin, J. Quantitative Extraction and Mass Spectrometry Analysis at a Single-Cell Level. *Anal. Chem.* **90,** 7937–7945 (2018).
67. Yin, L., Zhang, Z., Liu, Y., Gao, Y. & Gu, J. Recent advances in single-cell analysis by mass spectrometry. *Analyst* **144,** 824–845 (2019).
68. Ferreira, C. R., Eberlin, L. S., Hallett, J. E. & Cooks, R. G. Single oocyte and single embryo lipid analysis by desorption electrospray ionization mass spectrometry. *J. Mass Spectrom.* **47,** 29–33 (2012).
69. Yang, Y. *et al.* Single-cell analysis by ambient mass spectrometry. *TrAC Trends Anal. Chem.* **90,** 14–26 (2017).
70. Masuda, K., Abouleila, Y., Ali, A., Yanagida, T. & Masujima, T. in (ed. António, C.) 269–282 (Springer New York, 2018). doi:10.1007/978-1-4939-7819-9_19
71. Lee, J. K., Jansson, E. T., Nam, H. G. & Zare, R. N. High-Resolution Live-Cell Imaging and Analysis by Laser Desorption/Ionization Droplet Delivery Mass

Spectrometry. *Anal. Chem.* **88,** 5453–5461 (2016).
72. Bergman, H.-M. & Lanekoff, I. Profiling and quantifying endogenous molecules in single cells using nano-DESI MS. *Analyst* **142,** 3639–3647 (2017).
73. Liu, Y. *et al.* Study on Variation of Lipids during Different Growth Phases of Living Cyanobacteria Using Easy Ambient Sonic-Spray Ionization Mass Spectrometry. *Anal. Chem.* **86,** 7096–7102 (2014).
74. Shrestha, B. *et al.* Subcellular Metabolite and Lipid Analysis of Xenopus laevis Eggs by LAESI Mass Spectrometry. *PLoS One* **9,** e115173 (2014).
75. Shrestha, B., Patt, J. M. & Vertes, A. In Situ Cell-by-Cell Imaging and Analysis of Small Cell Populations by Mass Spectrometry. *Anal. Chem.* **83,** 2947–2955 (2011).
76. Shrestha, B. & Vertes, A. in (ed. Sriram, G.) 31–39 (Humana Press, 2014). doi:10.1007/978-1-62703-661-0_3
77. Zhang, L. & Vertes, A. Single-Cell Mass Spectrometry Approaches to Explore Cellular Heterogeneity. *Angew. Chemie Int. Ed.* **57,** 4466–4477 (2018).
78. Zhang, L. *et al.* In Situ metabolic analysis of single plant cells by capillary microsampling and electrospray ionization mass spectrometry with ion mobility separation. *Analyst* **139,** 5079–5085 (2014).
79. Onjiko, R. M., Moody, S. A. & Nemes, P. Single-cell mass spectrometry reveals small molecules that affect cell fates in the 16-cell embryo. *Proc. Natl. Acad. Sci.* **112,** 6545 LP-6550 (2015).
80. Sun, M. & Yang, Z. Metabolomic Studies of Live Single Cancer Stem Cells Using Mass Spectrometry. *Anal. Chem.* **91,** 2384–2391 (2019).
81. Pan, N., Rao, W., Standke, S. J. & Yang, Z. Using dicationic ion-pairing compounds to enhance the single cell mass spectrometry analysis using the single-probe: A microscale sampling and ionization device. *Anal. Chem.* **88,** (2016).
82. Rao, W., Pan, N. & Yang, Z. High Resolution Tissue Imaging Using the Single-probe Mass Spectrometry under Ambient Conditions. *J. Am. Soc. Mass Spectrom.* **26,** 986–993 (2015).
83. Rao, W., Pan, N., Tian, X. & Yang, Z. High-Resolution Ambient MS Imaging of Negative Ions in Positive Ion Mode: Using Dicationic Reagents with the Single-Probe. *J. Am. Soc. Mass Spectrom.* **27,** 124–134 (2016).
84. Liu, R., Pan, N., Zhu, Y. & Yang, Z. T-Probe: An Integrated Microscale Device for Online In Situ Single Cell Analysis and Metabolic Profiling Using Mass Spectrometry. *Anal. Chem.* **90,** 11078–11085 (2018).
85. Liu, R., Zhang, G. & Yang, Z. Towards rapid prediction of drug-resistant cancer cell phenotypes: single cell mass spectrometry combined with machine learning. *Chem. Commun.* **55,** 616–619 (2019).
86. Tian, X., Zhang, G., Shao, Y. & Yang, Z. Towards enhanced metabolomic data analysis of mass spectrometry image: Multivariate Curve Resolution and Machine Learning. *Anal. Chim. Acta* **1037,** 211–219 (2018).
87. Sun, M., Tian, X. & Yang, Z. Microscale Mass Spectrometry Analysis of Extracellular Metabolites in Live Multicellular Tumor Spheroids. *Anal. Chem.* **89,** 9069–9076 (2017).
88. Sun, M., Yang, Z. & Wawrik, B. Metabolomic Fingerprints of Individual Algal Cells

Using the Single-Probe Mass Spectrometry Technique. *Front. Plant Sci.* **9,** 571 (2018).
89. Roberts, B. L. *et al.* Persistent, Multi-Generational Reduction of Oxysterol-Binding Protein Caused by Compound Treatment Induces Prophylactic Anti-Viral Activity. *ACS Chem. Biol.* (2018). doi:10.1021/acschembio.8b00984
90. Standke, S. J., Colby, D. H., Bensen, R. C., Burgett, A. W. G. & Yang, Z. Mass Spectrometry Measurement of Single Suspended Cells Using a Combined Cell Manipulation System and a Single-Probe Device. *Anal. Chem.* **91,** 1738–1742 (2019).
91. Specht, H. & Slavov, N. Transformative Opportunities for Single-Cell Proteomics. *J. Proteome Res.* **17,** 2565–2571 (2018).
92. Duncan, M. W., Roder, H. & Hunsucker, S. W. Quantitative matrix-assisted laser desorption/ionization mass spectrometry. *Brief. Funct. Genomic. Proteomic.* **7,** 355–370 (2008).
93. Wollscheid, B. *et al.* Mass-spectrometric identification and relative quantification of N-linked cell surface glycoproteins. *Nat. Biotechnol.* **27,** 378 (2009).
94. Lombard-Banek, C., Reddy, S., Moody, S. A. & Nemes, P. Label-free Quantification of Proteins in Single Embryonic Cells with Neural Fate in the Cleavage-Stage Frog (Xenopus laevis) Embryo using Capillary Electrophoresis Electrospray Ionization High-Resolution Mass Spectrometry (CE-ESI-HRMS). *Mol. Cell. Proteomics* **15,** 2756–2768 (2016).
95. Lombard-Banek, C., Moody, S. A. & Nemes, P. Single-Cell Mass Spectrometry for Discovery Proteomics: Quantifying Translational Cell Heterogeneity in the 16-Cell Frog (Xenopus) Embryo. *Angew. Chem. Int. Ed. Engl.* **55,** 2454–2458 (2016).
96. Budnik, B., Levy, E., Harmange, G. & Slavov, N. SCoPE-MS: mass spectrometry of single mammalian cells quantifies proteome heterogeneity during cell differentiation. *Genome Biol.* **19,** 161 (2018).
97. Budnik, B., Levy, E. & Slavov, N. Mass-spectrometry of single mammalian cells quantifies proteome heterogeneity during cell differentiation. *bioRxiv* (2017).
98. Mao, S. *et al.* In Situ Scatheless Cell Detachment Reveals Correlation between Adhesion Strength and Viability at Single-Cell Resolution. *Angew. Chemie Int. Ed.* **57,** 236–240 (2017).
99. Linwen, Z. & Akos, V. Single-Cell Mass Spectrometry Approaches to Explore Cellular Heterogeneity. *Angew. Chemie Int. Ed.* **57,** 4466–4477 (2017).
100. Fu, Q. *et al. Application of porous metal enrichment probe sampling to single cell analysis using matrix-assisted laser desorption ionization time of flight mass spectrometry (MALDI-TOF-MS)*. *Journal of mass spectrometry : JMS* **51,** (2016).
101. Passarelli, M. K., Ewing, A. G. & Winograd, N. Single-Cell Lipidomics: Characterizing and Imaging Lipids on the Surface of Individual Aplysia californica Neurons with Cluster Secondary Ion Mass Spectrometry. *Anal. Chem.* **85,** 2231–2238 (2013).
102. Passarelli, M. K. *et al.* Single-Cell Analysis: Visualizing Pharmaceutical and Metabolite Uptake in Cells with Label-Free 3D Mass Spectrometry Imaging. *Anal. Chem.* **87,** 6696–6702 (2015).
103. Ostrowski, S. G., Kurczy, M. E., Roddy, T. P., Winograd, N. & Ewing, A. G. Secondary Ion MS Imaging To Relatively Quantify Cholesterol in the Membranes

of Individual Cells from Differentially Treated Populations. *Anal. Chem.* **79,** 3554–3560 (2007).
104. Ong, T.-H., Tillmaand, E. G., Makurath, M., Rubakhin, S. S. & Sweedler, J. V. Mass spectrometry-based characterization of endogenous peptides and metabolites in small volume samples. *Biochim. Biophys. Acta* **1854,** 732–740 (2015).
105. Ferreira, C. R., Pirro, V., Eberlin, L. S., Hallett, J. E. & Cooks, R. G. Developmental phases of individual mouse preimplantation embryos characterized by lipid signatures using desorption electrospray ionization mass spectrometry. *Anal. Bioanal. Chem.* **404,** 2915–2926 (2012).
106. Mizuno, H., Tsuyama, N., Harada, T. & Masujima, T. Live single-cell video-mass spectrometry for cellular and subcellular molecular detection and cell classification. *J. Mass Spectrom.* **43,** 1692–1700 (2008).
107. ESAKI, T. & MASUJIMA, T. Fluorescence Probing Live Single-cell Mass Spectrometry for Direct Analysis of Organelle Metabolism. *Anal. Sci.* **31,** 1211–1213 (2015).
108. Mizuno N.; Harada, T.; Masujima, T., H. . T. Live single-cell video-mass spectrometry for cellular and subcellular molecular detection and cell classification. *J Mass Spectrom.* (2008). doi:10.1002/jms.1460
109. Pan, N., Rao, W., Standke, S. J. & Yang, Z. Using Dicationic Ion-Pairing Compounds To Enhance the Single Cell Mass Spectrometry Analysis Using the Single-Probe: A Microscale Sampling and Ionization Device. *Anal. Chem.* **88,** 6812–6819 (2016).
110. Hu, P., Zhang, W., Xin, H. & Deng, G. Single Cell Isolation and Analysis. *Front. Cell Dev. Biol.* **4,** 116 (2016).
111. Wu, C., Wu, P., Zhao, H., Liu, W. & Li, W. Clinical Applications of and Challenges in Single-Cell Analysis of Circulating Tumor Cells. *DNA Cell Biol.* **37,** 78–89 (2017).
112. Schober, Y., Guenther, S., Spengler, B. & Römpp, A. Single Cell Matrix-Assisted Laser Desorption/Ionization Mass Spectrometry Imaging. *Anal. Chem.* **84,** 6293–6297 (2012).
113. Pulfer, M. & Murphy, R. C. Electrospray mass spectrometry of phospholipids. *Mass Spectrom. Rev.* **22,** 332–364 (2003).
114. Neumann, M. H. D., Bender, S., Krahn, T. & Schlange, T. ctDNA and CTCs in Liquid Biopsy - Current Status and Where We Need to Progress. *Comput. Struct. Biotechnol. J.* **16,** 190–195 (2018).
115. Jelonek, K., Ros, M., Pietrowska, M. & Widlak, P. Cancer biomarkers and mass spectrometry-based analyses of phospholipids in body fluids. *Clin. Lipidol.* **8,** 137–150 (2013).
116. Kataoka, H. New trends in sample preparation for clinical and pharmaceutical analysis. *TrAC Trends Anal. Chem.* **22,** 232–244 (2003).
117. Yan, L. *et al.* Single-cell RNA-Seq profiling of human preimplantation embryos and embryonic stem cells. *Nat. Struct. Mol. Biol.* **20,** 1131–1139 (2013).
118. Kalisky, T. & Quake, S. R. Single-cell genomics. *Nat. Methods* **8,** 311–314 (2011).
119. Boggio, K. J. *et al.* Recent advances in single-cell MALDI mass spectrometry imaging and potential clinical impact. *Expert Rev. Proteomics* **8,** 591–604 (2011).

120. Fujii S.; Lorenzo Tejedor, M.; Esaki, T.; Sakane, I.; Mizuno, H.; Tsuyama, N.; Masujima, T., T. . M. Direct metabolomics for plant cells by live single-cell mass spectrometry. *Nat. Protoc.* **10,** (2015).
121. Dueñas, M. E., Essner, J. J. & Lee, Y. J. 3D MALDI Mass Spectrometry Imaging of a Single Cell: Spatial Mapping of Lipids in the Embryonic Development of Zebrafish. *Sci. Rep.* **7,** 14946 (2017).
122. Pan, N. *et al.* The Single-Probe: A Miniaturized Multifunctional Device for Single Cell Mass Spectrometry Analysis. *Anal. Chem.* **86,** 9376–9380 (2014).
123. Rao, W., Pan, N., Tian, X. & Yang, Z. High-Resolution Ambient MS Imaging of Negative Ions in Positive Ion Mode: Using Dicationic Reagents with the Single-Probe. *J. Am. Soc. Mass Spectrom.* **27,** 124–134 (2016).
124. Rao, W., Pan, N. & Yang, Z. Applications of the Single-probe: Mass Spectrometry Imaging and Single Cell Analysis under Ambient Conditions. *J. Vis. Exp.* 53911 (2016). doi:10.3791/53911
125. Pan, N., Rao, W., Standke, S. J. & Yang, Z. Using Dicationic Ion-Pairing Compounds To Enhance the Single Cell Mass Spectrometry Analysis Using the Single-Probe: A Microscale Sampling and Ionization Device. *Anal. Chem.* **88,** 6812–6819 (2016).
126. Zhao, L. *et al.* Intracellular water-specific MR of microbead-adherent cells: the HeLa cell intracellular water exchange lifetime. *NMR Biomed.* **21,** 159–164 (2008).
127. Tahara, M. *et al.* Cell diameter measurements obtained with a handheld cell counter could be used as a surrogate marker of G2/M arrest and apoptosis in colon cancer cell lines exposed to SN-38. *Biochem. Biophys. Res. Commun.* **434,** 753–759 (2013).
128. Gregg, J. L., McGuire, K. M., Focht, D. C. & Model, M. A. Measurement of the thickness and volume of adherent cells using transmission-through-dye microscopy. *Pflügers Arch. - Eur. J. Physiol.* **460,** 1097–1104 (2010).
129. Boss, D. *et al. Measurement of absolute cell volume, osmotic membrane water permeability, and refractive index of transmembrane water and solute flux by digital holographic microscopy*. *Journal of biomedical optics* **18,** (2013).
130. Shashni, B. *et al.* Size-Based Differentiation of Cancer and Normal Cells by a Particle Size Analyzer Assisted by a Cell-Recognition PC Software. *Biol. Pharm. Bull.* **41,** 487–503 (2018).
131. Klein, E. *et al.* Properties of the K562 cell line, derived from a patient with chronic myeloid leukemia. *Int. J. cancer* **18,** 421–31 (1976).
132. Chong J., Soufan, O., Li, C., Caraus, I., Li, S., Bourque, G., Wishart, D.S., and Xia, J. MetaboAnalyst 4.0: towards more transparent and integrative metabolomics analysis. *Nucl. Acids Res.* (2018). doi:doi:10.1093/nar/gky310
133. Romano, P. *et al.* Geena 2, improved automated analysis of MALDI/TOF mass spectra. *BMC Bioinformatics* **17,** 61 (2016).
134. Huang, Q., Mao, S., Khan, M., Zhou, L. & Lin, J.-M. Dean flow assisted cell ordering system for lipid profiling in single-cells using mass spectrometry. *Chem. Commun.* **54,** 2595–2598 (2018).
135. Vasdekis, A. E. & Stephanopoulos, G. Review of methods to probe single cell metabolism and bioenergetics. *Metab. Eng.* **27,** 115–135 (2015).

136. Polat, A. N. & Özlü, N. Towards single-cell LC-MS phosphoproteomics. *Analyst* **139,** 4733–4749 (2014).
137. Svatoš, A. Single-cell metabolomics comes of age: new developments in mass spectrometry profiling and imaging. *Anal. Chem.* **83,** 5037–5044 (2011).
138. Junot, C., Fenaille, F., Colsch, B. & Bécher, F. High resolution mass spectrometry based techniques at the crossroads of metabolic pathways. *Mass Spectrom. Rev.* **33,** 471–500 (2014).
139. Murakami, I. *et al.* Acute-phase ITIH4 levels distinguish multi-system from single-system Langerhans cell histiocytosis via plasma peptidomics. *Clin. Proteomics* **12,** 16 (2015).
140. Zavalin, A. *et al.* Direct imaging of single cells and tissue at sub-cellular spatial resolution using transmission geometry MALDI MS. *J. Mass Spectrom.* **47,** i–i (2012).
141. Krismer, J., F. Steinhoff, R. & Zenobi, R. *Single-cell MALDI Tandem Mass Spectrometry: Unambiguous Assignment of Small Biomolecules from Single Chlamydomonas reinhardtii Cells*. *CHIMIA International Journal for Chemistry* **70,** (2016).
142. Ong, T.-H. *et al.* Classification of Large Cellular Populations and Discovery of Rare Cells Using Single Cell Matrix-Assisted Laser Desorption/Ionization Time-of-Flight Mass Spectrometry. *Anal. Chem.* **87,** 7036–7042 (2015).
143. Urban, P. L. Quantitative mass spectrometry: an overview. *Philos. Trans. A. Math. Phys. Eng. Sci.* **374,** 20150382 (2016).
144. Thomas, M. *et al.* Visualization of high resolution spatial mass spectrometric data during acquisition. *Conf. Proc. ... Annu. Int. Conf. IEEE Eng. Med. Biol. Soc. IEEE Eng. Med. Biol. Soc. Annu. Conf.* **2012,** 5545–5548 (2012).
145. Luchette, M., Korideck, H., Makrigiorgos, M., Tillement, O. & Berbeco, R. Radiation dose enhancement of gadolinium-based AGuIX nanoparticles on HeLa cells. *Nanomedicine Nanotechnology, Biol. Med.* **10,** 1751–1755 (2014).
146. L Rothenberg, M. *Irinotecan (CPT-11): Recent Developments and Future Directions-Colorectal Cancer and Beyond*. *The oncologist* **6,** (2001).
147. Rubakhin, S. S. & Sweedler, J. V. Quantitative Measurements of Cell−Cell Signaling Peptides with Single-Cell MALDI MS. *Anal. Chem.* **80,** 7128–7136 (2008).
148. Lin, J. H. & Lu, A. Y. H. Role of Pharmacokinetics and Metabolism in Drug Discovery and Development. *Pharmacol. Rev.* **49,** 403 LP-449 (1997).
149. Kubo, S. *et al.* Acylated cholestane glycosides from the bulbs of Ornithogalum saundersiae. *Phytochemistry* **31,** 3969–3973 (1992).
150. Zhou, Y. *et al.* OSW-1: a natural compound with potent anticancer activity and a novel mechanism of action. *J. Natl. Cancer Inst.* **97,** 1781–1785 (2005).
151. Burgett, A. W. G. *et al.* Natural products reveal cancer cell dependence on oxysterol-binding proteins. *Nat. Chem. Biol.* **7,** 639–647 (2011).
152. Garcia-Prieto, C. *et al.* Effective killing of leukemia cells by the natural product OSW-1 through disruption of cellular calcium homeostasis. *J. Biol. Chem.* **288,** 3240–3250 (2013).
153. Wills, Q. F. & Mead, A. J. Application of single-cell genomics in cancer: promise and challenges. *Hum. Mol. Genet.* **24,** R74–R84 (2015).

154. Kann, B., Offerhaus, H. L. & Otto, C. Raman microscopy for cellular investigations — From single cell imaging to drug carrier uptake visualization. *Adv. Drug Deliv. Rev.* **89,** 71–90 (2015).
155. Pan, N. *et al.* The single-probe: a miniaturized multifunctional device for single cell mass spectrometry analysis. *Anal. Chem.* **86,** 9376–9380 (2014).
156. Collins, F. S. & Varmus, H. A New Initiative on Precision Medicine. *N. Engl. J. Med.* **372,** 793–795 (2015).
157. Roychowdhury, S. & Chinnaiyan, A. M. Advancing precision medicine for prostate cancer through genomics. *J. Clin. Oncol.* **31,** 1866–73 (2013).
158. Sawyer, M. & Ratain, M. J. Body Surface Area as a Determinant of Pharmacokinetics and Drug Dosing. *Invest. New Drugs* **19,** 171–177 (2001).
159. PINKEL, D. The use of body surface area as a criterion of drug dosage in cancer chemotherapy. *Cancer Res.* **18,** 853–6 (1958).
160. Bardin, C. *et al.* Therapeutic drug monitoring in cancer – Are we missing a trick? *Eur. J. Cancer* **50,** 2005–2009 (2014).
161. Kang, J. S. & Lee, M. H. Overview of therapeutic drug monitoring. *Korean J. Intern. Med.* **24,** 1–10 (2009).
162. Nguyen, L. V., Vanner, R., Dirks, P. & Eaves, C. J. Cancer stem cells: an evolving concept. *Nat. Rev. Cancer* **12,** 133–143 (2012).
163. CRISTOFANILLI, M. Circulating Tumor Cells, Disease Progression, and Survival in Metastatic Breast Cancer. *Semin. Oncol.* **33,** 9–14 (2006).
164. Gerlinger, M. *et al.* Intratumor Heterogeneity and Branched Evolution Revealed by Multiregion Sequencing. *N. Engl. J. Med.* **366,** 883–892 (2012).
165. Marusyk, A., Almendro, V. & Polyak, K. Intra-tumour heterogeneity: a looking glass for cancer? *Nat. Rev. Cancer* **12,** 323–334 (2012).
166. Andersson, H. & van den Berg, A. Microtechnologies and nanotechnologies for single-cell analysis. *Curr. Opin. Biotechnol.* **15,** 44–49 (2004).
167. Wang, D. & Bodovitz, S. Single cell analysis: the new frontier in ‘omics’. *Trends Biotechnol.* **28,** 281–290 (2010).
168. Shapiro, E., Biezuner, T. & Linnarsson, S. Single-cell sequencing-based technologies will revolutionize whole-organism science. *Nat. Rev. Genet.* **14,** 618–630 (2013).
169. Lecault, V., White, A. K., Singhal, A. & Hansen, C. L. Microfluidic single cell analysis: from promise to practice. *Curr. Opin. Chem. Biol.* **16,** 381–390 (2012).
170. Schmid, A., Kortmann, H., Dittrich, P. S. & Blank, L. M. Chemical and biological single cell analysis. *Curr. Opin. Biotechnol.* **21,** 12–20 (2010).
171. Rubakhin, S. S., Lanni, E. J. & Sweedler, J. V. Progress toward single cell metabolomics. *Curr. Opin. Biotechnol.* **24,** 95–104 (2013).
172. Masujima, T. Live single-cell mass spectrometry. *Anal. Sci.* **25,** 953–60 (2009).
173. Urban, P. L., Schmid, T., Amantonico, A. & Zenobi, R. Multidimensional Analysis of Single Algal Cells by Integrating Microspectroscopy with Mass Spectrometry. *Anal. Chem.* **83,** 1843–1849 (2011).
174. Greving, M. P., Patti, G. J. & Siuzdak, G. Nanostructure-Initiator Mass Spectrometry Metabolite Analysis and Imaging. *Anal. Chem.* **83,** 2–7 (2011).
175. Miura, D., Fujimura, Y. & Wariishi, H. In situ metabolomic mass spectrometry imaging: Recent advances and difficulties. doi:10.1016/j.jprot.2012.02.011

176. Zemski Berry, K. A. *et al.* MALDI Imaging of Lipid Biochemistry in Tissues by Mass Spectrometry. *Chem. Rev.* **111,** 6491–6512 (2011).
177. and, P. N. & Vertes*, A. Laser Ablation Electrospray Ionization for Atmospheric Pressure, in Vivo, and Imaging Mass Spectrometry. (2007). doi:10.1021/AC071181R
178. Chughtai, K. & Heeren, R. M. A. Mass Spectrometric Imaging for Biomedical Tissue Analysis. *Chem. Rev.* **110,** 3237–3277 (2010).
179. von der Maase, H. *et al.* Gemcitabine and Cisplatin Versus Methotrexate, Vinblastine, Doxorubicin, and Cisplatin in Advanced or Metastatic Bladder Cancer: Results of a Large, Randomized, Multinational, Multicenter, Phase III Study. *J. Clin. Oncol.* **18,** 3068–3077 (2000).
180. de Sousa Cavalcante, L. & Monteiro, G. Gemcitabine: Metabolism and molecular mechanisms of action, sensitivity and chemoresistance in pancreatic cancer. *Eur. J. Pharmacol.* **741,** 8–16 (2014).
181. Wickremsinhe, E. *et al.* Preclinical Absorption, Distribution, Metabolism, and Excretion of an Oral Amide Prodrug of Gemcitabine Designed to Deliver Prolonged Systemic Exposure. *Pharmaceutics* **5,** 261–276 (2013).
182. van Nuland, M. *et al.* Ultra-sensitive LC–MS/MS method for the quantification of gemcitabine and its metabolite 2′,2′-difluorodeoxyuridine in human plasma for a microdose clinical trial. *J. Pharm. Biomed. Anal.* **151,** 25–31 (2018).
183. Bowen, C., Wang, S. & Licea-Perez, H. Development of a sensitive and selective LC–MS/MS method for simultaneous determination of gemcitabine and 2,2-difluoro-2-deoxyuridine in human plasma. *J. Chromatogr. B* **877,** 2123–2129 (2009).
184. Jansen, R. S., Rosing, H., Schellens, J. H. M. & Beijnen, J. H. Simultaneous quantification of 2′,2′-difluorodeoxycytidine and 2′,2′-difluorodeoxyuridine nucleosides and nucleotides in white blood cells using porous graphitic carbon chromatography coupled with tandem mass spectrometry. *Rapid Commun. Mass Spectrom.* **23,** 3040–3050 (2009).
185. Bapiro, T. E. *et al.* A novel method for quantification of gemcitabine and its metabolites 2’,2’-difluorodeoxyuridine and gemcitabine triphosphate in tumour tissue by LC-MS/MS: comparison with (19)F NMR spectroscopy. *Cancer Chemother. Pharmacol.* **68,** 1243–53 (2011).
186. Pan, N. *et al.* The Single-Probe: A Miniaturized Multifunctional Device for Single Cell Mass Spectrometry Analysis. *Anal. Chem.* **86,** 9376–9380 (2014).
187. Gregg, J. L., McGuire, K. M., Focht, D. C. & Model, M. A. Measurement of the thickness and volume of adherent cells using transmission-through-dye microscopy. *Pflugers Arch.* **460,** 1097–104 (2010).
188. S. Chou, T. *et al. Stereospecific Synthesis of 2-Deoxy-2,2-difluororibonolactone and Its Use in the Preparation of 2'-Deoxy-2',2'-difluoro-β-D-ribofuranosyl Pyrimidine Nucleosides: The Key Role of Selective Crystallization*. *Synthesis-stuttgart* **1992,** (1992).
189. Chou, T. S. *et al.* Stereospecific Synthesis of 2-Deoxy-2,2-difluororibonolactone and Its Use in the Preparation of 2’-Deoxy-2’,2’-difluoro-β-D-ribofuranosyl Pyrimidine Nucleosides: The Key Role of Selective Crystallization. *Synthesis (Stuttg).* 565–570 (1992).

Appendix A

(a)

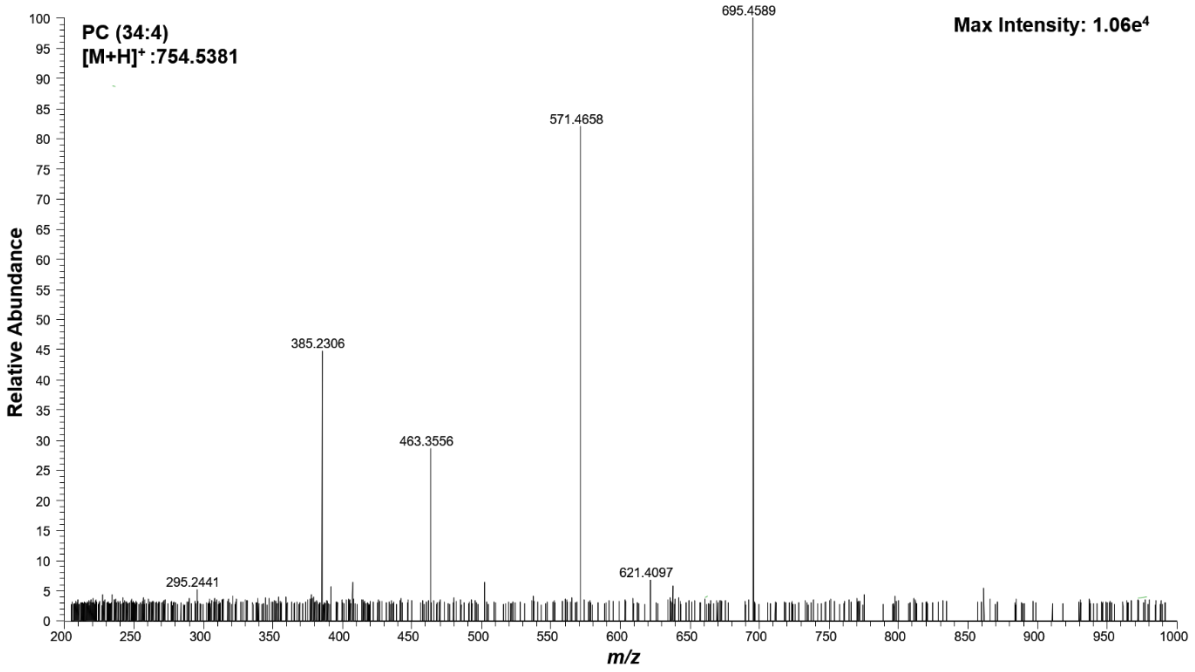

(b)

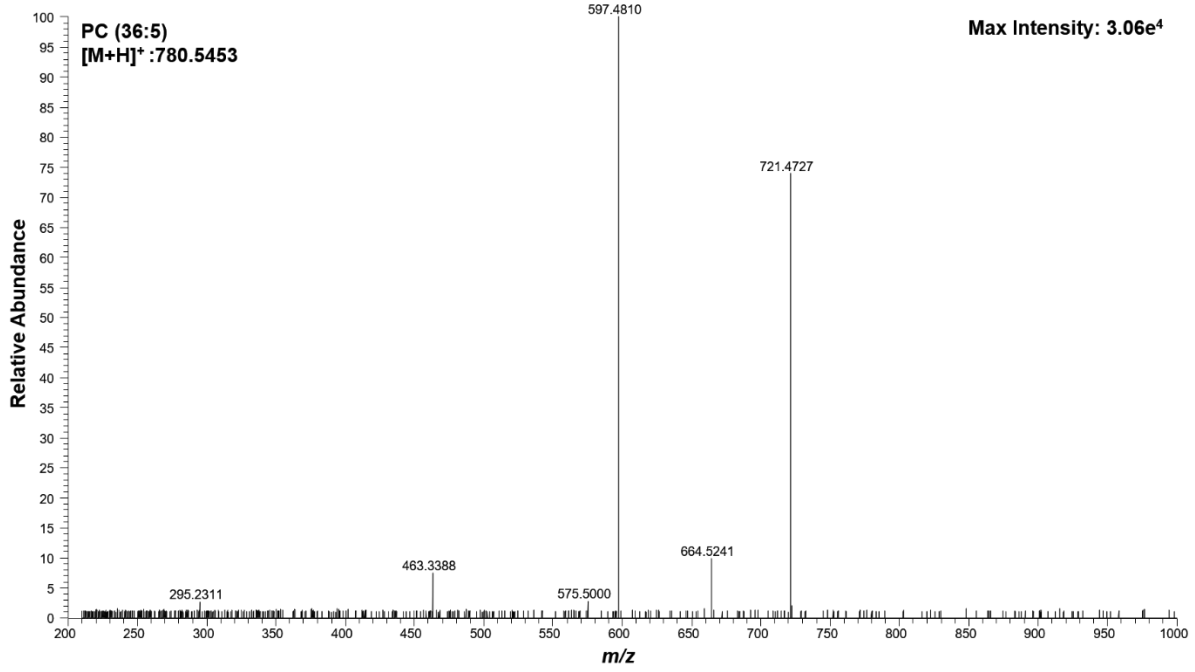

(c)

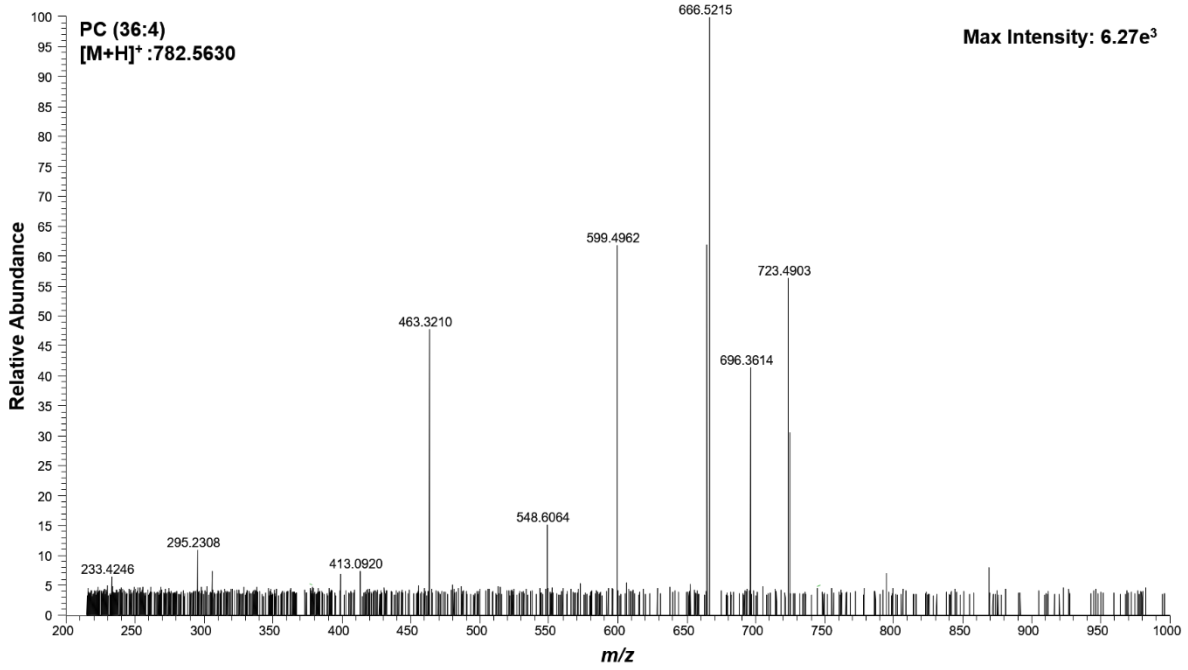
PC (36:4)
[M+H]+ :782.5630
Max Intensity: 6.27e3
Relative Abundance
m/z
666.5215
599.4962
723.4903
463.3210
696.3614
548.6064
295.2308
233.4246
413.0920

(d)

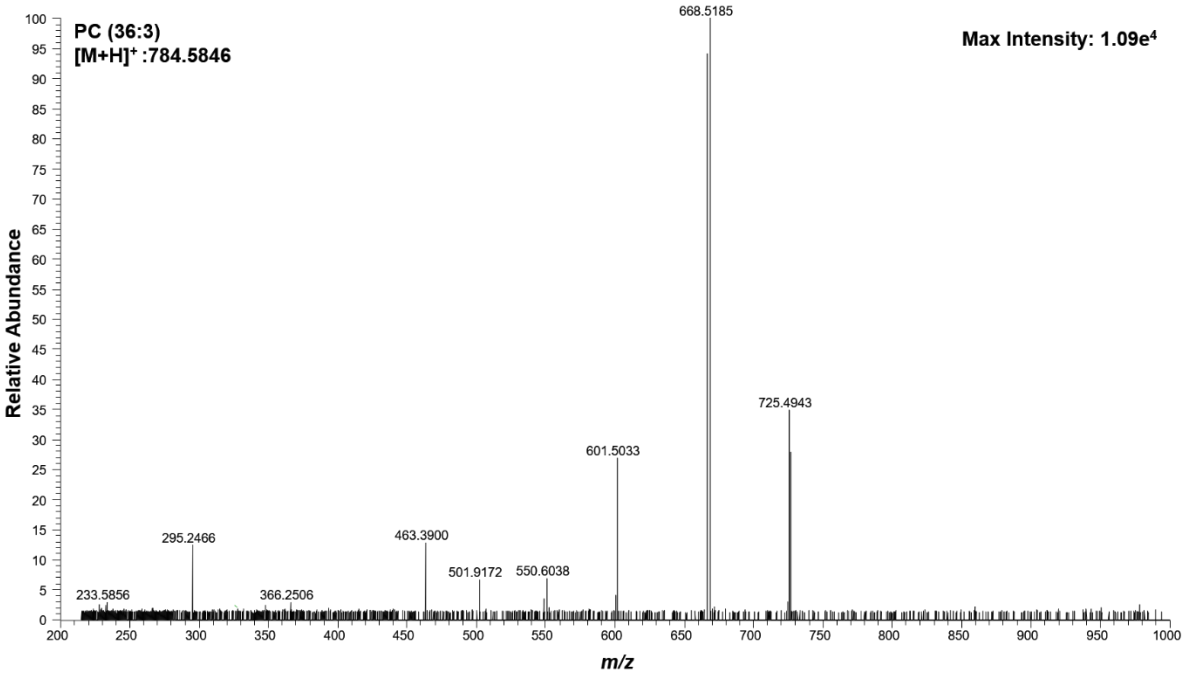
PC (36:3)
[M+H]+ :784.5846
Max Intensity: 1.09e4
Relative Abundance
m/z
668.5185
725.4943
601.5033
295.2466
463.3900
501.9172
550.6038
233.5856
366.2506

(e)

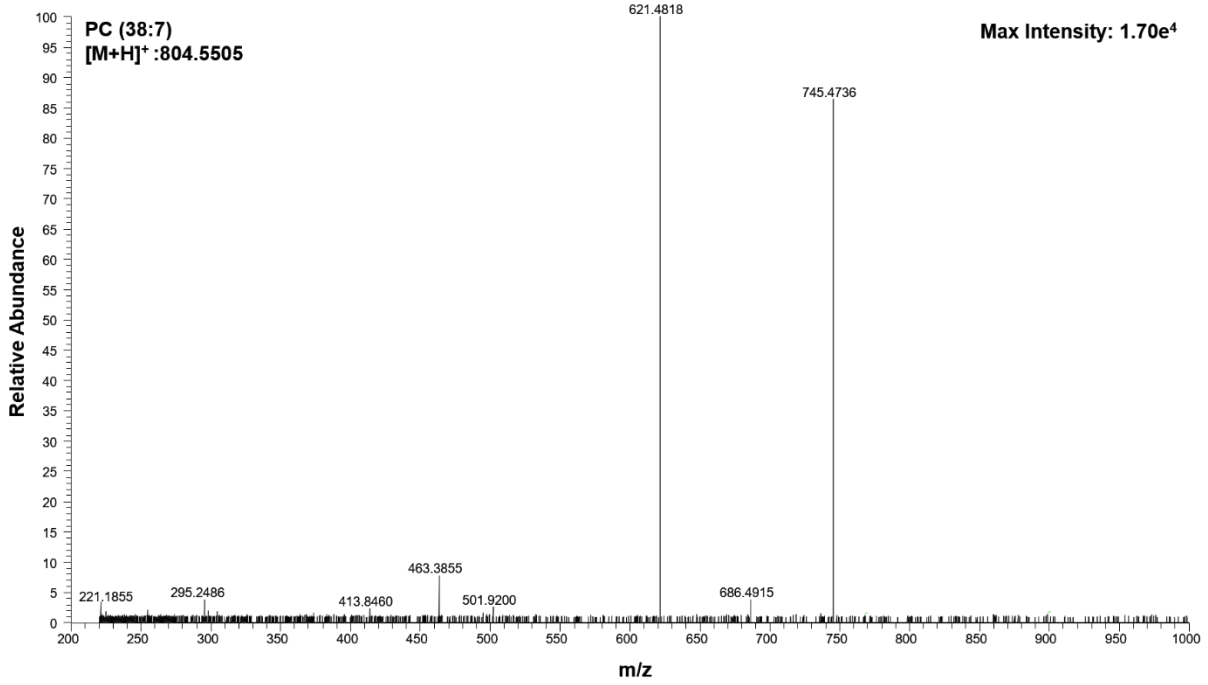
PC (38:7)
[M+H]+ :804.5505
Max Intensity: 1.70e4
621.4818
745.4736
463.3855
221.1855
295.2486
413.8460
501.9200
686.4915
Relative Abundance
m/z

(f)

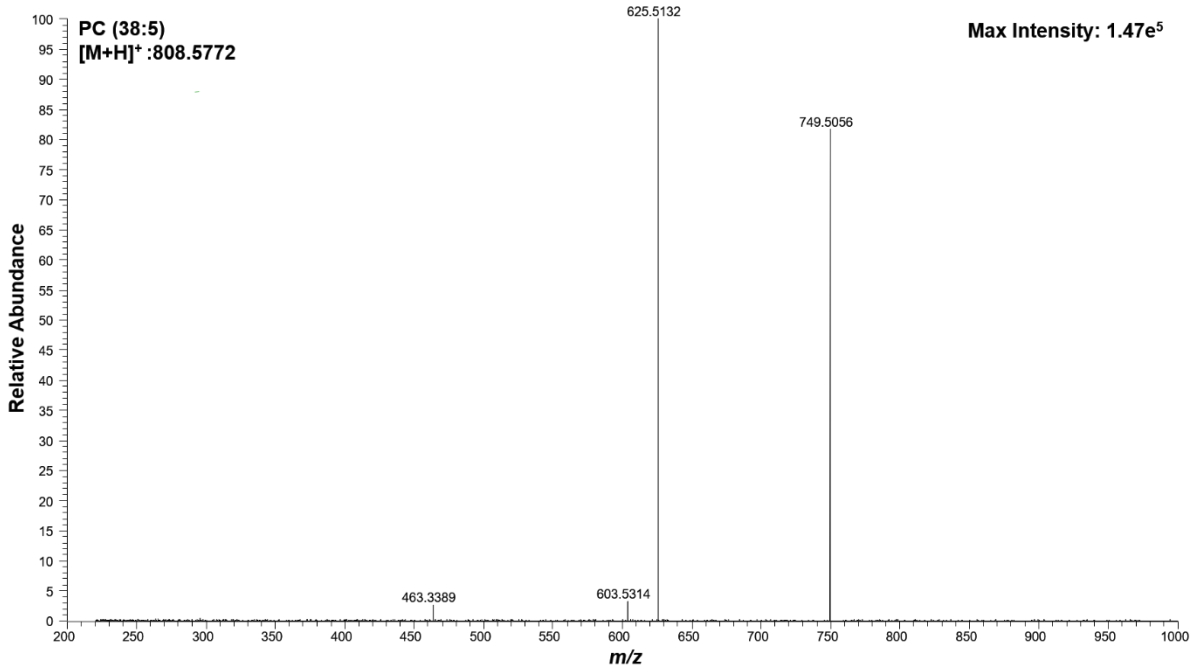
PC (38:5)
[M+H]+ :808.5772
Max Intensity: 1.47e5
625.5132
749.5056
463.3389
603.5314
Relative Abundance
m/z

(g)

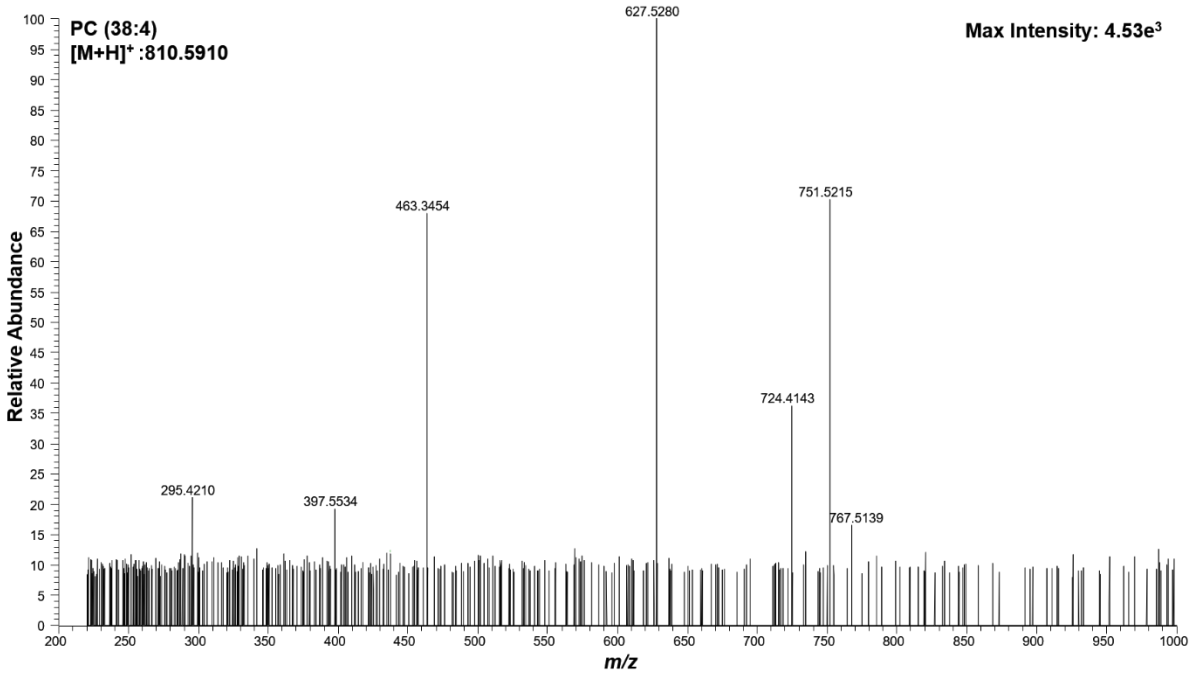

(h)

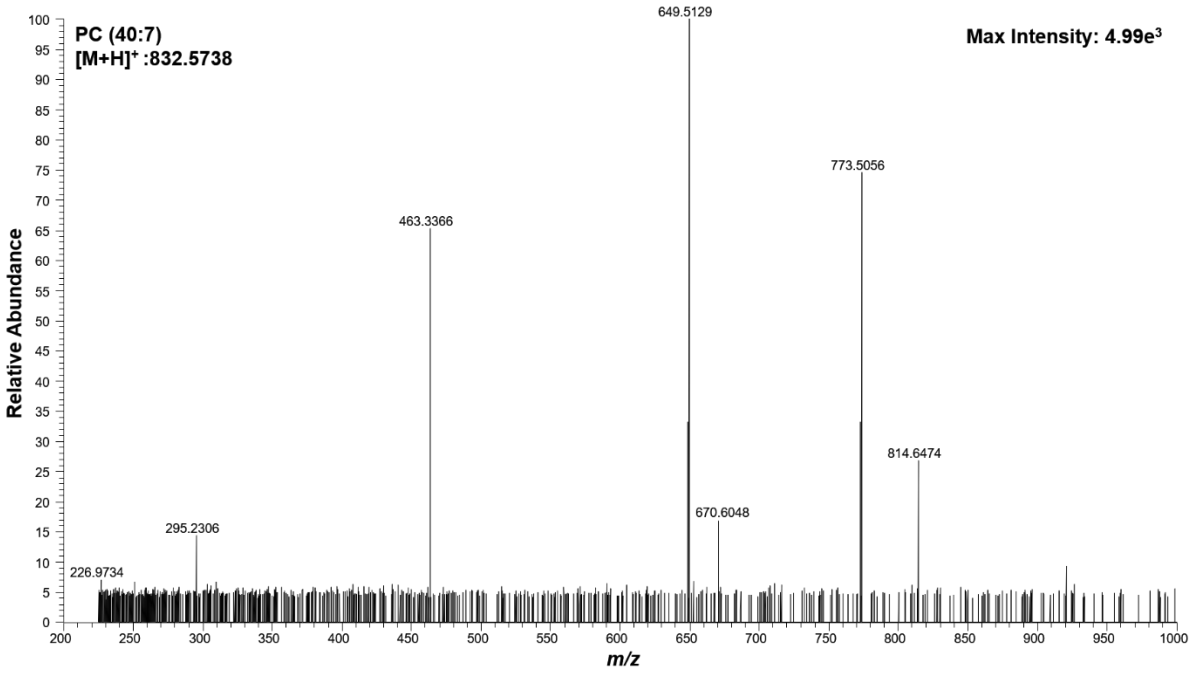

Figure A1. MS/MS verification of lipids with 10-40 manufacturer's unit energy at: (a) *m/z* 754.5 (b) *m/z* 780.5 (c) *m/z* 782.5 (d) *m/z* 784.5 (e) *m/z* 804.5 (f) *m/z* 808.5 (g) *m/z* 810.5 (h) *m/z* 832.5.

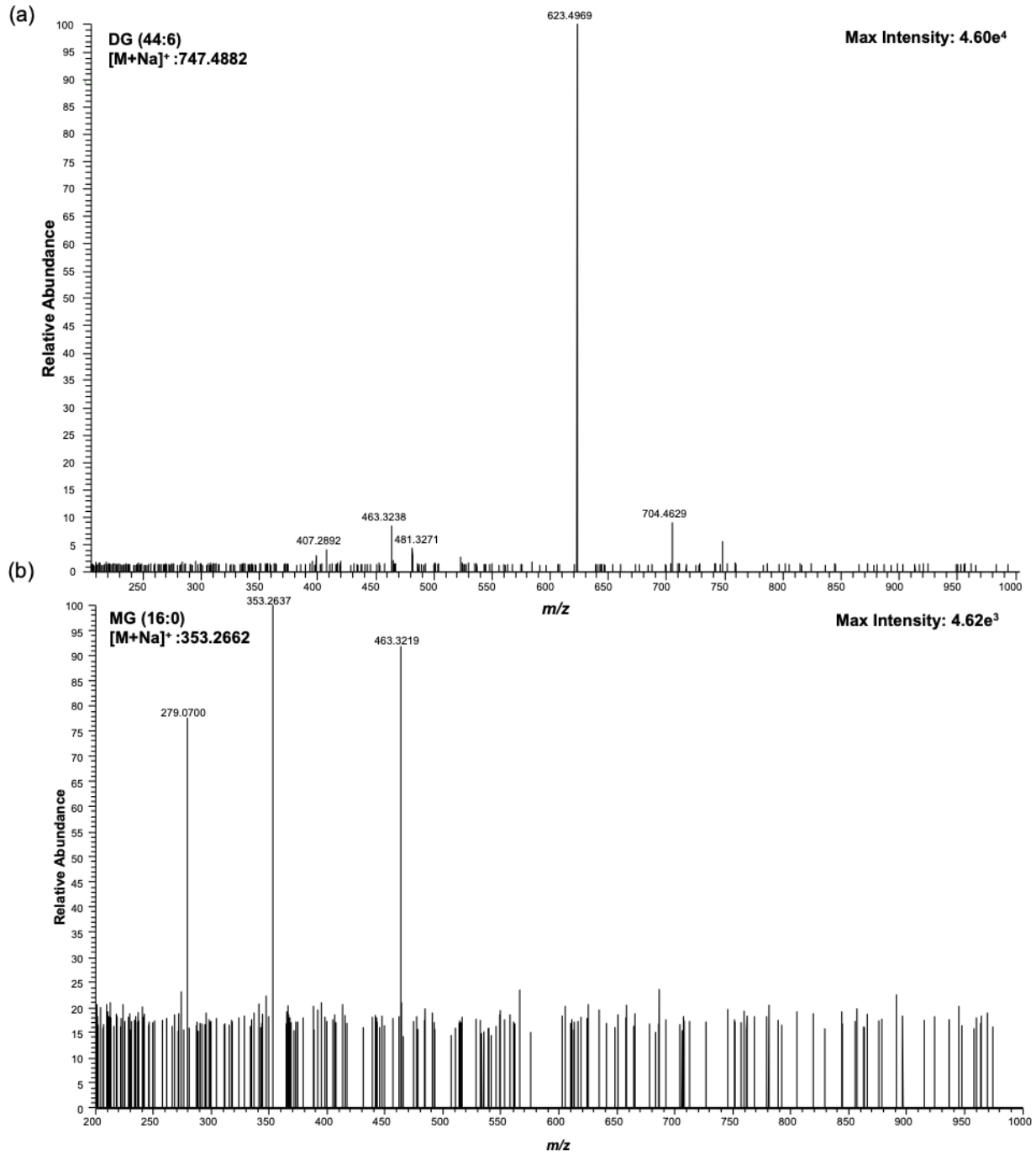

Figure A2. MS/MS verification of lipids with 10-40 manufacturer's unit energy at: (a) *m/z* 747.4 (b) *m/z* 353.2

Appendix B

B.1. Methods

B.1.1. Cell Cytotoxicity Assay.

T24 cell lines were grown in McCoy's medium supplemented with 10% synthetic FBS and 1% penicillin-streptomycin. All cells were maintained in an incubator at 37°C under 5% CO_2, and they were passaged around 75% confluency. Cells (5000 cells/well) were plated into 96-well plates in 75 µL of medium. After 24 h, a time-zero plate was produced by adding 25 µL of medium and 20 µL of CellTiter-Blue (Promega) to the wells and then incubating the plates at 37 °C for 90 min. Fluorescence (560 nm excitation; 590 nm emission) was detected using a Tecan Infinite M200 to establish cell viability at time of dosing. Then, compounds were serially diluted in medium and delivered to the cells as 4x solutions in 25 µL of medium. After 48 h, CellTiter-Blue was added, and the fluorescence was recorded as described above. Growth relative to untreated cells was calculated, and this data was fitted to a four-parameter dose-response curve using GraphPad Prism 8.

B.1.2. Isotopically-Labeled Gemcitabine.

Stable-isotopically labeled gemcitabine was accessed through a short sequence of reactions following the synthetic route that scientists at Eli Lily published in 1991.[188] The starting material 3,5-di-O-benzoate-2-deoxy-2,2-difluoro-D-ribofuranose 4.3 (**Scheme B1**) was purchased commercially as a mixture of both anomers. The hemiacetal mixture was then activated as glycosyl donor by conversion of the free hydroxyl group to a mesyl group in 4.4 with good yield (82%). The glycosyl acceptor

was prepared from commercially available 2-13C, 1,3-15N2 cytosine 4.5 (Scheme 35). Glycosyl acceptor 4.6 was prepared in situ from heating the mixture of cytosine 4.5 and hexamethyldisilane to reflux in presence of ammonium sulfate for 45 minutes. Utilizing the Vorbrueggen glycosylation method, the mesylated glycosyl donor 4.4 was reacted with silylated glycosyl acceptor 4.6 and trimethylsilyl trifluoromethanesulfonate as the activator in refluxing 1,2-dichloroethane for 48 hours. This reaction produced a mixture of protected isotopically labeled gemcitabine 4.7 (76% yield). The glycosylation reaction was presumed to proceed through an SN1 pathway involving an oxonium ion intermediate, which resulted in a mixture of nucleoside anomers with the ratio of α : β being 1.3 : 1 as measured through 1H NMR.

Treating the mixture 4.7 with ammonia in anhydrous methanol effectively removed both benzoyl protecting groups. The anomeric mixture of deprotected nucleoside were successfully separated through semi-preparative reverse-phase HPLC to afford desired β-anomer (4.8 in 34% yield) and α-anomer (4.9 in 4.0% yield). The desired β-nucleoside 4.8 was then converted to the hydrochloride salt of gemcitabine 4.10 in the presence of equimolar HCl in isopropanol. The molecular weight of the stable-isotopically labeled gemcitabine 4.10 was confirmed through high resolution mass spectrometry.

B.1.3. Compound Data.

Compound **4.4 (Scheme S1)** was synthesized as previously described.[189] To a solution of 2-Deoxy-2,2-difluoro-D-ribofuranose-3,5-dibenzoate (200.0 mg, 0.529 mmol) in anhydrous DCM (2 mL, 0.26 M) at 0°C was added triethylamine (103 µL, 0.74 mmol),

followed by methanesulfonyl chloride (49 µL, 0.634 mmol). The reaction mixture was stirred at RT for 4h15m, when it was completed base on TLC analysis. The reaction mixture was diluted with DCM (20 mL), washed with 1N HCl (15 mL), 5% $NaHCO_3$ solution (15 mL), DI H_2O (15 mL), and brine. The organic phase was dried over Na_2SO_4 and filtered. The solvent was removed in vacuo to afford mixture of products (α:β = 1.3:1) as a sticky yellow gel (200 mg, 82% yield). Products # was used in the next step without further purification. ^{1}H NMR (400 MHz, Chloroform-d) δ 8.07 (dt, J = 8.5, 1.5 Hz, 5H), 8.05 – 8.02 (m, 2H), 7.66 – 7.61 (m, 2H), 7.58 (td, J = 7.5, 1.4 Hz, 2H), 7.46 (dtd, J = 15.6, 7.7, 2.4 Hz, 9H), 6.13 (d, J = 6.3 Hz, 1H), 6.03 (d, J = 6.5 Hz, 0H), 5.93 (dd, J = 15.0, 6.8 Hz, 1H), 5.57 (dd, J = 16.4, 4.3 Hz, 1H), 4.85 (q, J = 4.1 Hz, 1H), 4.79 – 4.70 (m, 2H), 4.70 – 4.57 (m, 3H), 3.17 (s, 3H), 3.02 (s, 3H). ^{13}C NMR (101 MHz, Chloroform-d) δ 166.01, 165.92, 165.09, 164.95, 134.35, 134.29, 133.74, 133.60, 130.26, 130.19, 129.86, 129.23, 129.16, 128.85, 128.82, 128.79, 128.64, 128.14, 127.98, 123.49, 123.13, 121.01, 120.74, 120.61, 120.45, 118.26, 117.93, 99.99, 99.74, 99.52, 99.28, 99.21, 98.96, 98.79, 98.54, 82.83, 82.80, 82.77, 79.84, 79.76, 71.34, 71.17, 70.98, 70.81, 69.75, 69.60, 69.49, 69.34, 63.06, 62.55, 40.42, 40.30.

Compounds **4.7** were synthesized with procedure adapted from Chou et al.[189] A suspension of isotopically labeled cytosine **4.5** (25.0 mg, 0.219 mmol), ammonium sulfate (1.2 mg, 0.009 mmol) in hexamethyldisilazane (300 µL, 1.4 mmol) was heated under reflux (130°C) for 45 minutes. The reaction mixture was then cooled to RT. Under N_2 atmosphere, to this reaction mixture was added 1,2-dichloroethane (0.75 mL, 0.3 M) and trimethylsilyl trifluoromethanesulfonate (40 µL, 0.144 mmol). The clear, colorless solution was stirred at RT for 45 minutes. To the reaction mixture was then added **4.4**

(66 mg, 0.144 mmol, dissolved in 0.66 mL 1,2-dichloroethane). The reaction mixture was heated under reflux (90°C). The reaction progress was monitored by TLC (5% MeOH/$CHCl_3$, UV). 1,2-DCE was added periodically to keep the same reaction concentration. After 72 hours, the reaction was completed based on TLC analysis. The reaction mixture was cooled to RT, the solvent was removed *in vacuo* to afford a thick gel, which was dissolved in EtOAc (40 mL), washed with DI H_2O (5 mL x 3), 5% $NaHCO_3$ solution (5 mL). The organic phased was dried over Na_2SO_4 and filtered. The solvent was removed *in vacuo* to afford crude mixture (64.8 mg), which was purified through silica gel column chromatography (eluted with MeOH/$CHCl_3$ gradient, 2% to 10% MeOH) to afford desired products 5 as a white powder (52.7 mg, 76% yield). ^{1}H NMR (500 MHz, Chloroform-d) δ 8.10 – 8.03 (m, 6H), 8.03 – 7.99 (m, 2H), 7.67 – 7.56 (m, 4H), 7.51 – 7.41 (m, 10H), 6.68 (t, J = 7.0 Hz, 1H), 6.56 (bs, 1H), 5.83 (dd, J = 7.6, 3.6 Hz, 1H), 5.78 (dt, J = 10.3, 5.2 Hz, 1H), 5.70 (dd, J = 7.6, 3.7 Hz, 1H), 5.64 (d, J = 13.1 Hz, 1H), 4.86 – 4.75 (m, 2H), 4.68 (dd, J = 12.4, 4.6 Hz, 1H), 4.64 (d, J = 5.0 Hz, 2H), 4.55 (td, J = 4.7, 3.3 Hz, 1H).

Compounds **4.8** and **4.9** were synthesized with procedure adapted from Chou *et al*.[189]To a suspension of **4.7** (47.6 mg, 0.10 mmol) in anhydrous MeOH (2 mL) at RT was added NH_3 solution in MeOH (100 µL, 7M solution). The reaction mixture was stirred at RT and the reaction progress was monitored by TLC (10% MeOH/$CHCl_3$, UV). The reaction was completed after 16h by TLC. The solvent was removed *in vacuo* to afford an oily residue, which was resuspended in DI H_2O (10 mL) and EtOAc (5 mL). The aqueous phase was extracted with EtOAc (5 mL) while the organic phase was washed with DI H_2O (5 mL). The combined aqueous phase was concentrated *in vacuo*

to afford crude product as a clear gel (25 mg, 94%). The crude mixture was purified through LCMS (C18 column, condition) to afford **4.9** (α-anomer-10.5 mg, 39.5%) and **4.8** (β-anomer-9.0 mg, 33.9%).

Compounds **4.10** were synthesized with procedure adapted from Chou *et al*.[189] **4.8** (9.0 mg) was dissolved in DI H_2O (0.5 mL) and isopropanol (0.5 mL), then HCl solution (6 µL of 6N solution) was added. The mixture was mixed for 5 minutes, then the solvent was removed in vacuo to afford **4.10** as a white solid (10.1 mg). ^{1}H NMR (400 MHz, Deuterium Oxide) δ 8.06 – 7.98 (m, 1H), 6.33 – 6.22 (m, 2H), 4.40 (td, J = 11.7, 8.3 Hz, 1H), 4.18 – 4.09 (m, 1H), 4.04 (d, J = 12.3 Hz, 1H), 3.89 (dd, J = 13.1, 4.4 Hz, 1H). ^{13}C NMR (101 MHz, Deuterium Oxide) δ 160.58 (d, J = 14.2 Hz), 144.62 (d, J = 12.6 Hz), 121.62 (t, J = 260.5 Hz), 96.44 (d, J = 3.7 Hz), 86.30 – 84.66 (m), 81.81 (d, J = 7.7 Hz), 71.46 – 68.07 (m), 60.12. ^{19}F NMR (376 MHz, Deuterium Oxide) δ -116.75 (dd, J = 13.0, 5.5 Hz), -117.39 (dd, J = 12.9, 5.4 Hz), -118.00, -118.64. IR and HRSM HRMS calcd for $C_8{}^{13}CH_{11}F_2N^{15}N_2O_4 + H^+$- $[M+H]^+$: 267.0765; found 267.0730.

B.2. Figures

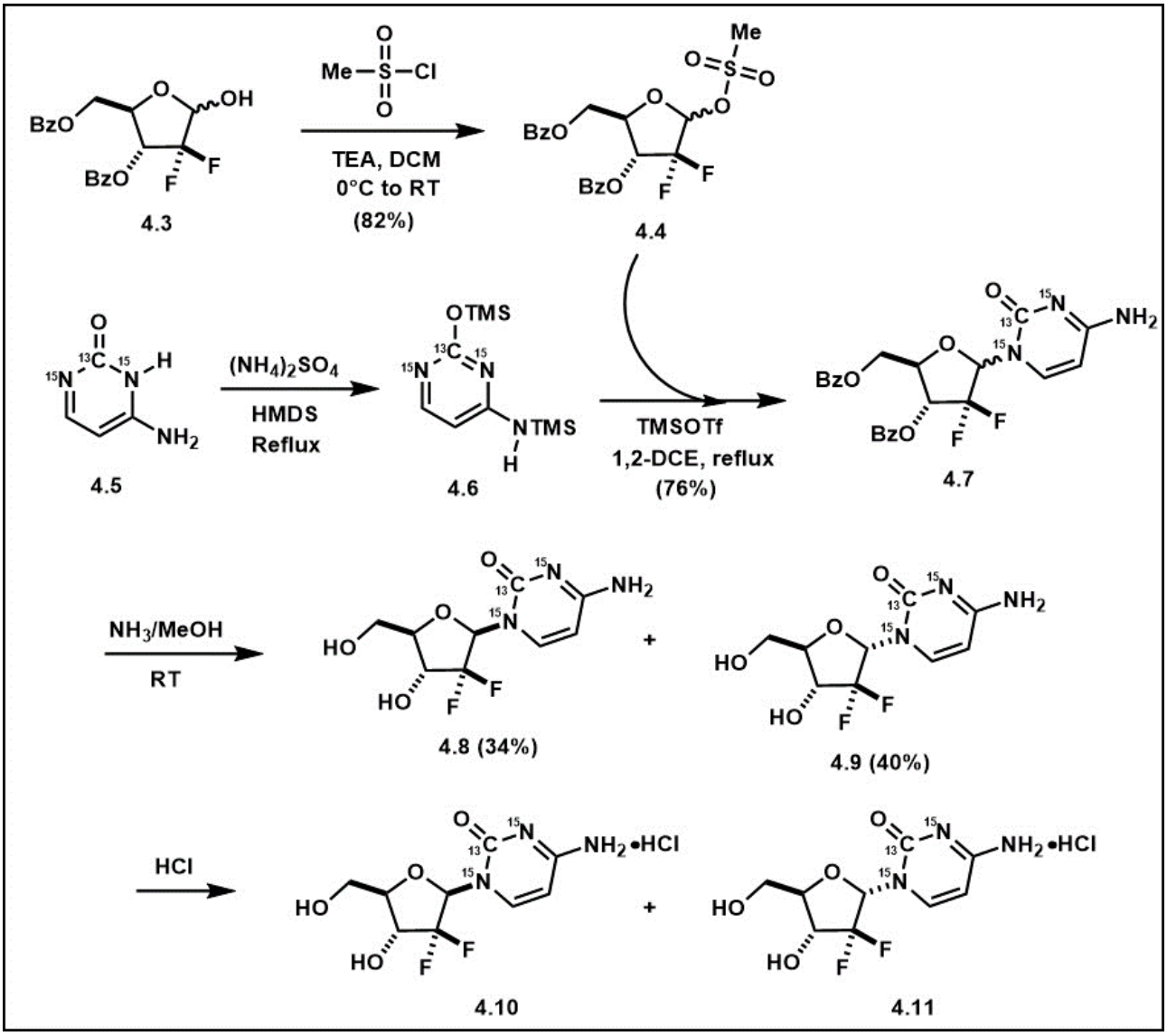

Scheme B1: Synthesis of stable-isotopically labeled Gemcitabine.

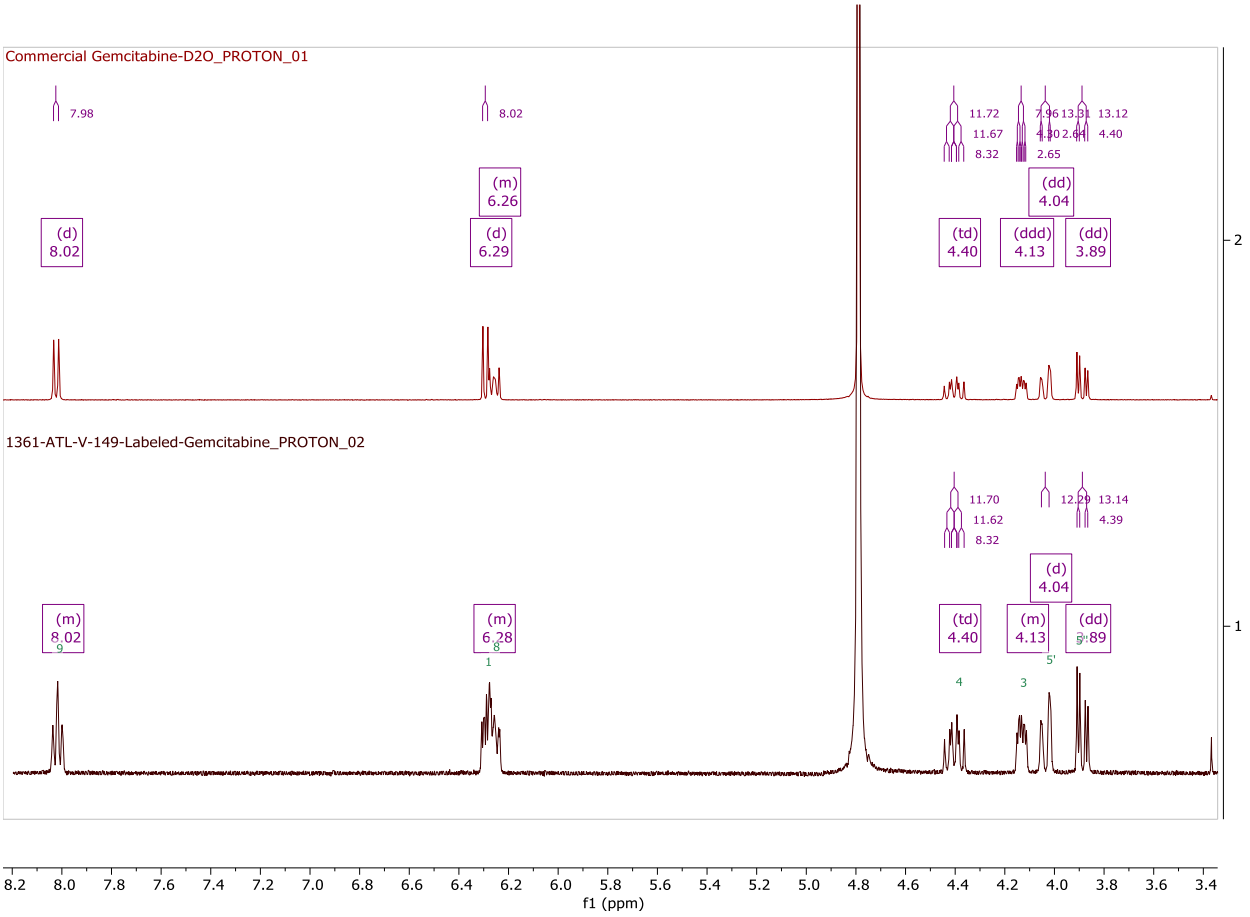

Figure B1. ^{1}H NMR spectra of non-labeled gemcitabine (top) and labeled gemcitabine (bottom).

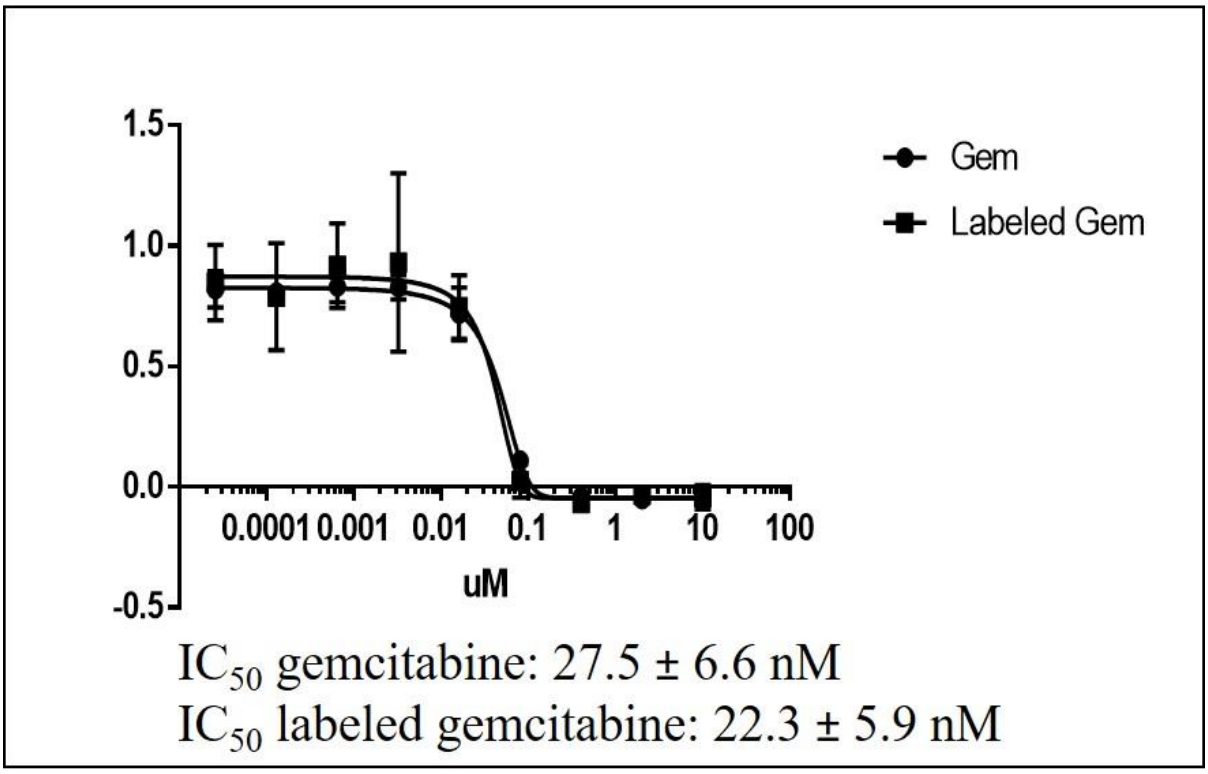

Figure B2. Cytotoxicity assay of non-labeled gemcitabine (Gem) and stable-isotopically labeled gemcitabine (Labeled Gem) on T-24 cell line.

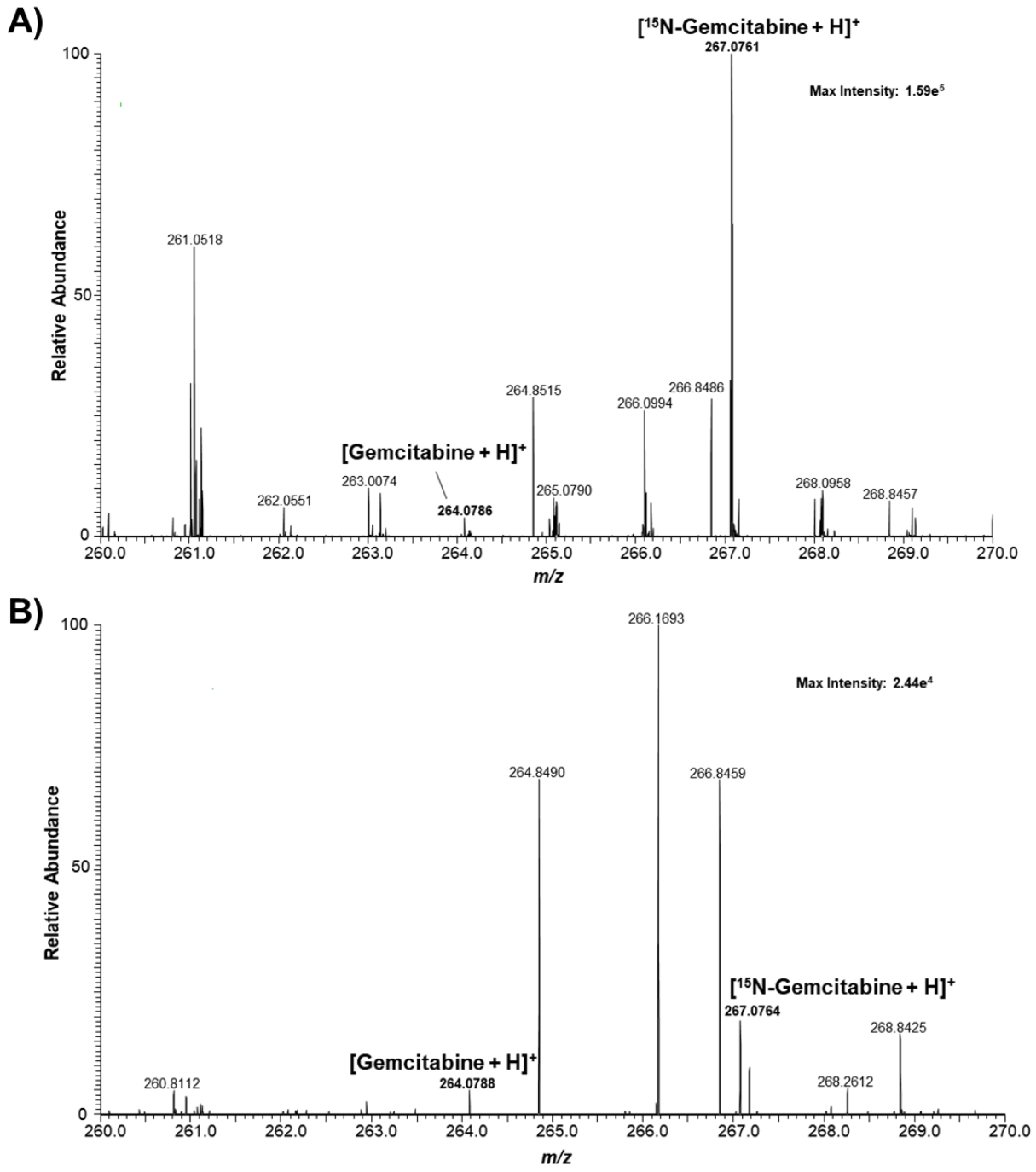

Figure B3. Mass spectrum of gemcitabine and $^{15}N_3$-gemcitabine after gemcitabine treatment (10 µM, 1 h). (a) Spectrum from a single T24 cell and (b) spectrum from a single K562 cell.

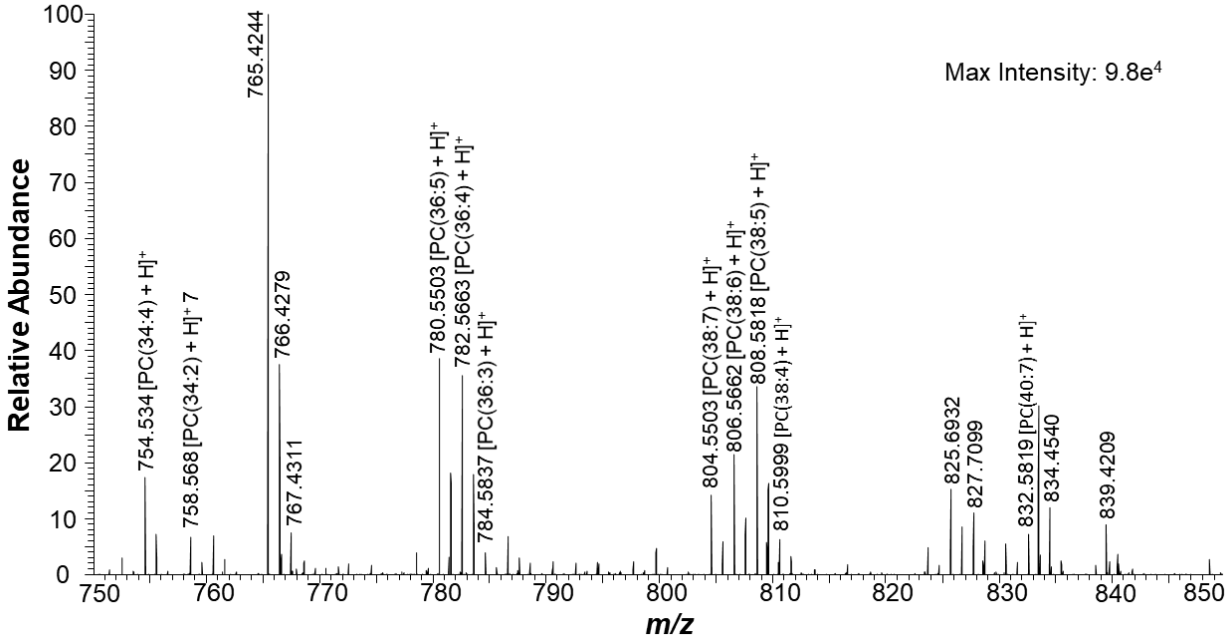

Figure B4. Mass spectrum of a single cell isolated from a bladder cancer patient qualitatively detecting phospholipids.

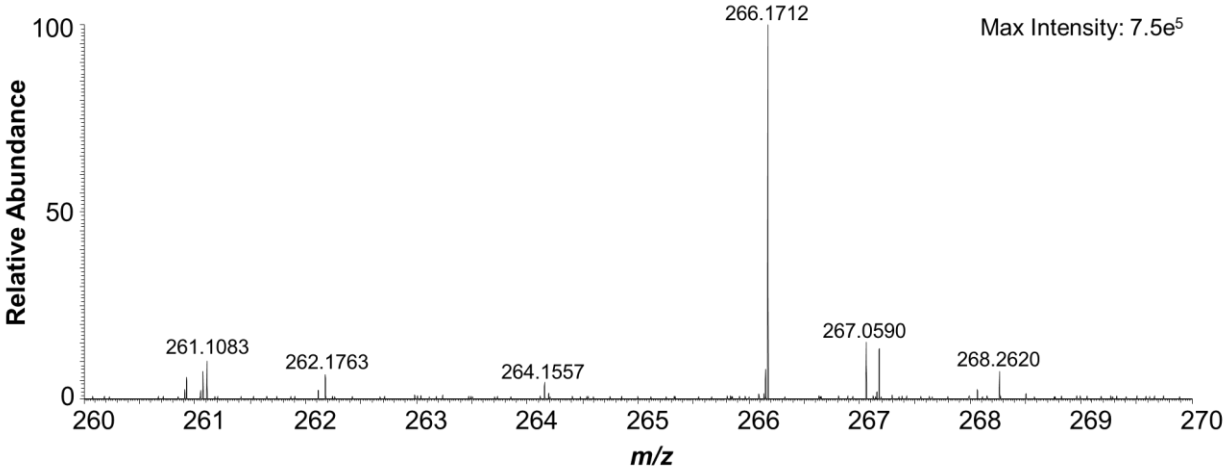

Figure B5. Mass spectrum of a single cell isolated from an untreated bladder cancer patient.

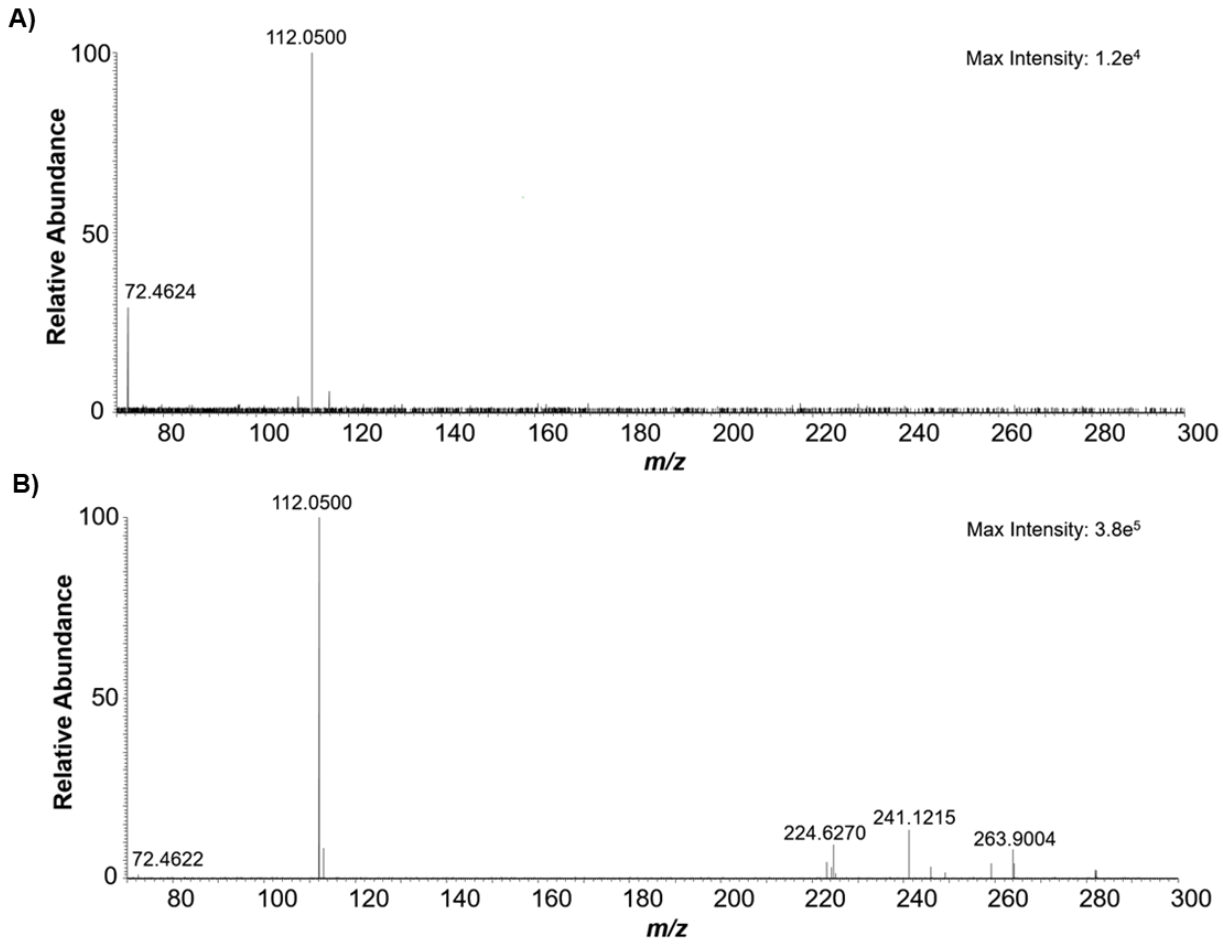

Figure B6: MS/MS spectra of Gemcitabine. A) MS/MS spectra of gemcitabine analyzed from a single cell isolated from bladder cancer patient 1. B) MS/MS of gemcitabine analyzed from a spiked solution.

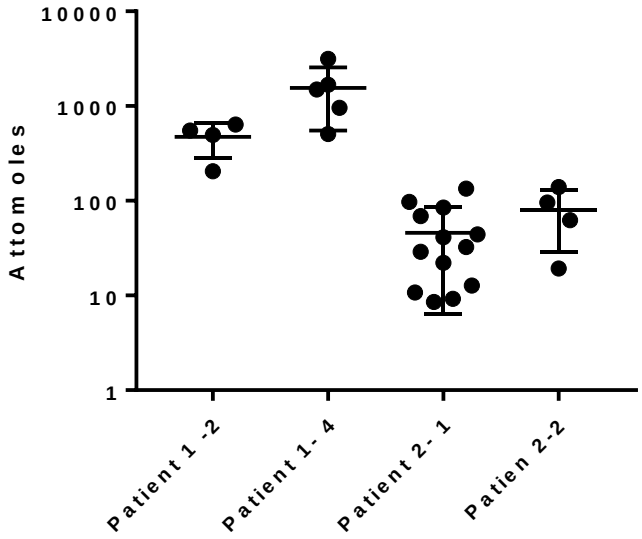

Figure B7: Scatter plot depicting single cell quantification of gemcitabine from bladder cancer patient urinary cells.

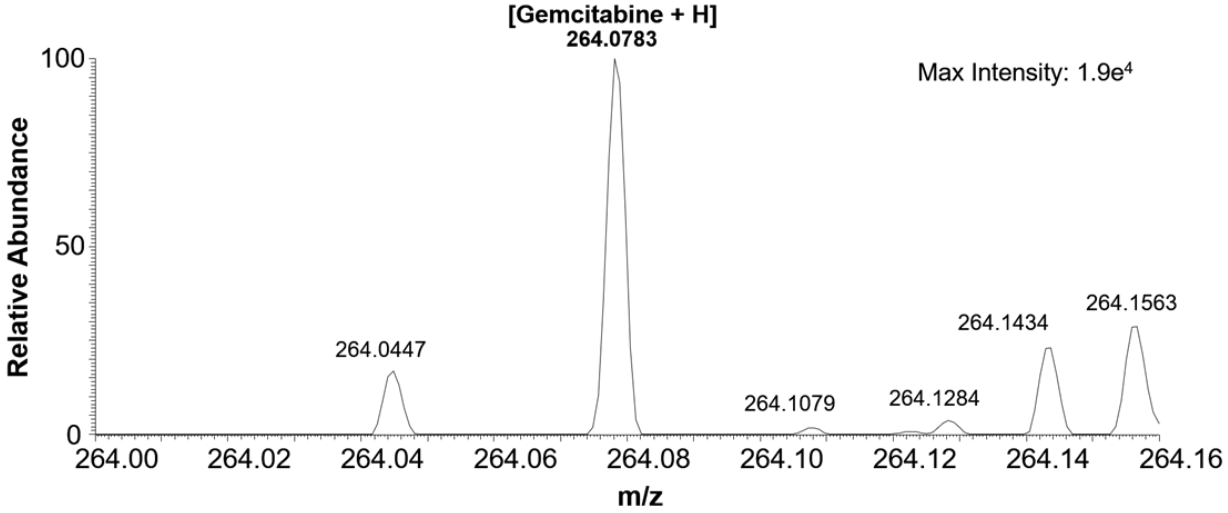

Figure B8: Spectrum of Gemcitabine depicting the limit of quantification (LOQ) utilizing the single probe in a 5nM gemcitabine solution in acetonitrile.